

UNCLASSIFIED

AD 269 773

Reproduced

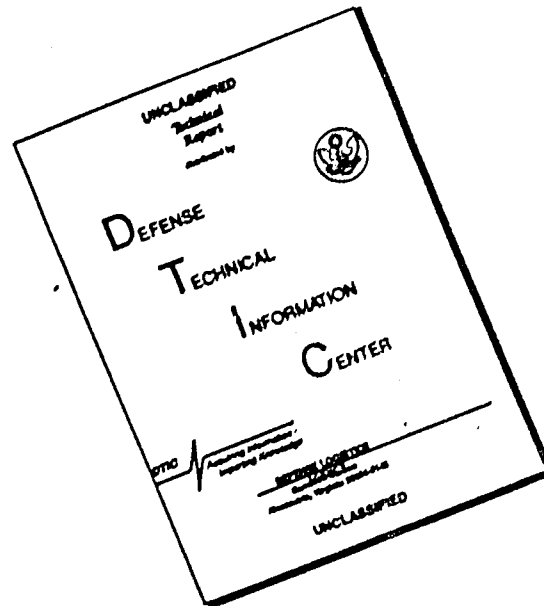
by who

ARMED SERVICES TECHNICAL INFORMATION AGENCY
ARLINGTON HALL STATION
ARLINGTON 12, VIRGINIA



UNCLASSIFIED

DISCLAIMER NOTICE



THIS DOCUMENT IS BEST QUALITY AVAILABLE. THE COPY FURNISHED TO DTIC CONTAINED A SIGNIFICANT NUMBER OF PAGES WHICH DO NOT REPRODUCE LEGIBLY.

NOTICE: When government or other drawings, specifications or other data are used for any purpose other than in connection with a definitely related government procurement operation, the U. S. Government thereby incurs no responsibility, nor any obligation whatsoever; and the fact that the Government may have formulated, furnished, or in any way supplied the said drawings, specifications, or other data is not to be regarded by implication or otherwise as in any manner licensing the holder or any other person or corporation, or conveying any rights or permission to manufacture, use or sell any patented invention that may in any way be related thereto.

CATALOGED
AS AD NO. 269773

WADC TECHNICAL REPORT 59-575
Part II

62-1-6
NOX
269 773

OXIDATION OF TUNGSTEN AND TUNGSTEN BASED ALLOYS

P. E. Blackburn
K. F. Andrew
E. A. Gulbransen
F. A. Brassart

Westinghouse Electric Corporation
Research Laboratories

JUNE 1961

Directorate of Materials & Processes
Contract No. AF 33 (616)-5770
Project No. 7351

ASTIA
EX-117-50
15 AUG 1961
TIPER

AERONAUTICAL SYSTEMS DIVISION
AIR FORCE SYSTEMS COMMAND
UNITED STATES AIR FORCE
WRIGHT-PATTERSON AIR FORCE BASE, OHIO

NOTICES

When Government drawings, specifications, or other data are used for any purpose other than in connection with a definitely related Government procurement operation, the United States Government thereby incurs no responsibility nor any obligation whatsoever; and the fact that the Government may have formulated, furnished, or in any way supplied the said drawings, specifications, or other data, is not to be regarded by implication or otherwise as in any manner licensing the holder or any other person or corporation, or conveying any rights or permission to manufacture, use, or sell any patented invention that may in any way be related thereto.

Qualified requesters may obtain copies of this report from the Armed Services Technical Information Agency, (ASTIA), Arlington Hall Station, Arlington 12, Virginia.

This report has been released to the Office of Technical Services, U. S. Department of Commerce, Washington 25, D. C., for sale to the general public.

Copies of ASD Technical Reports and Technical Notes should not be returned to the Aeronautical Systems Division unless return is required by security considerations, contractual obligations, or notice on a specific document.

FOREWORD

This report was prepared by the Research Laboratories of Westinghouse Electric Corporation under USAF Contract No. AF 33(616)-5770. The contract was initiated under Project No. 7351, "Metallic Materials", Task No. 73512, "Refractory Materials." The work was administered under the direction of the Materials Central, Directorate of Advanced Systems Technology, Wright Air Development Division, with Lt. W. E. Smith acting as project engineer.

This report covers work conducted from August 1959 to December 1960.

The authors are indebted to Dr. R. J. Ruka for his help in x-ray diffraction techniques. We are also grateful to I. Spitzberg for his assistance in making the x-ray diffraction measurements and in determining the oxidation rates of tungsten at high temperatures.

ABSTRACT

This paper describes the results of studies related to the oxidation of tungsten and its alloys.

The pressure of WO_3 polymers over WO_2 was measured in a tungsten Knudsen cell and found to agree with measurements in a platinum cell. Literature data for WO_2 and WO_3 were combined with vapor pressures determined in this project to give thermodynamic values for $W_{18}O_{49}$ and $W_{20}O_{58}$.

Tungsten oxidation rates have been measured from 800° to $1700^\circ C$ and in pressures of oxygen between 2×10^{-1} and 10^{-2} atmospheres. The effects of oxygen pressure indicate that the rate may be governed by oxygen dissociating to atoms at the reacting surface. The oxidation rate is demonstrated to be independent of the oxide evaporation rate. All of the evidence indicates that if an oxide barrier layer is present at temperatures above $800^\circ C$ it must be very thin.

Studies on the oxidation of tantalum-tungsten alloys between 800° and $1200^\circ C$ indicate that the 50-50 alloy has the greatest oxidation resistance, oxidizing at a rate as much as 10 times slower than tungsten alone.

PUBLICATION REVIEW

This report has been reviewed and is approved.

FOR THE COMMANDER



I. PERIMUTTER
Chief, Physical Metallurgy Branch
Metals and Ceramics Laboratory
Directorate of Materials and Processes

TABLE OF CONTENTS

	Page
GENERAL INTRODUCTION	1
SECTION I. VAPOR PRESSURES AND THERMODYNAMICS OF TUNGSTEN OXIDES AND MIXED OXIDES OF TUNGSTEN	2
INTRODUCTION	2
APPARATUS	3
SAMPLE MATERIAL	5
PROCEDURE	5
RESULTS	6
1. Vapor Pressures over Tungsten Oxides	6
2. Thermodynamics	12
3. Tungsten Oxide Pressures over Mixed Oxides of Tungsten	16
DISCUSSION	18
SECTION II. KINETICS OF OXIDATION	19
INTRODUCTION	19
EXPERIMENTAL - MICROBALANCE SYSTEM	19
1. Microbalance	19
2. Samples	19
RESULTS	21
1. Kinetic Study	21
A. Effect of Temperature	21
B. Effect of Pressure	25
2. X-ray Study	32
3. Metallographic Study	36
DISCUSSION - MICROBALANCE SYSTEM	36
EXPERIMENTAL - PRESSURE MEASURING SYSTEM	40
RESULTS	48
1. Kinetic Study	48
A. Effect of Temperature	48
DISCUSSION - PRESSURE CHANGE METHOD	50
SECTION III. OXIDATION OF TUNGSTEN AT HIGH TEMPERATURES	52
APPARATUS	52
SAMPLES	52
PROCEDURE	52
RESULTS	52
SECTION IV. SUMMARY AND CONCLUSIONS	71
LIST OF REFERENCES	73

LIST OF ILLUSTRATIONS

	Page
1. Induction Vacuum Furnace	413C483 . . . 4
2. W_3O_9 Pressure over $WO_2 + W$	517364 . . . 10
3. Logarithm of W_3O_9 Pressure over Tungsten Oxides at $1150^\circ C$	515726 . . . 11
4. Tungsten Oxide Pressure over the W-Ta-O and W-Hf-O Systems	515727 . . . 17
5. Photograph of Invar Balance	RM 19222. . . 20
6. Photographs of W and W-Ta Specimens	RM 19218. . . 22
7. Evaporation of WO_3 vs. Static Gas Pressure	517243 . . . 24
8. Effect of Temperature on Oxidation of 75W-25Ta Alloy, $900^\circ - 1200^\circ C$	517137 . . . 26
9. Effect of Temperature on Oxidation of 90W-10Ta Alloy, $900^\circ - 1200^\circ C$	517135 . . . 27
10. Effect of Temperature on Oxidation of 50W-50Ta Alloy, $800^\circ - 1200^\circ C$	517134 . . . 28
11. Oxidation of W and W-Ta Alloys, $1200^\circ C$	517312 . . . 29
12. Effect of Pressure on Oxidation of W at $1200^\circ C$, 7.6 cm - 0.76 cm	517138 . . . 30
13. Oxidation Rate vs. Oxygen Pressure	517363 . . . 31
14. X-Ray Diffraction Data of 90W-10Ta Oxide vs. Standard Patterns	RM 19240. . . 33
15. X-Ray Diffraction Data of 75W-25Ta Oxide vs. Standard Patterns	RM 19234. . . 34
16. X-Ray Diffraction Data of 50W-50Ta Oxide vs. Standard Patterns	RM 19239. . . 35
17. Photomicrographs of Metal-Oxide Interfaces, Pure W	RM 19217. . . 37
18. Photomicrographs of Metal-Oxide Interfaces, 90W-10Ta and 75W-25Ta	RM 19216. . . 38
19. Photomicrographs of Metal-Oxide Interfaces, 50W-50Ta	RM 19221. . . 39

LIST OF ILLUSTRATIONS (CONT'D)

20.	Effect of Temperature on Oxidation of 50W-50Ta Alloy, 900°-1200°C, Log-Log	517367 . . .	41
21.	Effect of Temperature on Oxidation of 75W-25Ta Alloy, 900°-1200°C, Log-Log	517330 . . .	42
22.	Effect of Temperature on Oxidation of 90W-10Ta Alloy, 900°-1200°C, Log-Log	517368 . . .	43
23.	Effect of Temperature on Linear Rate Constants	517385 . . .	44
24.	Photograph of Pressure Measuring Device	RM 19223. . .	45
25.	Details of Furnace Tube and Sample Support	193A943 . . .	46
26.	Schematic Diagram of Reaction System	193A942 . . .	47
27.	Effect of Temperature on Oxidation of W, 1200°-1250°C	517267 . . .	49
28.	Oxidation of Tungsten Wire Sample, 1200°-1300°C	493453 : . .	51
29.	System for High Temperature Oxidation Measurements	194A478 . . .	53
30.	Furnace Detail with Platinum Susceptor in Place	194A477 . . .	54
31.	Oxygen Gauge Schematic Diagram	294B629 . . .	55
32.	Oxidation of W in 21% O ₂ -79% Ar. Induction Heating	517242 . . .	58
33.	Oxidation of W in 21% O ₂ -79% Ar. Induction Heating	517244 . . .	59
34.	Photograph of Oxidized W Samples. Induction Heating	RM 19219. . .	60
35.	Oxidation of W in 21% O ₂ -79% Ar. Radiation Heating	517237 . . .	61
36.	Oxidation of W in 21% O ₂ -79% Ar. Radiation Heating	517239 . . .	62
37.	Photograph of Oxidized W Samples. Radiation Heating	RM 19220. . .	63
38.	Logarithm of the Rate Constants for Formation and Vaporization of WO ₃ vs. 1/T	517236 . . .	65
39.	Logarithm of Evaporation Rate of WO ₃ vs. 1/T	517238 . . .	66
40.	Logarithm of W Oxidation Rate vs. 1/T (21% O ₂ -79% Ar)	517240 . . .	68
41.	Logarithm of Oxidation Rate of W at 100 mm and 5 x 10 ⁻² mm vs. 1/T	517378 . . .	70

LIST OF TABLES

	Page
1. W_3O_9 Pressure over WO_2 in a Tungsten Knudsen Cell	6
2. Estimated Percentages of Gas Species over WO_2 and WO_3 at $1506^\circ C$	7
3. Estimated Heat and Entropy of Sublimation of WO_3 to the Given Gas Species	7
4. Heat and Free Energy of Formation of WO_3	12
5. Heat and Free Energy of Formation of WO_2	13
6. Heat and Free Energy of Formation of $1/18 W_{18}O_{49}$	15
7. Heat and Free Energy of Formation of $1/20 W_{20}O_{58}$	16
8. Effect of Temperature on Oxidation of W Alloys	23
9. Effect of Pressure on Oxidation of W at $1200^\circ C$	32
10. Spectrographic Analysis of Oxide Films	36
11. Metallographic Examination of Oxidized W and W-Ta Alloys	36
12. Summary of Kinetic Data for Oxidation of Tungsten Alloys	40
13. Oxidation of Tungsten in 21% O_2 -79% Ar, Inductive Heating	57
14. Oxidation of Tungsten in 21% O_2 -79% Ar, Radiant Heating	64

OXIDATION OF TUNGSTEN AND TUNGSTEN BASED ALLOYS

GENERAL INTRODUCTION

This report covers the results obtained during the past year on studies of the oxidation of tungsten and tungsten alloys. A previous report¹, WADC Technical Report 59-575, describes the work which was carried out during the first 18 months of the project. The earlier study included: 1) Measurements of oxidation rates on pure tungsten from 500 to 1300°C in oxygen pressures 10^{-1} to 10^{-3} atmospheres. 2) Phase diagram studies and vapor pressure measurements over the tungsten oxides. 3) X-ray diffraction analysis of the oxide films. It was concluded that, a) oxidation is diffusion controlled below 600°C, b) from 650 to 950°C the sample is covered with a thin protective layer underneath a cracked thicker oxide, c) above 1200°C and below 10^{-1} atmospheres the oxide vaporizes as fast as it is formed, d) the four tungsten oxides vaporize as polymers of WO_3 , e) the four oxides are WO_3 , $W_{20}O_{58}$, $W_{18}O_{49}$, and WO_2 , all with narrow homogeneity ranges of about .04 oxygen atoms/tungsten atom at 1300°C, f) most of the oxide formed during oxidation is WO_3 .

During the past year the research on oxidation of tungsten and its alloys has been continued by 1) measuring vapor pressure over WO_2 and mixed oxides of tungsten with hafnium and tantalum, 2) calculation of thermal properties of $W_{18}O_{49}$ and $W_{20}O_{58}$ from 298 to 1800°K, 3) measurement of oxidation rates of tungsten to 1700°C and of tungsten-tantalum alloys to 1200°C, 4) further study of the effects of oxygen pressure and vaporization rate on the oxidation of tungsten, 5) x-ray and metallographic studies of the oxide film.

Manuscript released by the authors December 1960, for publication as a WADC Technical Report.

SECTION I. VAPOR PRESSURES AND THERMODYNAMICS OF
TUNGSTEN OXIDES AND MIXED OXIDES OF TUNGSTEN

INTRODUCTION

A necessary constituent of any study involving oxidation is a thorough knowledge of the physical and chemical characteristics of the oxides. With this in mind, we have measured the vapor pressures of the four oxides of tungsten and their phase limits. This study reports: 1) additional data for the vapor over WO_2 , 2) an examination of factors involved in establishing equilibrium between gas and solid, 3) thermodynamic values for the tungsten oxides, 4) research into the mixed oxides of tungsten.

The vapor pressures over WO_3 given in WADC-TR-59-575 were in fairly good agreement with those obtained by previous authors, namely, Ueno², Berkowitz et al³, and Blackburn et al⁴. However, there was some discrepancy among these data for the heat and entropy of vaporization. Some of this discrepancy could be attributed to uncertainties in the slope and intercept of the Van't Hoff curves at the 95% level. The data obtained in the Technical Report was over a much broader temperature range than the preceding work, leading to a greater level of confidence in the two thermodynamic factors. One source of error which was not considered is the presence of gas species other than W_3O_9 . This occurrence would lead to changes in both entropy and heat of vaporization, since the relative amounts of the other species change with temperature. This effect is examined in the present report.

Of the remaining tungsten oxides, i.e. $W_{20}O_{58}$, $W_{18}O_{49}$, and WO_2 , only the vapor pressure over WO_2 has been previously studied. In that research, by Blackburn, Hoch, and Johnston, the heat and entropy of vaporization were inconsistent with the available thermal data for WO_2 and WO_3 . However, the vapor pressures over WO_2 given in the WADC report were generally in accord with the appropriate thermal values. Since these latter data were obtained using a platinum Knudsen cell, there existed the possibility that equilibrium had not been attained inside the cell. For this reason a tungsten Knudsen cell is used in this study.

Until recently there has been some question about the composition of the stable oxide phases of tungsten, as well as uncertainty about the thermodynamic data for these oxides.

Coughlin⁵ has calculated thermal values for WO_2 , W_4O_{11} , and WO_3 from estimated heat content data, from heat of formation of WO_3 found by Huff et al⁶, and from reduction equilibria published by Wöhler et al⁷ and by Shibata⁸. Since the phase designated by Coughlin as W_4O_{11} is generally accepted by crystallographers⁹ as $W_{18}O_{49}$, new values for this phase can be calculated. A thorough study of WO_2 and WO_3 has just been published by King, Weller and Christensen¹⁰. This study includes low temperature heat capacity and high temperature heat content data for these two oxides. Furthermore, there have been two recent reduction equilibria studies by Vasil'eva et al¹¹ and by Griffis¹². This work includes values for $W_{20}O_{58}$ which were missing in the earlier research. Mah¹³ has determined the heat of formation of both WO_2

and WO_3 , and Beard¹⁴ has measured the enthalpy, heat capacity, and entropy of WO_3 from 0° to $1000^\circ C$. The entropy of WO_3 at $298^\circ K$ was calculated from low temperature heat capacity data measured by Seltz et al¹⁵. No entropy data are available for $W_{18}O_{49}$ and $W_{20}O_{58}$. King's data, when combined with the vapor pressure measurements in this research, permit calculation of more accurate thermal values for $W_{18}O_{49}$ and $W_{20}O_{58}$ than has formerly been possible. The values given in our last WADC report were based on earlier, less complete data.

The possibility of finding alloys of tungsten with better oxidation resistance than tungsten itself is another objective of this project. With this in mind, we have attempted to find alloying additions in which the metal and its oxides would satisfy some of the following conditions: 1) low vapor pressure compared to WO_3 , 2) high melting point, 3) formation of a stable mixed oxide with WO_3 and a consequent lowering of the W_3O_9 vapor pressure, 4) formation by the mixed oxide of a coherent adhesive film on the underlying alloy.

The third condition is tested by determining W_3O_9 pressure as a function of the concentration of the added constituent. This procedure leads to the discovery of the composition of the mixed oxides as well as to their effect on the W_3O_9 pressure. In most cases information about vapor pressures of the metal and its oxide, and about corresponding melting points are available in the literature. The last condition, formation of a protection oxide layer, is found by studying the oxidation of the alloys. Further discussion of this problem is reserved for another section of this report.

APPARATUS

The apparatus used for this study is essentially the same as that described in Section I WADC Technical Report 59-575. It is formed of a vacuum system constructed of Pyrex tubing and metal Alpert valves. The furnace, which was sealed to the balance section, consisted of a mullite tube heated by radiation from a thick walled molybdenum susceptor. The susceptor was enclosed in a separately pumped vacuum jacket to prevent it from oxidizing while it was being heated by a controlled induction furnace. A susceptor wall thickness of 0.7 cm was necessary to successfully shield the sample inside the furnace tube from the magnetic field within the induction coil.

The molybdenum furnace has recently been replaced with a new vacuum furnace shown in Figure 1. In this system the induction coil is inside a water cooled brass shell which is pumped through a liquid nitrogen trap by a 720 l.oil diffusion pump. The susceptor is made of tungsten in order to perform experiments at higher temperatures. The principal limitation on temperature is the availability of gas tight refractory ceramics. Alumina may be used to 1900° while stabilized zirconia is useful to $2200^\circ C$. Counter balanced airplane cable is used for the furnace suspension, permitting ready replacement of induction coil, susceptor and furnace tube.

Weight changes of the Knudsen cells were measured by a quartz spring balance sealed inside the vacuum system. Springs with sensitivities of 14 and $41 \mu g/10^{-3} cm$ were used.

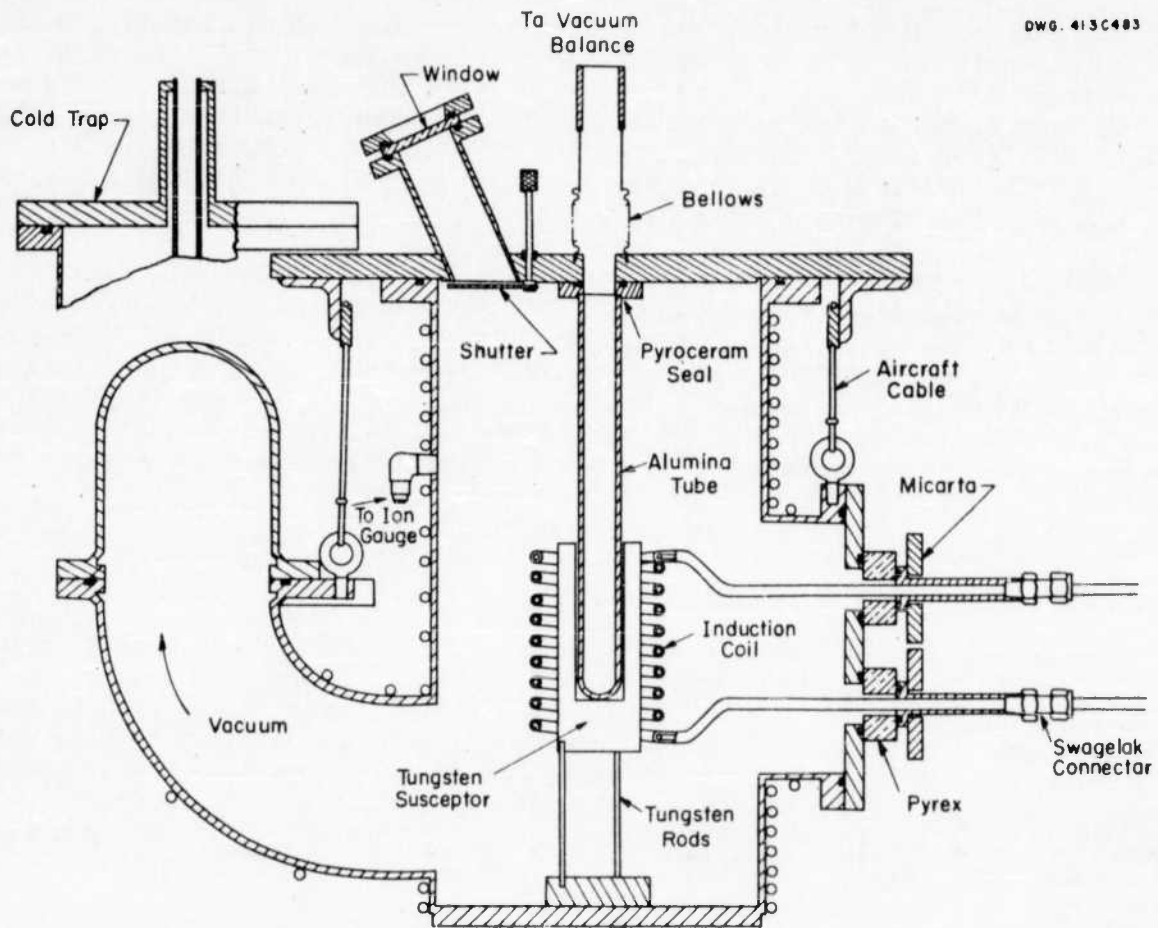


Fig. 1 - Induction vacuum furnace.

Knudsen cells were constructed of 3 mil platinum and 5 mil tungsten sheet. The latter was used for WO₂ measurements while all other runs were made in platinum cells.

SAMPLE MATERIAL

Tungsten trioxide was obtained by dehydrating tungstic acid at 800° in air. The impurities in weight per cent as determined by spectroscopic analysis were: Al, 0.002; Cd, 0.003; Co, 0.008; Cr, 0.005; Fe, 0.006; Li, 0.010; Ni, 0.003; Si, 0.002; Sr, 0.002; Ti, 0.020; V, 0.020; Zn, 0.004. Tungsten dioxide was made by mixing trioxide and metal and heating in a sealed platinum bomb at 1500°C for 1/2 hour. X-ray analysis of this material indicated weak lines for W₁₈O₄₉ as well as WO₂ lines. The oxygen-tungsten ratio was found to be 1.96 from chemical analysis. The impurities in the tungsten were: Ca, 0.001; Cu, 0.004; Fe, 0.002; Si, 0.001; Mo, 0.004; Nb, 0.010; Zr, 0.040. Mixed oxides were made by mechanically combining WO₃ and the second oxide in an agate mortar. The mixture was then reacted in a sealed platinum container for 1/2 hour at 1500°C. These materials were used: Ta₂O₅, 99.9+%; TiO₂, 99.9%; and HfO₂, 96.4%. The latter compound had the following percentages of impurities: Al, 0.640; B, 0.001; Cr, 0.006; Fe, 0.200; Mg, 0.030; Mn, 0.004; Ni, 0.002; Pb, 0.002; Si, 0.110; Ti, 0.60; V, 0.002; and ZrO₂, 1.800.

PROCEDURE

A weighed Knudsen cell was filled with oxide powder, re-weighed, and suspended from a spring balance inside the evacuated system. The change in spring extension as a function of time at constant temperature was recorded. A traveling microscope was used to measure spring extension and length was converted to weight change by using a calibration curve for the spring. The orifice area was found by taking a photomicrograph of the orifice and measuring the area of the magnified hole with a planimeter, then reducing to the original area with the appropriate magnification factor. This procedure was necessary in the case of the tungsten sample because of the irregular hole which was drilled in the cell. These areas were also corrected for the Clausing factor due to hole thickness and thermal expansion of the metal.

Pressures were calculated from the rate of gas effusion, $\frac{m}{tA}$ using the formula,

$$P = \frac{m}{tA} \sqrt{\frac{2\pi RT}{M}} \quad (1)$$

where m is the weight of the effused gas in time t from an orifice of corrected area A, R is the gas constant, T the absolute temperature, and M the molecular weight of the gas species.

The temperature was measured with a platinum vs platinum 10%-rhodium thermocouple enclosed in the bottom of the molybdenum susceptor. The thermocouple was calibrated as a function of temperature and distance from the bottom of the tube, and was standardized against a second thermocouple inserted into the mullite tube. The calibration curve was then used to compute the temperature of the run. Since

the sample temperature changed as the cell moved inside the furnace tube, it was necessary to correct the pressures to a single temperature. This was done by use of the following formula

$$P_{(T_{av})} = \frac{m}{tA} \sqrt{\frac{2\pi RT}{M}} \left(10^a \frac{(T_{av}-T)}{T T_{av}} \right) \quad (2)$$

where

$$\log P = \frac{-a}{T} + B \quad (3)$$

T is the temperature of the sample, and T_{av} is the average temperature for the complete measurement.

RESULTS

1. Vapor Pressures over Tungsten Oxides

The vapor pressures over WO_2 measured with a tungsten Knudsen cell, are given in Table 1. These values were calculated assuming that the gas phase was all W_3O_9 . In fact, this is not the case, for there are significant amounts of polymers of WO_3 over WO_2 in this temperature range as will be discussed in more detail later. The vapor pressures determined with a tungsten cell are 26% lower than those measured with a platinum cell.

TABLE 1

W_3O_9 Pressure over WO_2 in a Tungsten Knudsen Cell

Temperature °K	Time Sec.	Weight Loss μg	Effective Area ^a cm ² x 10 ³	W_3O_9 Pressure Atm. x 10 ⁶
1526	3532	4969	5.63	8.35
1567	1535	6160	5.64	24.2
1586	2039	13973	5.64	41.5
1604	641	8206	5.64	77.7
1624	358	8217	5.64	140
1630	155	5166	5.64	204
1663	154	11203	5.64	450
1664	128	9560	5.64	460
1669	57	11634	5.65	1270

^a Area of Knudsen cell multiplied by Clausing factor and corrected for thermal expansion.

Table 2 lists estimated amounts of the gas species over WO_2 and WO_3 at $1506^\circ C$.

TABLE 2

Estimated Percentages of Gas Species over WO_2 and WO_3 at $1506^\circ K$

Gas Species	% Over WO_2	% Over WO_3
WO_3	3.7	0.0095
W_2O_6	13	4.1
W_3O_9	84	69
W_4O_{12}	0.16	27
W_5O_{15}	0.037	0.21

These figures were derived by assuming the following values for the heat and entropy of sublimation of WO_3 to the given species.

TABLE 3

Estimated Heat and Entropy of Sublimation of WO_3 to the Given Gas Species

Gas Species	ΔH_{1500} kcal/mole of gas	ΔS_{1500} kcal/mole of gas
WO_3	115	40
W_2O_6	120	56
W_3O_9	121	63
W_4O_{12}	151	81
W_5O_{15}	167	82

The heats of vaporization to W_4O_{12} and W_5O_{15} were taken from Berkowitz et al.³ The entropies of vaporization to tetramer and pentamer were determined from the ratios of these species to W_3O_9 at $1492^\circ K$ as given by Berkowitz et al, while the entropies for the first two species are estimates by Aekermann et al¹⁶. The heat for W_2O_6 was based on the assumption that its pressure is 5% of the trimer at $1492^\circ K$. (Berkowitz estimates that both monomer and dimer are less than 5% of the trimer.) The heat of vaporization of the monomer was based on the supposition that the heat of dissociation of dimer to monomer is 110 kcal/mole. In an analogous system, Blackburn et al found the heat of dissociation of Mo_3O_9 (g) to $3 MoO_3$ (g) to be 220 kcal.

The equilibrium constant at a given temperature for the various species in

equilibrium with WO_3 (s) may be calculated from Table 3. The ratios of these species over WO_2 is then calculated from the total pressure over WO_2 .

In WADC Technical Report 59-575, the heat and entropy of vaporization of WO_3 to W_3O_9 were given as $\Delta H = 123.6$ kcal/mole of W_3O_9 and $\Delta S = 65.5$ e.u./mole of W_3O_9 . These values were derived from the slope of the $\log P$ vs $1/T$ curve without correcting for the presence of other species. The corrected heat and entropy of vaporization of WO_3 to W_3O_9 are

$$\Delta H = 121.3 \pm 1.9 \text{ kcal/mole of } W_3O_9$$

and

$$\Delta S = 63.2 \text{ e.u./mole of } W_3O_9$$

It should be pointed out that only thermodynamic values for the trimer and tetramer have been measured. Hence the correction to the slope of the Van't Hoff plot as well as the percentages in Table 2, are necessarily tentative.

A least squares fit of the values obtained using a platinum cell in Technical Report 59-575 gives for the reaction



$$\Delta H = 151.3 \pm 6.4 \text{ kcal/mole of } W_3O_9$$

and

$$\Delta S = 76.3 \text{ e.u./mole of } W_3O_9$$

while the values given in Table 1 give for reaction (4) using a tungsten cell

$$\Delta H = 152.8 \pm 8.9 \text{ kcal/mole of } W_3O_9$$

and

$$\Delta S = 76.6 \text{ e.u./mole of } W_3O_9$$

where the spread in ΔH is calculated at the 95% confidence level. The data obtained with the tungsten cell are about 9% greater than that calculated from free energies derived by King et al¹⁰ for WO_2 and WO_3 (See Tables 4 and 5). The heat and entropy of vaporization for reaction (4) may be calculated from King's data and the heat and entropy of vaporization of WO_3 . That is

	$\Delta H_{1600}^{\text{cal}}$	$\Delta S_{1600}^{\text{cal}}$
$9/2 WO_2 (s) \longrightarrow 3 WO_3 (s) + 3/2 W (s)$	27,600	9.9
$3 WO_3 (s) \longrightarrow W_3O_9 (g)$	123,600	65.5
$9/2 WO_2 (s) \longrightarrow W_3O_9 (g) + 3/2 W (s)$	151,200	75.4

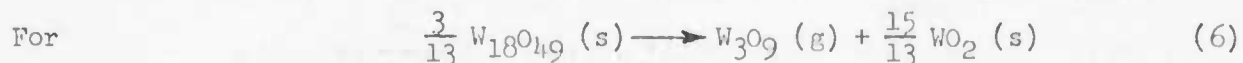
This excellent agreement for the heat and entropy may be compared to those given by Blackburn et al.⁴ for the same reaction in a platinum cell. Blackburn found $\Delta H = 90.2$ kcal and $\Delta S = 40.5$ e.u./mole of W_3O_9 . The data from this research is plotted in Figure 2 along with Blackburn's data. It is believed that the principal reason for the large discrepancy in these two sets of data is the fact that Blackburn et al attempted to measure the disproportionation of WO_2 at temperatures where equilibrium in the solid phase is not readily attained. Measurements of vapor pressure as a function of oxide composition have shown that the solid phase does not approach equilibrium below $1200^\circ C$ at a rate equal to or greater than the effusion rate of W_3O_9 (g) from the Knudsen cell. Figure 3 shows data obtained at $1150^\circ C$. The dashed line shows the expected curves as determined at higher temperatures. The lack of agreement indicates a failure to attain equilibrium. The gas phase presents no difficulties since the pressure measured over WO_3 by both Langmuir and Knudsen methods are in excellent agreement at $900^\circ C$. (See WADC TR 59-575.)

It was suggested in the preceding report that the failure to reach equilibrium at lower temperatures was due to a diffusion controlled reaction. However, diffusion control occurs only if the heat of diffusion is greater than the heat of vaporization. Such a condition is not involved here, because equilibrium is attained at higher, not lower temperatures. Hence, the activated process controlling the reaction at low temperatures must operate at greater speed than the effusion rate at high temperatures, and at a lower rate than the anticipated effusion rate at low temperatures. This situation requires the activated process to have a heat of activation in excess of 152 kcal (the heat of disproportionation of WO_2 (s) to $W + W_3O_9$ (g)). In terms of other processes which have been studied, such as surface diffusion, adsorption, desorption, this is an unusually high value for a heat of activation. Heats of diffusion usually fall between 10 and 80 kcal. The parabolic oxidation of tungsten, which appears to occur initially at lower temperatures, yields a heat of diffusion between 30 and 60 kcal/mole of oxygen. Since this reaction requires 1 1/2 moles of oxygen for the formation of W_3O_9 from WO_2 , i.e.



the heat of activation should be between 45 and 90 kcal. Another possible explanation is nucleation and growth of the other phases. Very little research has been done on this process, so the limits of the heats of activation are not known.

Although the values for the W_3O_9 (g) pressure resulting from disproportionation of $W_{18}O_{49}$ and $W_{20}O_{58}$ to W_3O_9 (g) and the next lower oxide were given in WADC TR 59-575, thermodynamic values were not given. Since these will be used to calculate free energies of formation for the tungsten oxides, the values are given below.



$$\Delta H = 122.0 \pm 2.9 \text{ kcal/mole of } W_3O_9$$

and

$$\Delta S = 59.6 \text{ e.u./mole of } W_3O_9$$

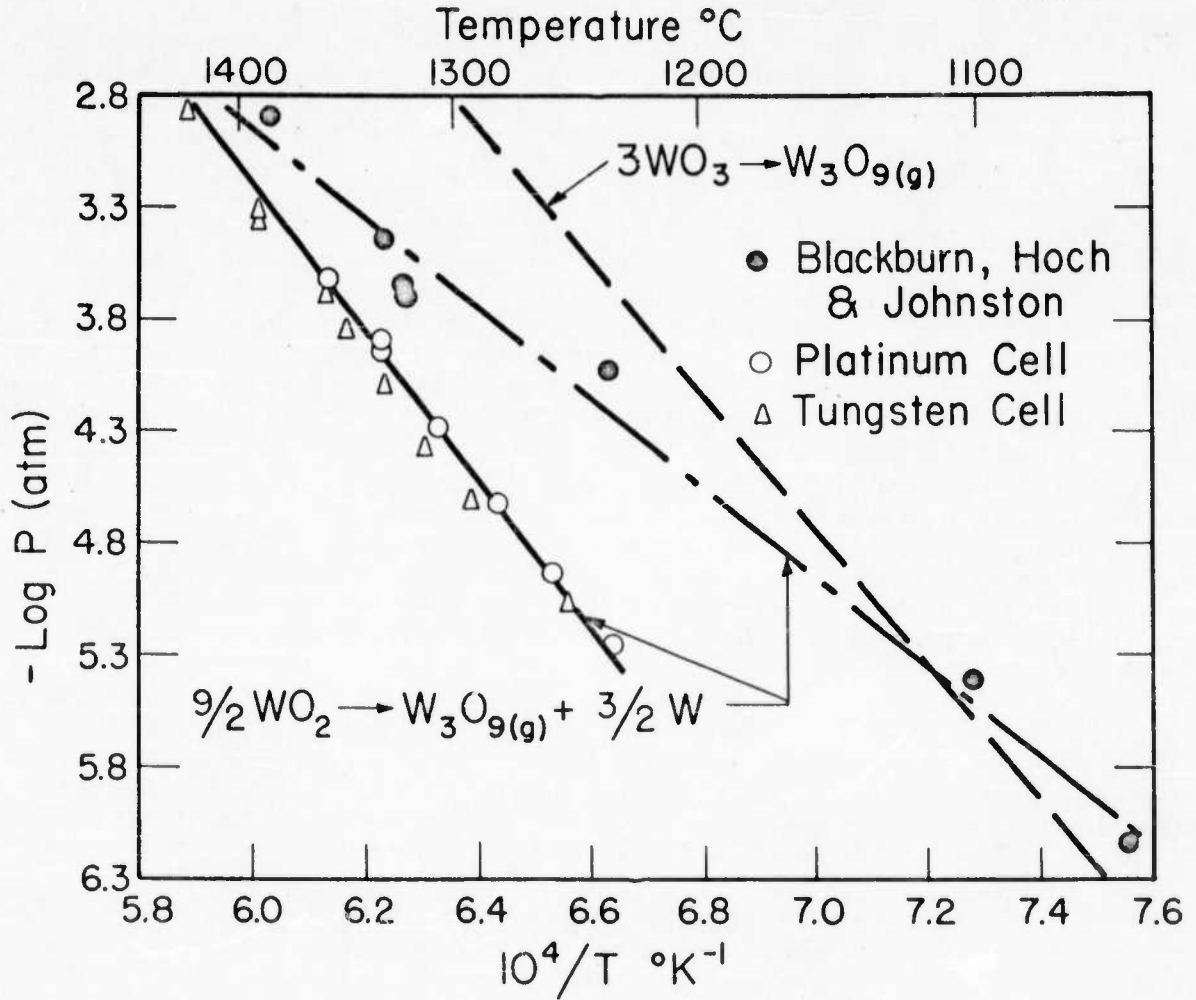


Fig. 2 - W_3O_9 pressure over $\text{WO}_2 + \text{W}$.

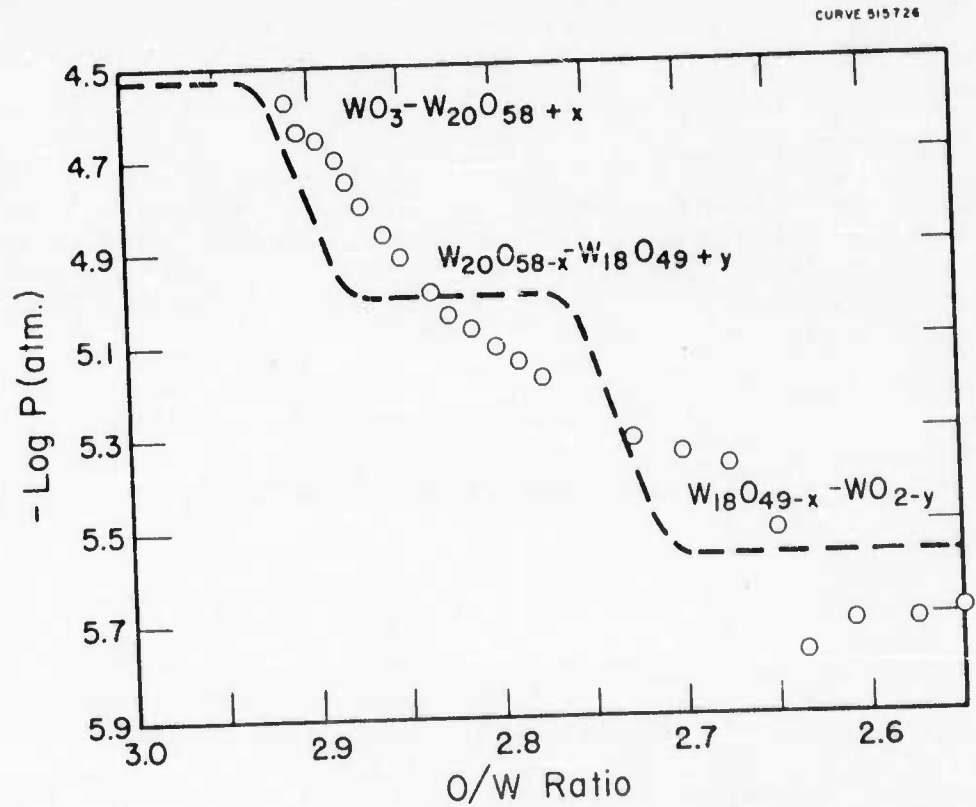
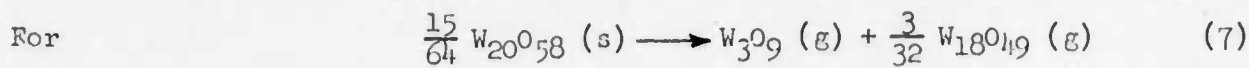


Fig.3-Logarithm of W_3O_9 pressure over tungsten oxides from WO_3 to $\text{WO}_{2.5}$ at 1150°C .



$$\Delta H = 128.3 \pm 9.8 \text{ kcal/mole of } \text{W}_3\text{O}_9$$

and

$$\Delta S = 66.5 \text{ e.u./mole of } \text{W}_3\text{O}_9$$

where the uncertainty in the heat of vaporization is at the 95% confidence level.

2. Thermodynamics

King et al¹⁰ have measured the low temperature heat capacity and high temperature heat content for WO_2 and WO_3 . They have tabulated these two functions in the range where each was measured as well as the entropy at 298.15 and at high temperatures. These authors have also calculated the heat and free energy of formation for WO_3 and WO_2 . Their values are presented in Tables 4 and 5.

TABLE 4

Heat and Free Energy of Formation of WO_3 ¹⁰

Temperature °K	$-\Delta H$ kcal/mole of WO_3	$-\Delta F^0$ kcal/mole of WO_3
298.15	201.45	182.65
400	201.25	176.2
500	200.9	170.0
600	200.45	163.85
700	200.0	157.75
800	199.5	151.75
900	199.0	145.85
1000	198.5	139.95
1050	198.25	137.05
1050	197.85	137.05
1100	197.65	134.15
1200	197.15	128.4
1300	196.7	122.65
1400	196.25	117.0
1500	195.75	111.35
1600	195.25	105.75
1700	194.75	100.15
1745	194.55	97.65
1745	177.0	97.65
1800	176.35	95.15
1900	175.25	90.65
2000	174.2	86.25

TABLE 5

Heat and Free Energy of Formation of WO_2 ¹⁰

Temperature K	$-\Delta H$ kcal/mole of WO_2	$-\Delta F^0$ kcal/mole of WO_2
298.15	140.95	127.6
400	140.8	123.05
500	140.6	118.65
600	140.3	114.30
700	139.95	110.0
800	139.6	105.75
900	139.2	101.55
1000	138.85	97.35
1100	138.45	93.25
1200	138.05	89.15
1300	137.65	85.05
1400	137.25	81.05
1500	136.8	77.05
1600	136.3	73.1
1700	135.7	69.15
1800	135.0	65.25
1900	134.25	61.4
2000	133.4	57.6

The values given in Tables 4 and 5 when combined with the vapor pressures over the four oxides may be used to calculate thermal values for the two intermediate oxides, $W_{18}O_{49}$ and $W_{20}O_{58}$. The following equations were used for $W_{18}O_{49}$:

	ΔH_{1600} cal	ΔS_{1600} e.u.
$\frac{13}{54} W_3O_9 (g) + \frac{5}{18} WO_2 (s) \longrightarrow \frac{1}{18} W_{18}O_{49} (s)$	-29,760	-15.21
$\frac{13}{18} W (s) + \frac{13}{12} O_2 (g) \longrightarrow \frac{13}{18} WO_3 (s)$	-141,010	-40.40
$\frac{13}{18} WO_3 (s) \longrightarrow \frac{13}{54} W_3O_9 (g)$	+29,760	+15.70
$\frac{5}{18} W (s) + \frac{5}{18} O_2 (g) \longrightarrow \frac{5}{18} WO_2 (s)$	-37,860	-10.97
<hr/>		
$W (s) + \frac{49}{36} O_2 (g) \longrightarrow \frac{1}{18} W_{18}O_{49} (s)$	-178,870	-50.88

In calculating the heats of vaporization for the two intermediate oxides it was assumed that the value found for WO_3 would yield quantities with better internal consistency than those found experimentally (Equations 6 and 7). The spread for each of

these heats determined at the 95% level includes the heat for W_3O_3 . Thus it is not possible to eliminate the supposition that they all are equal. If the heats of vaporization of W_3O_3 , $W_{20}O_{58}$ and $W_{18}O_{49}$ are equal, it follows that the heats of formation of the two intermediate oxides are a linear function of their oxygen concentration. The entropy for vaporization of $W_{18}O_{49}$ and $W_{20}O_{58}$ was calculated by least squares giving the value used at $1600^\circ K$. Since the heat of formation at 1600° is a linear function of the oxygen concentration, the same procedure may be used at 298.15 where the values are again determined from Tables 4 and 5. An average heat capacity term ΔC_p was found by dividing the difference in these two heats by the temperature interval. That is

$$\Delta C_p = \frac{\Delta H_{1600} - \Delta H_{298}}{(1600-298)} \quad (8)$$

The heat of formation then is

$$\Delta H_T = \Delta H_0 + \Delta C_p T \quad (9)$$

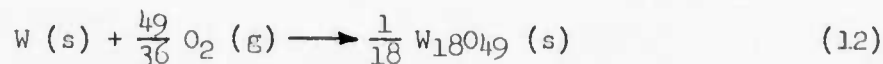
where ΔH_0 is

$$\Delta H_{298} - 298\Delta C_p \quad (10)$$

The free energy of formation is

$$\Delta F = \Delta H_0 + \Delta C_p T - T\Delta S_{298} - T\Delta C_p \ln T/298 \quad (11)$$

where ΔS_{298} is found by calculating ΔF at 1600 from ΔH_{1600} and ΔS_{1600} . The free energy equation for



is

$$\Delta F = - 185,960 + 87.99 T - 10.20 T \log T \quad (13)$$

The thermal values for the formation of $W_{18}O_{49}$ are given in Table 6.

TABLE 6

Heat and Free Energy of Formation of $1/18 W_{18}O_{49}$

Temperature °K	$-\Delta H$ kcal/mole of $1/18 W_{18}O_{49}$	$-\Delta F^{\circ}$ kcal/mole of $1/18 W_{18}O_{49}$
298.15	184.650	167.25
400	184.20	161.40
500	183.75	155.70
600	183.30	150.15
700	182.85	144.70
800	182.40	139.25
900	181.95	133.80
1000	181.55	128.55
1100	181.10	123.30
1200	180.65	118.05
1300	180.20	112.85
1400	179.75	107.70
1500	179.30	102.55
1600	178.85	97.45
1700	178.40	92.40
1800	178.00	87.30

Using the same procedure for $W_{20}O_{58}$ the following reactions are needed:

	ΔH_{1600} cal	ΔS_{1600} e.u.
$\frac{16}{75} W_{30}O_9 (g) + \frac{1}{50} W_{18}O_{49} (s) \longrightarrow \frac{1}{20} W_{20}O_{58} (s)$	-26,360	-13.48
$\frac{16}{25} W (s) + \frac{24}{25} O_2 (g) \longrightarrow \frac{16}{25} WO_3 (s)$	-124,960	-35.80
$\frac{16}{25} WO_3 (s) \longrightarrow \frac{16}{75} W_{30}O_9 (g)$	+26,360	+13.92
$\frac{9}{25} W (s) + \frac{49}{100} O_2 (g) \longrightarrow \frac{1}{50} W_{18}O_{49} (s)$	-64,390	-18.32
<hr/>		
$W (s) + \frac{29}{20} O_2 (g) \longrightarrow \frac{1}{20} W_{20}O_{58} (s)$	-189,350	-53.68

ΔC_p and ΔS_{298} are calculated as they were for $W_{18}O_{49}$ and substituted in equation 11 to give the free energy of formation of $1/20 W_{20}O_{58}$

$$\Delta F = -196,770 + 92.57 T - 10.69 T \log T \quad (14)$$

Table 7 gives the free energy and heat of formation of $1/20 W_{20}O_{58}$ using equation 14.

TABLE 7

Heat and Free Energy of Formation of $1/20 \text{ W}_{20}\text{O}_{58}$

Temperature °K	$-\Delta H$ kcal/mole of $1/20 \text{ W}_{20}\text{O}_{58}$	$-\Delta F^\circ$ kcal/mole of $1/20 \text{ W}_{20}\text{O}_{58}$
298.15	195.40	177.05
400	194.90	170.90
500	194.45	164.90
600	194.00	159.05
700	193.55	153.30
800	193.10	147.50
900	192.60	141.80
1000	192.15	136.30
1100	191.70	130.70
1200	191.20	125.20
1300	190.75	119.70
1400	190.30	114.25
1500	189.80	108.85
1600	189.35	103.45
1700	188.90	98.10
1800	188.45	92.80

3. Tungsten Oxide Pressures over Mixed Oxides of Tungsten

Two refractory oxides have been reacted with WO_3 , and the vapor pressure of the mixture determined by rate of effusion at a constant temperature. The added oxide is limited to a few compounds by the following considerations: a) the oxide must have a vapor pressure less than WO_3 , b) the melting point of the oxide must be greater than WO_3 , c) the metallic component of the oxide must be one which can be alloyed with tungsten. This requires a metal with a low vapor pressure. With regard to condition (c), experience has shown that an alloying element with a vapor pressure greater than chromium is lost too rapidly at the alloying temperature to remain in significant amounts in the tungsten.

$\log P/P_0$ versus the WO_3 concentration in mixed oxides of tantalum and hafnium are plotted in Figure 4. In this case, P is the measured pressure of W_3O_9 while P_0 is the W_3O_9 pressure over WO_3 . Each system was measured at a constant temperature. The W_3O_9 pressure over the W-Hf-O system decreased smoothly to about one quarter of that over pure WO_3 . The decrease in pressure to 25 mole % WO_3 is equivalent to that calculated from the entropy of mixing in an ideal solution. Below 25 mole % the measured pressure is higher than that calculated from the entropy of mixing. There was no evidence for the formation of a stable compound in this system. An explanation for the failure to form a stable mixed oxide is the large size of the hafnium $+4$ ion, about 20% greater than $\text{W} +4$. This exceeds the generally accepted rule that ionic substitution in a lattice is only likely to occur when the ionic diameters are within 15% of each other. The observed decrease in the W_3O_9 pressure over this system could be due to the formation of the solid solution as suggested above, or perhaps to some rate limiting factor such as effusion through the remaining HfO_2 powder.

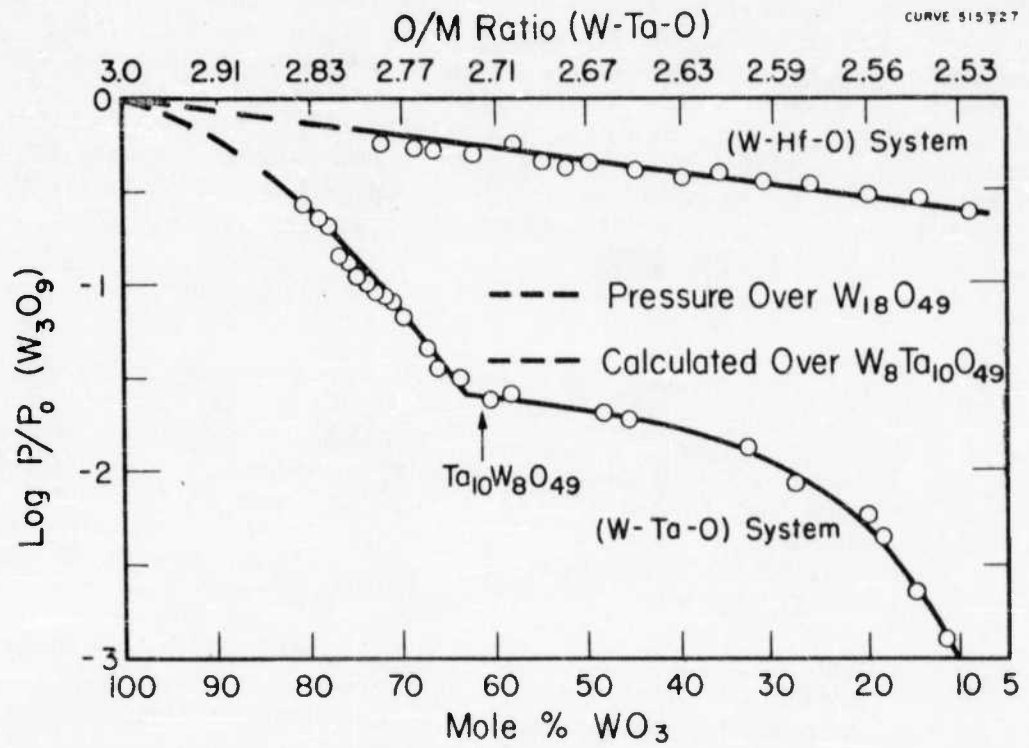


Fig.4-Tungsten oxide pressures over W-Ta-O system at 1403°C and over W-Hf-O system at 1258 °C.

In the Ta-W-O system the W_3O_9 pressure decreased to about 2.5% of the pressure over WO_3 at 63 mole % WO_3 . There is a break in the curve at this point followed by a further decrease in the W_3O_9 pressure with Ta_2O_5 enrichment. This break occurs at an oxygen/metal ratio of 2.730. This is very close to the oxygen-metal ratio in $W_{18}O_{49}$, suggesting that the compound formed may be a tantalum substituted tungsten oxide with composition $Ta_{10}W_8O_{49}$. As further evidence for this hypothesis the level of the W_3O_9 pressure over $W_{18}O_{49}$ is indicated in Figure 4, along with the additional lowering of the pressure in $Ta_{10}W_8O_{49}$ caused by the entropy of mixing. The measured pressure is in fairly good agreement with that calculated over $Ta_{10}W_8O_{49}$. The shapes of the curves on either side of the break suggest that this compound forms a solid solution with WO_3 on the one hand, Ta_2O_5 on the other, and a narrow 2 phase region. A curve calculated on this assumption is in fair agreement with the measured curve. The measured curve falls below the calculated curve and decreases much more rapidly at the tantalum-rich end. Here again, as in the Hf-W-O system, evaporation limiting factors may influence the shape of the curve. Analysis of the starting material and of the residue of a measurement at $1200^\circ C$ on the Ta-W-O system indicates that less than 1% of the vapor consisted of tantalum oxide.

DISCUSSION

The vapor pressure over WO_2 as measured with a platinum cell is in fairly good agreement with that measured with a tungsten cell. It was assumed that equilibrium in the platinum cell might be hampered by the solution of tungsten in platinum. However, the results indicate that this effect, or others, only resulted in a pressure difference of 26%. The results of both measurements yield values which are in good agreement with the thermal data for WO_2 and WO_3 . The earlier vapor pressure measurements of Blackburn, Hoch and Johnston were found to be in error due to failure to attain equilibrium in the solid phase at temperatures below $1200^\circ C$.

The amount of gas species other than W_3O_9 has been calculated from estimated heats and entropies of vaporization. Of the three other species only one, W_4O_{12} , has been measured accurately. There is a lack of consistency among the thermal values for the four species estimated in this research. The uncertainty in the correction to the thermal values for W_3O_9 is such that the magnitude of the heat and entropy could be increased rather than decreased should more accurate values be available.

The heat and free energy of formation of the $W_{18}O_{49}$ and $W_{20}O_{58}$ have been calculated from literature data and the vapor pressures measured here. In making these calculations the gas phase over the oxides was assumed to consist entirely of W_3O_9 . A calculation was made for WO_2 at $1506^\circ K$ in which the gas species is significantly different from that over WO_3 . The free energy of formation was computed by considering the other species. In this case, there was less than 250 calories difference between the two methods of calculation. Since there is considerable doubt about the thermal values for the other species, and since the maximum error is less than 250 cal, there is no justification for a more complex treatment of the data than has been used here.

SECTION II. KINETICS OF OXIDATION

INTRODUCTION

In an earlier study¹ the kinetics of the oxidation of tungsten sheet and wire specimens were studied between 500 and 1300°C over the pressure range of 10^{-1} to 10^{-3} atmospheres of oxygen. The results showed: 1) A protective oxide was formed below 600°C. 2) From 650-950°C a protective oxide scale was formed initially. After reaching a certain thickness the oxide scale cracked away from the metal at local areas which gave easy access of oxygen to the metal and a linear rate of oxidation. 3) Between 1000 and 1300°C the mechanism of oxidation changed with temperature and pressure. At 1200°C and higher, the rate of oxidation was determined by the rate at which oxygen arrived at the surface, by diffusion of the volatilized oxide away from the surface and by geometrical considerations of the sample surface area.

Two difficulties were encountered in the earlier study. First, the sheet specimens had a laminar structure and therefore oxidized more rapidly at the edges. This was observed for oxidations above 800°C. Second, since the wire specimens were only 9 mils in diameter, the metal was quickly consumed by oxidation.

In this study: 1) a modification of our earlier microbalance method is described for extending the range of the oxidation experiments and for elimination of the edge type of reaction, 2) measurements are presented on the oxidation of pure tungsten rod samples over the temperature range of 950 to 1200°C and for oxygen pressures of 0.01 to 0.10 atmospheres, 3) measurements are presented on the rate of oxidation of three tungsten-tantalum alloys from 800 to 1200°C at 0.1 atmospheres of oxygen pressure, 4) a new method is described for the study of the kinetics of oxidation of tungsten based on oxygen consumption of the metal, 5) crystal structure studies are made of the oxide scales and, 6) an interpretation of the kinetic data is developed.

EXPERIMENTAL - MICROBALANCE SYSTEM

1. Microbalance

A new type of balance was designed to utilize tungsten specimens weighing up to 10 gm. The beam and support were designed to fit the conventional microbalance reaction system. Invar metal was used in the construction. The over-all length of the beam was 14.5 cm and the weight of the beam was about 46 gm. The Invar balance was gold plated and is shown in Figure 5. Calibration of the balance showed a sensitivity ranging from 38.9×10^{-6} gm/0.001 cm deflection for a specimen weight of 0.9680 gm to 43.5×10^{-6} gm/0.001 cm deflection for a 5.2256 sample. The specimens were placed in a small platinum bucket suspended by a platinum wire from the beam end. The techniques used were similar to those used in our earlier study¹.

2. Samples

The pure tungsten specimens were machined from rod. The alloy specimens were machined from small buttons which had been prepared by the arc melting of pure powders

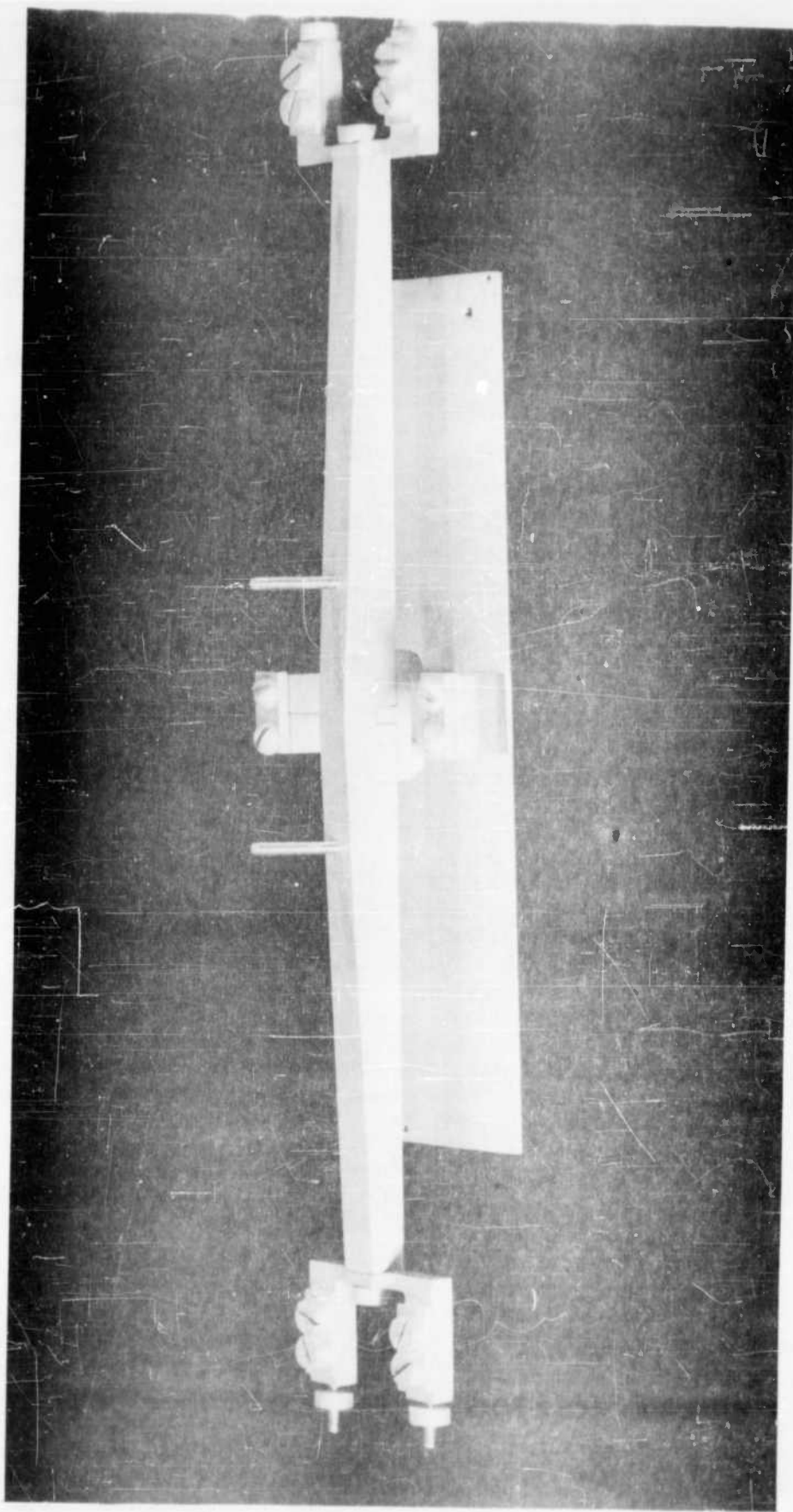


Fig. 5 -- Invar Balance

in an argon atmosphere. They were then polished through 4/0 polishing paper and washed with petroleum ether and alcohol. Photographs of the unreacted specimens are shown in A and C of Figure 6.

A spectrographic analysis of pure tungsten showed the following in parts per million: Ti, < 10; Nb, < 100; Mo, < 40; Fe, 15; Si, 10; B, < 10; Be, 1; Mn, < 1; Mg, < 10; Cr, < 10; Al, < 10; V, < 40; Ni, < 5; Cu, 25; Ag, < 1; Ca, < 10.

Kinetic studies were made on pure W, 50W-50Ta, 75W-25Ta, and 90W-10Ta. The alloy compositions are nominal weight percents. The sizes of the specimens were varied depending upon the amount of reaction expected. The pure W specimens weighed from 0.4613 gms to 0.9544 gms with surface areas from 0.505 cm² to 0.700 cm².

RESULTS

1. Kinetic Study

A. Effect of Temperature

The Invar balance was used to study the reaction of W-Ta alloys with oxygen and the effect of pressure on the oxidation of tungsten at 1200°C. The alloy data are summarized in Table 8.

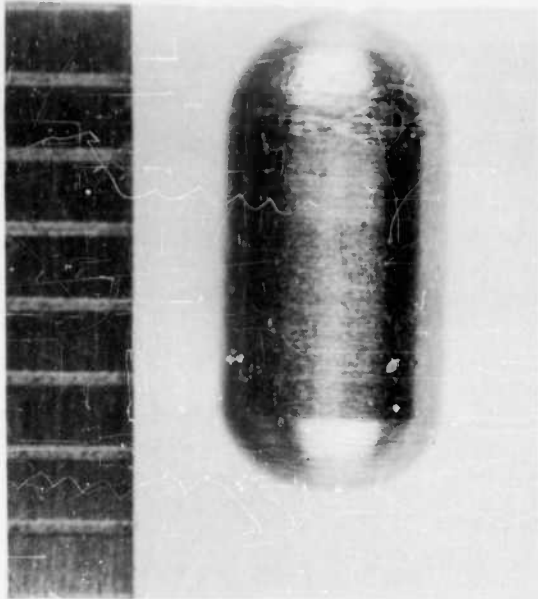
Due to the vaporization of WO₃ at 1100°C and above, it was necessary to correct the data obtained using the balance. It was assumed that the rate of loss of oxide by vaporization is linear. To find the amount vaporized, the oxide scale was removed mechanically and the remaining tungsten was weighed. The amount of oxide formed is then

$$(W_i - W_f) \frac{M(WO_3)}{M(W)} \quad (15)$$

where W_i is the weight of unreacted tungsten, W_f , the weight of descaled metal, $M(WO_3)$ and $M(W)$ are the molecular weights of WO₃ and W, respectively. The amount of oxide remaining on the sample is

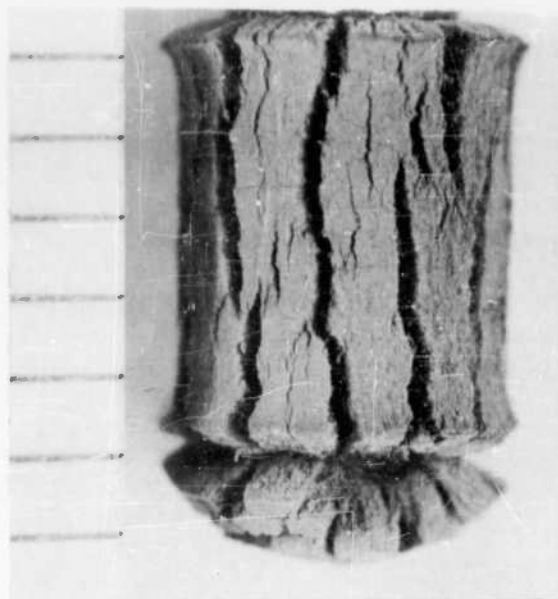
$$W_f - W_o \quad (16)$$

where W_o is the weight of the specimen after oxidation. The difference between 15 and 16 is the weight of oxide lost by vaporization. This is divided by the time and sample area and added to the measured weight change to obtain the oxidation curve.



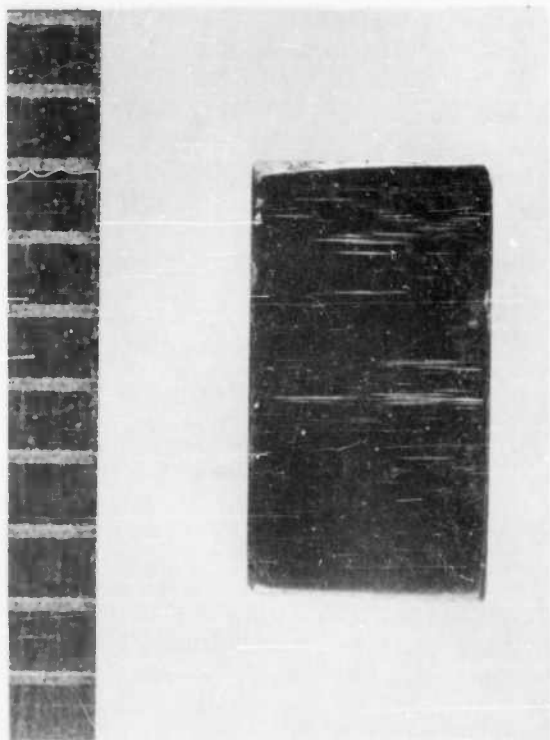
10 X

A. Unreacted W



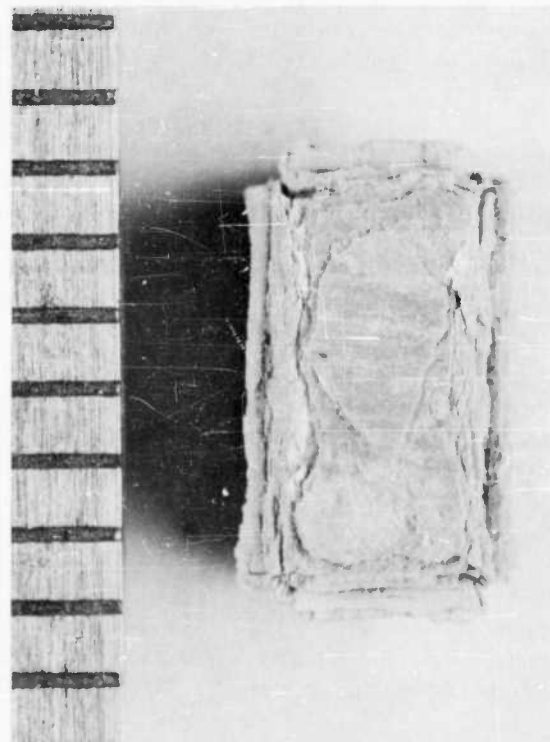
10 X

B. W oxidized at 1050°C
7.6 cm of Hg of O_2 - 80 min.



10 X

C. Unreacted W-Ta alloy



10 X

D. 90W - 10Ta alloy oxidized at
 1000°C - 7.6 cm of Hg of O_2 - 2 hr.

Fig. 6 --Photographs of W and W-Ta Specimens

TABLE 8

Effect of Temperature on Oxidation of W Alloys 7.6 cm of Hg of Oxygen

Alloy	Temp. °C	Wt. Gain (mg/cm ²) at Time (min)			
		30	60	120	180
90W-10Ta	900	7.1	14.6	28.8	42.8
	1000	11.7	24.2	49.3	--
	1050	13.3	28.2	54.1	--
	1100 *	23.4	48.7	--	--
	1200 *	56.6	98.6	--	--
75W-25Ta	900	4.5	7.4	12.8	17.2
	1000	10.3	17.8	31.0	43.1
	1050	16.1	30.0	40.8	34.3
	1100 *	36.3	66.1	--	--
	1200 *	56.5	98.6	180.0	--
50W-50Ta	800	1.3	1.9	2.6	3.2
	900	2.9	4.5	7.5	11.9
	1000	6.7	9.4	13.8	17.2
	1000	5.2	7.4	10.5	12.9
	1000	6.3	8.8	12.5	14.9
	1100	8.3	11.6	16.2	20.2
	1200	12.3	17.2	24.1	29.2

* Wt. gains corrected for loss of WO₃ by vaporization.

The vaporization rate of WO₃ as a function of pressure was measured at 1000, 1100 and 1200°C. This data is shown in Figure 7 along with some values taken from Speiser's¹⁷ curve determined at a pressure of one atmosphere. It was believed that these curves could be used to correct the balance data. However, at 1200°C and pressures less than 0.1 atm. the vaporization rate of the oxidizing samples (as determined above) was less than that in Figure 7. At 1200°C and 0.1 atm. the vaporization rates were about the same. This suggests that oxidation is independent of the vaporization rate, since at lower pressures the oxidation rate is not fast enough to produce the vaporization rate of pure WO₃.

The corrections to the weight gain curves for vaporization of oxide were made on W, 90W-10Ta and 75W-25Ta, but not on the 50W-50Ta samples. The oxide scale on the latter samples adhered to the metal so tightly that it was impossible to remove without also removing metal. The curves for 50W-50Ta represent the difference between oxygen reaction and oxide loss. The oxide loss is believed to be less for 50W-50Ta than for the others. The oxidation rate of these samples will be measured during the next year with the induction furnace apparatus described in the following section.

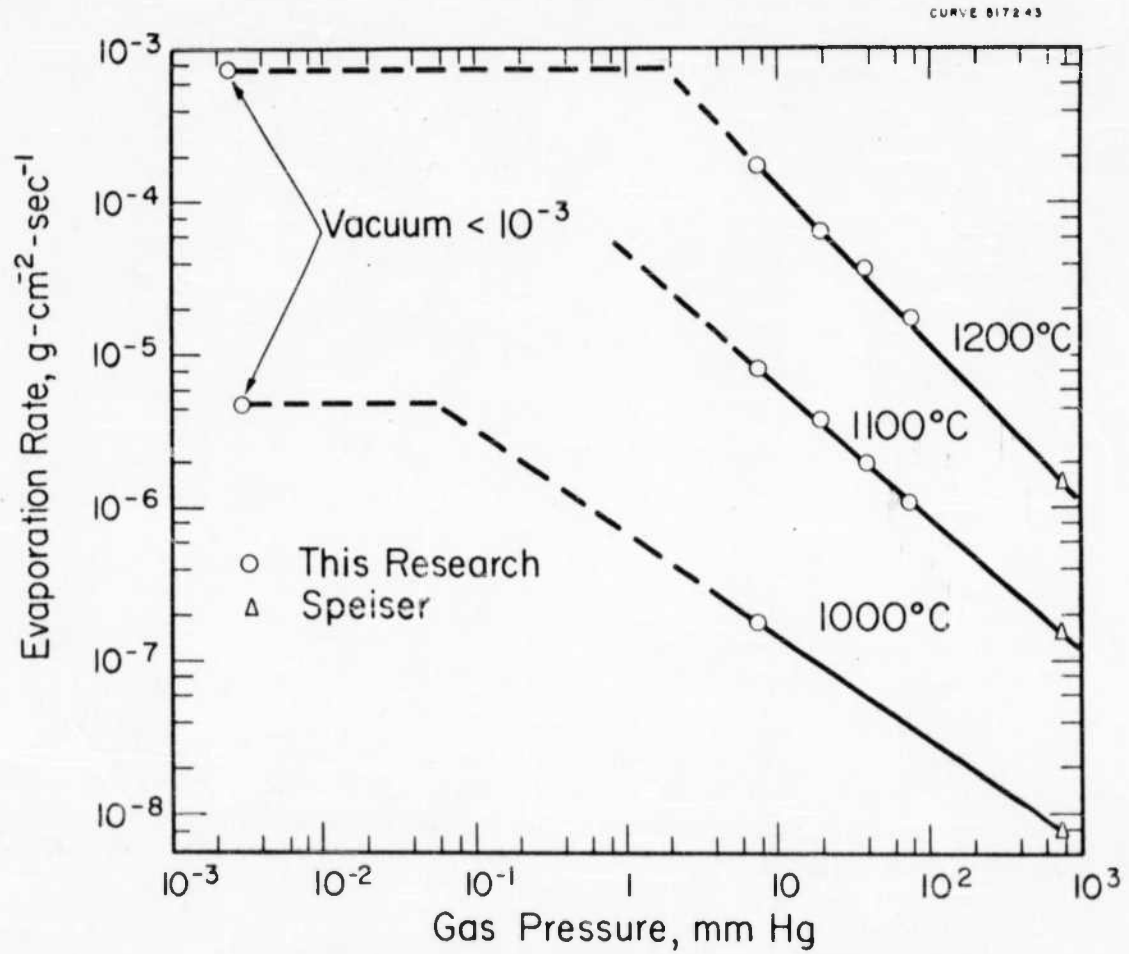


Fig. 7 -Evaporation of WO_3 versus static gas pressure.

The effect of temperature on the oxidation of alloys 50W-50Ta, 75W-25Ta and 90W-10Ta is shown in Figures 8, 9 and 10, respectively. The results are graphed as weight gain versus time plots for three hour runs.

In Figure 8 are plotted the weight gain curves for the oxidation of the 75W-25Ta alloy over the temperature range of 900-1200°C. These appear to be more linear than the curves of the 50W-50Ta alloy. With the exception of the 50W-50Ta alloy and at temperatures of 1100°C and above, corrections were made to our final weight gain curves for the loss in weight due to the vaporization of WO_3 .

The weight gain curves for the 90W-10Ta alloy are seen in Figure 9. The curve for the 1200°C oxidation shows a slight decrease in the rate after the first few minutes of oxidation. In general the shape of the curves is linear.

Figure 10 shows the oxidation curves of the 50W-50Ta alloy for the temperature range 800-1200°C at an oxygen pressure of a tenth of an atmosphere. The curves indicate a decrease in rate as the reaction proceeds. In curve B, a slight increase in rate may be seen after about two hours of reaction. Examination of this specimen indicated that this was due to the exposure of some fresh metallic surface to the oxygen atmosphere during the course of the oxidation.

A comparison of the oxidation of W with these three alloys at 1200°C and 0.76 cm of oxygen is plotted in Figure 11. Pure tungsten oxidizes the fastest and 50W-50Ta, the slowest. The 75W-25Ta and the 90W-10Ta show the same rate of oxidation.

B. Effect of Pressure

The Invar balance was used to oxidize tungsten in the pressure range of 0.76 cm to 7.6 cm of oxygen and the results are tabulated in Table 9. This data, obtained at 1200°C, is plotted in Figure 12. The oxidation rate from these four measurements is plotted in Figure 13 along with Langmuir's¹⁸ data for lower pressures. In addition to these values, three measurements were taken from the rate of weight loss of tungsten wire reacted at low pressures with oxygen reported in WADC TR 59-575¹. The latter weight losses of WO_3 were converted to oxygen reaction by multiplying by $48/231.86$, the ratio of the oxygen to oxide molecular weights. Langmuir¹⁸ found that the oxidation rate is proportional to the collision rate of oxygen on the surface at pressures below 50 μ . A least squares fit to data from this research gives the following:

$$\log K = 0.433 \log P - 4.93 \quad (17)$$

where K is the oxidation rate in $g\text{-cm}^{-2}\text{-sec}^{-1}$ and P is the pressure in mm. The coefficient for $\log P$ is 0.433 ± 0.225 , determined at the 95 per cent level. This broad region of uncertainty includes the value 0.5 which would be the case if the higher pressure oxidation were controlled by the rate of dissociation of molecular oxygen to atoms. More accurate data is required to definitely establish the pressure sensitivity of the oxidation rate. Further investigation of this problem is planned.

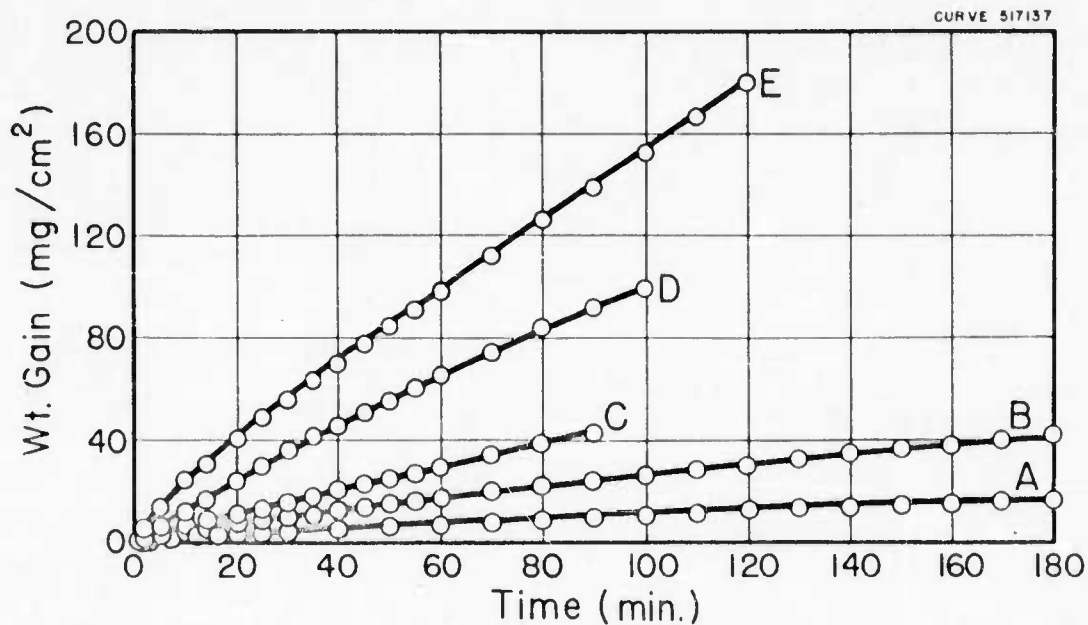


Fig.8-Effect of temperature on oxidation of 75W-25 Ta alloy,
 900°C-1200°C, 7.6 cm of Hg of O₂.
 A-900°C, B-1000°C, C-1050°C, D-1100°C, E-1200°C
 (curves A, B and C not corrected for vaporization of WO₃)

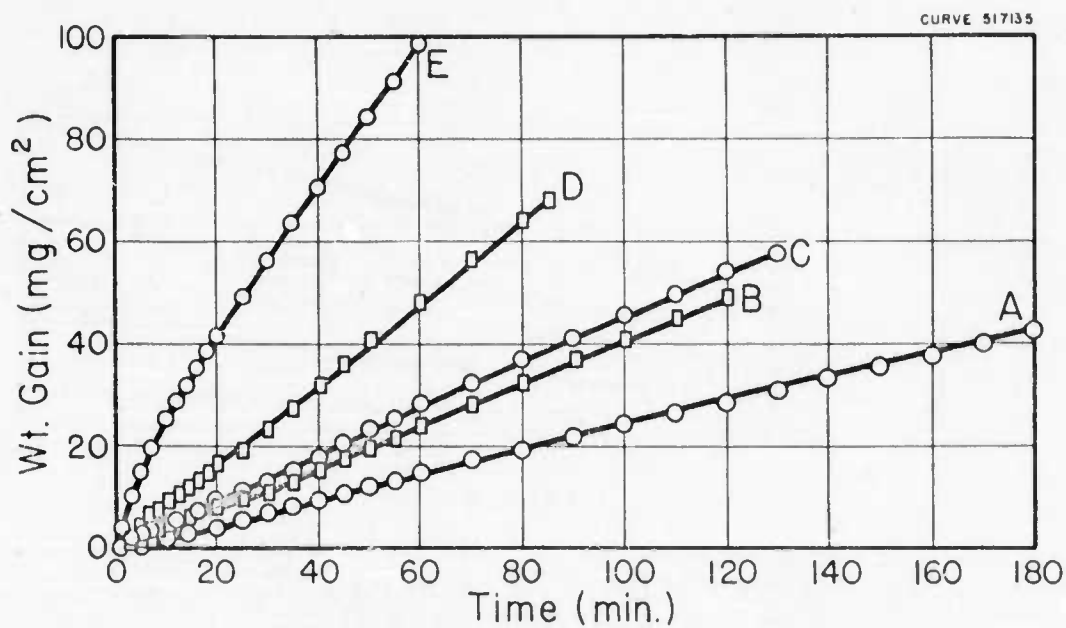


Fig. 9—Effect of temperature on oxidation of 90W-10Ta alloy,
 900°C-1200°C, 7.6 cm of Hg of O₂.
 A—900°C, B—1000°C, C—1050°C, D—1100°C, E—1200°C.
 (curves A, B and C not corrected for vaporization of WO₃)

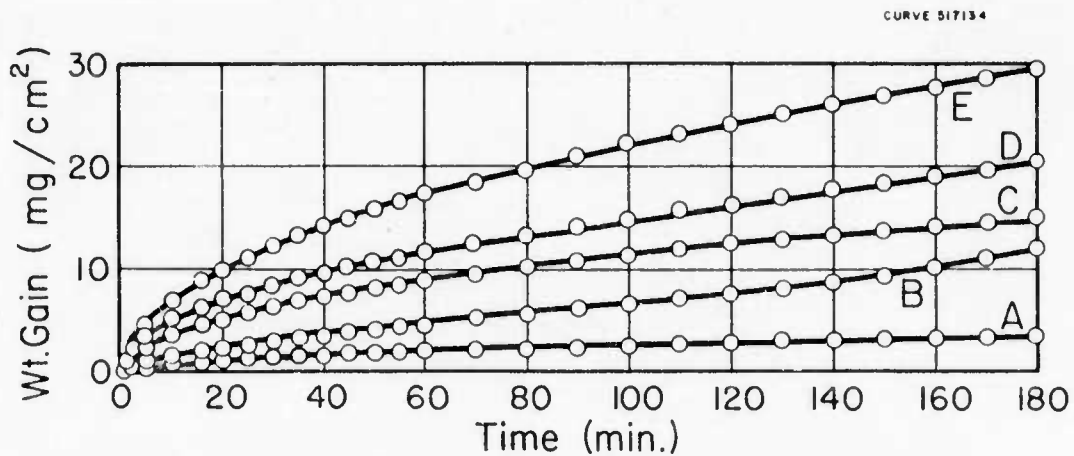


Fig. 10—Effect of temperature on oxidation of 50W-50Ta alloy.
 800°C-1200°C - 7.6 cm of Hg of O₂
 A-800°C, B-900°C, C-1000°C,
 D-1100°C, E-1200°C.
 (curves A, B, C, D and E not corrected for vaporization
 of WO₃)

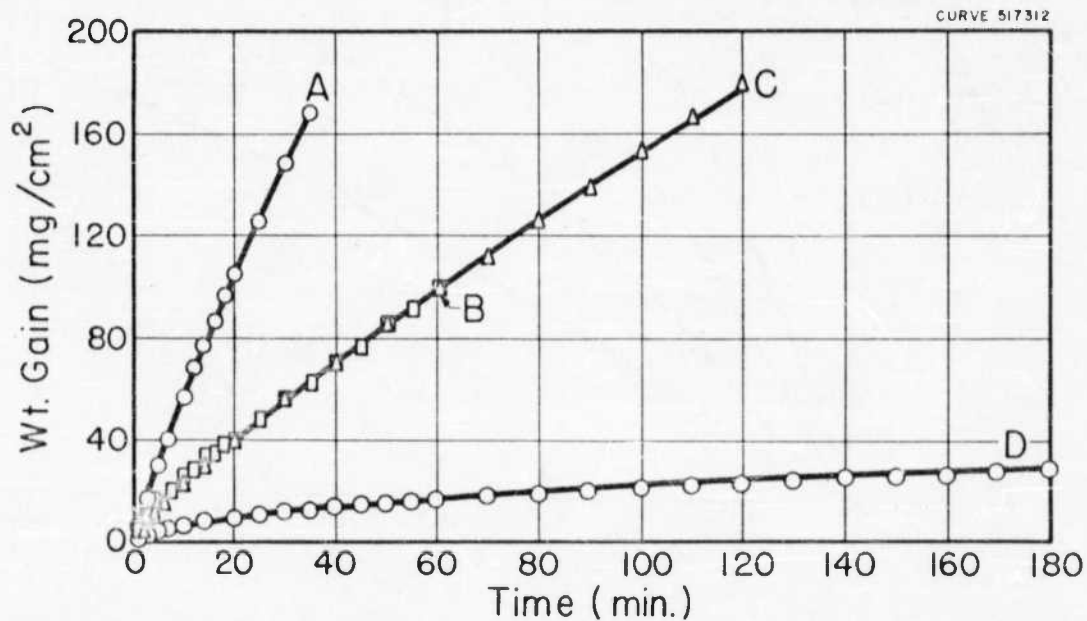


Fig. II—Oxidation of W and W-Ta alloys, 1200°C, 7.6 cm of Hg of O₂.
 A—Pure W, B—90W-10Ta, C—75W-25Ta, D—50W-50Ta.
 (curve D not corrected for vaporization of WO₃)

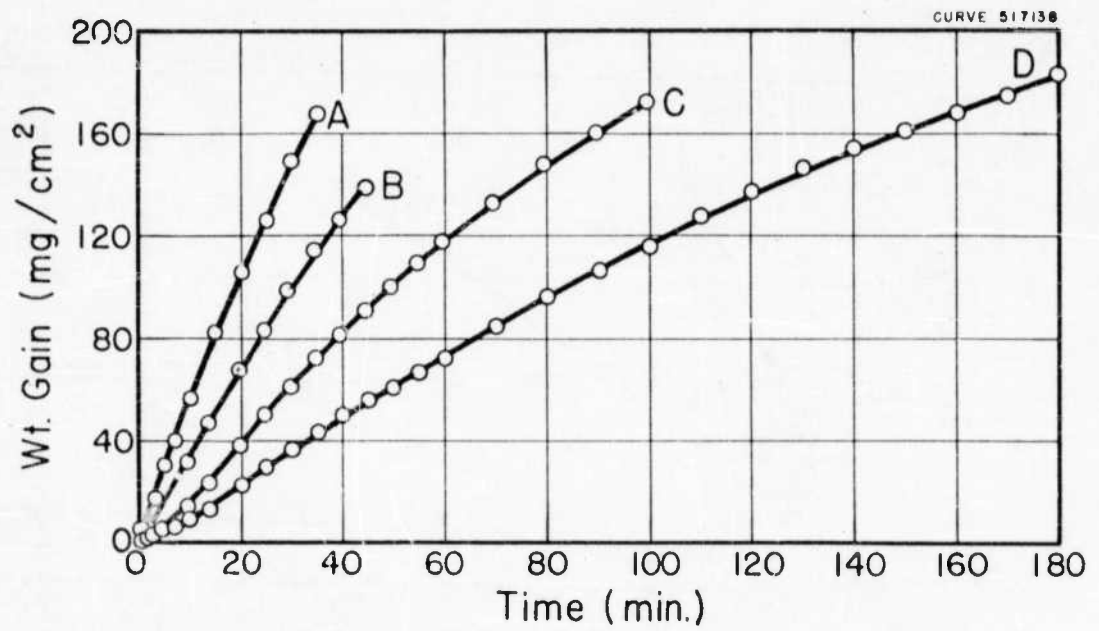


Fig. 12—Effect of pressure on oxidation of tungsten, 1200°C,
 7.6 cm—0.76 cm of Hg of O₂.
 A—7.6 cm, B—3.8 cm, C—1.9 cm, D—0.76 cm.

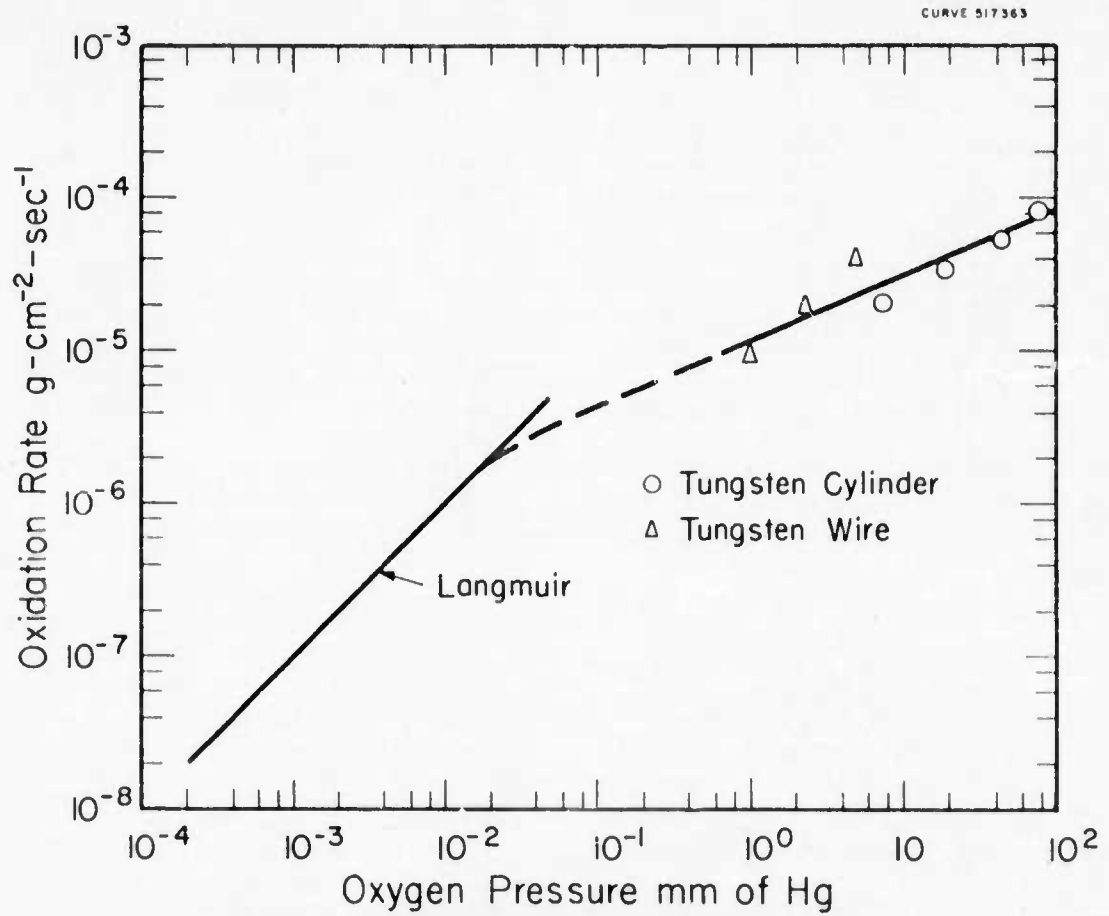


Fig.13-Oxidation rate versus oxygen pressure at 1200°C.

TABLE 9

Effect of Pressure on Oxidation of Tungsten-1200°C

O ₂ Pressure cm of Hg	^a Wt. Gain (mg/cm ²) at Time (min)			
	30	60	120	180
7.6	^b 149	---	---	---
3.8	99	---	---	---
1.9	61.5	118	---	---
0.76	37	73	138	187

^aCorrected for Wt. loss due to vaporization of WO₃ by calculation.^bCorrected from vaporization curve for WO₃. (See Figure 7).

2. X-ray Study

The scales on selected specimens were examined by X-ray diffraction. A 9 cm Unicam camera with Ni K_α radiation was used. The d-spacings are plotted in Figures 14 through 16. In each case the d-spacings and intensities of the unknown oxide are compared to: 1) Magneli's¹⁹ values for the low temperature form of WO₃, 2) Magneli's²⁰ values for W₁₈O₄₉ and, 3) X-ray data obtained in this research from a sample believed to be a mixed oxide with composition Ta_{0.56}W_{1.44}O_{2.72}. The values for Ta₂O₅ were not included since the agreement with these lines was not as good as for the three chosen. X-ray spectra of the loose outer oxide removed from two samples of 90W-10Ta are presented in Figure 14. Samples of oxide scale from the outside surface and from material next to the 75W-25Ta alloy were used for the diffraction lines shown in Figure 15. The surface scales from two 50W-50Ta samples were used for the lines given in Figure 16. All of the above samples were heated at temperature in a vacuum from 10 to 15 minutes after the conclusion of the oxidation run. This may have resulted in partial reduction of the oxide scales by their reaction with the underlying metal. We have shown in the vapor pressure measurements that equilibrium is not readily established in the solid phase below a temperature of 1200 to 1250°C. This may account for the failure to find identifiable phases.

Although the patterns were similar to those of tungsten oxides, no clean-cut identification could be made. Significant differences in number, position and intensity of lines were observed. No oxides of tantalum could be identified although spectrographic analysis of the scales showed tantalum was present up to as much as 60 per cent. The results of the analysis are shown in Table 10. This evidence seems to indicate the scales are a complex oxide such as W_xTa_yO_n in which tantalum has replaced tungsten.

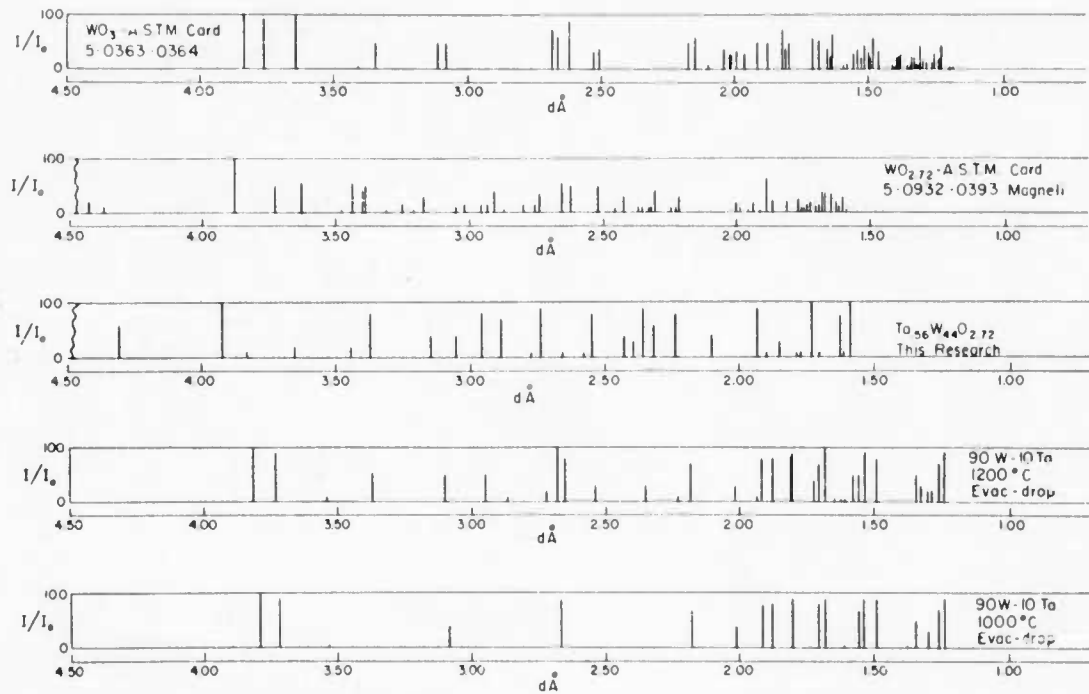


Fig. 14 -- X-ray diffraction data of 90W-10Ta oxide vs standard patterns

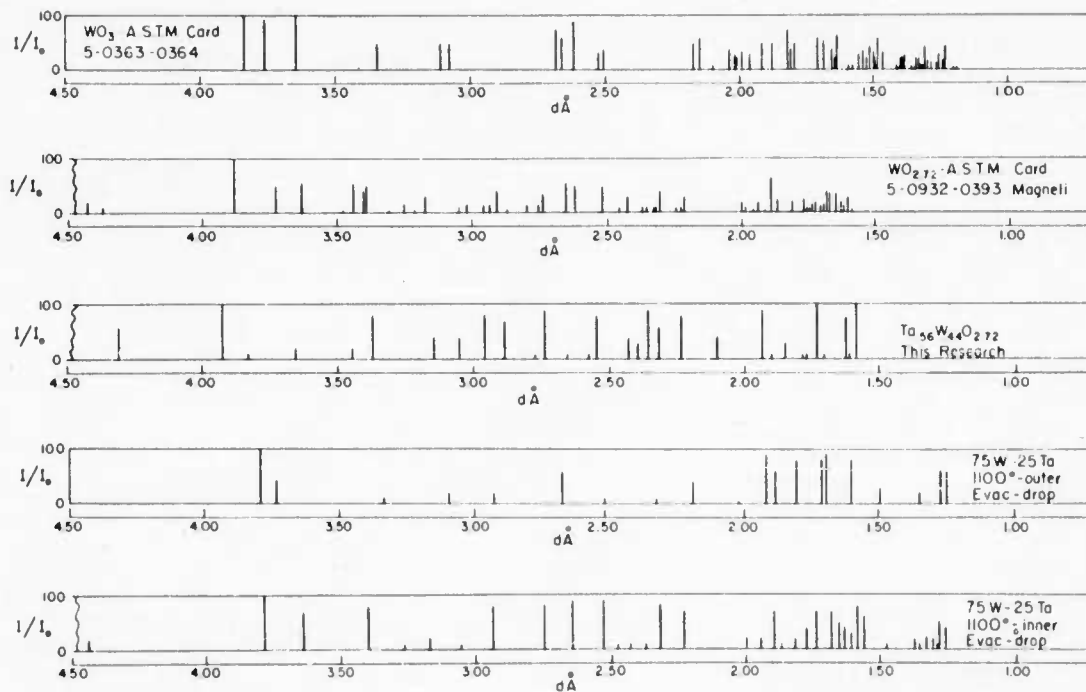


Fig. 15 --X-ray diffraction data of 75W-25Ta oxide vs standard patterns

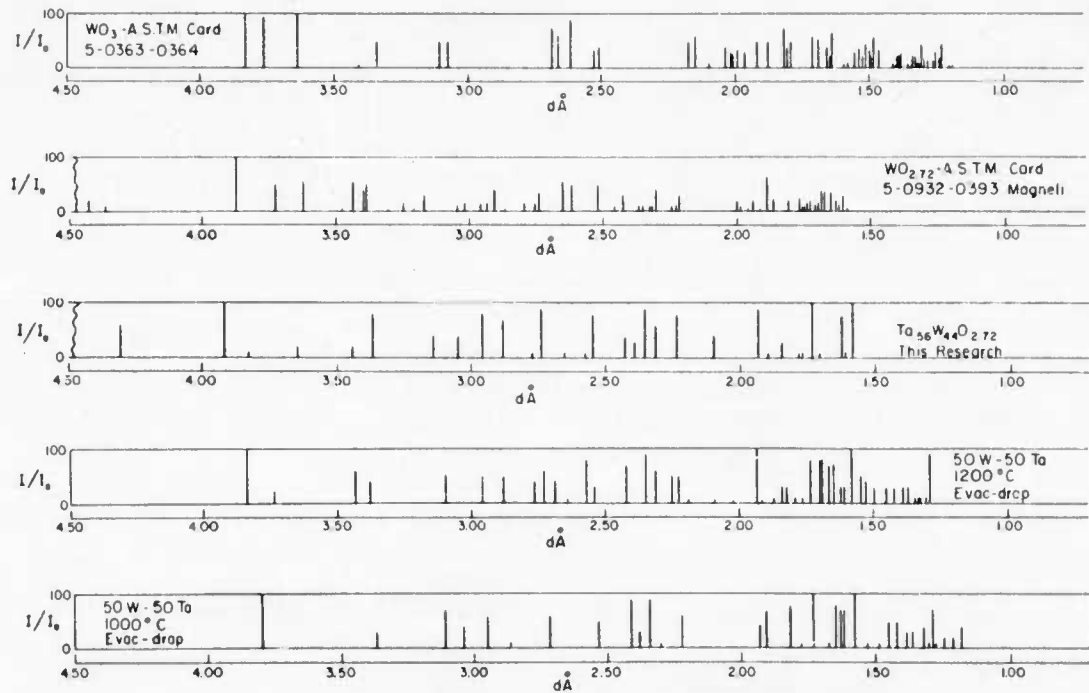


Fig. 16 -- X-ray diffraction data of 50W-50Ta oxide vs standard patterns

TABLE 10

Spectrographic Analysis of Oxide Films

Specimen	Oxidation			a% Ta Analytical	b% Ta Calculated
	Temp. °C	Wt. Change* mg/cm ²	WO ₃ Loss mg/cm ²		
90W-10Ta	1100	62.3	5.7	16.0	7.8
90W-10Ta	1200	47.5	51.0	24.5	7.8
75W-25Ta	1100	58.8	3.3	39.2	19.6
75W-25Ta	1200	38.9	141.1	53.5	19.6
50W-50Ta	1200	29.2	--	60.0	39.8

^aError estimated 10-20 per cent of amount present.

^bPer cent Ta assuming Ta-W ratio in oxide same as in alloy.

*Uncorrected for evaporation.

3. Metallographic Study

Random specimens were chosen for metallographic examination. The results are shown in Figures 17 through 19, and Table 11 summarizes the information. No conclusive interpretations can be made from these few results. Worthy of note is the lack of penetration by the oxide along crystallographic planes of the metal.

TABLE 11

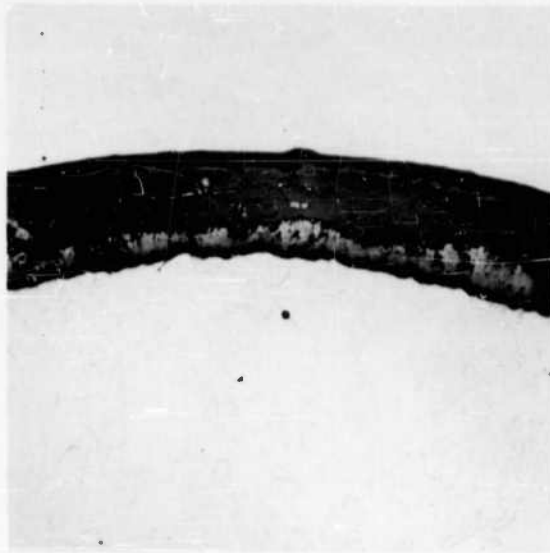
Metallographic Examination of Oxidized W and W-Ta Alloys

Specimen	Oxidation		Metallographic Results and Oxide Phases Present
	Temp. °C	Wt. Change mg/cm ²	
W	1100	116.8*	3 Phases-No metal penetration
W	1200	168.6*	2 Phases-Slight metal penetration
90W-10Ta	1100	68.0*	1 Phase-Metal penetration
75W-25Ta	1100	99.6*	1 Phase-No metal penetration
50W-50Ta	1200	29.2	2 Phases-No metal penetration

*Corrected for vaporization of WO₃.

DISCUSSION - MICROBALANCE SYSTEM

The equation $W^n = kt$ was used to describe the rate of oxidation where W = weight gain, k = oxidation rate constant, t = time and n = slope of logarithmic plot of the

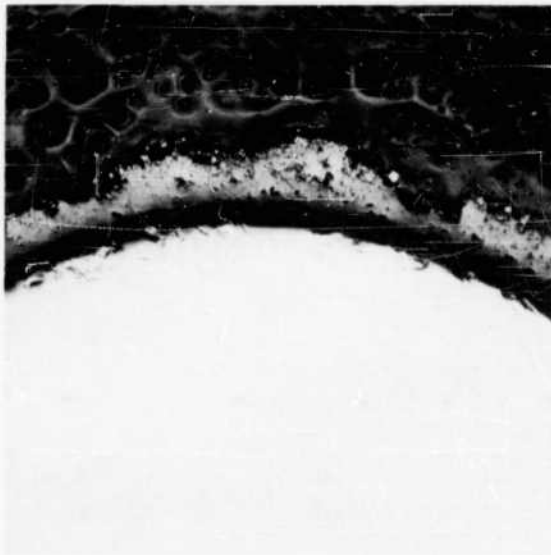


100X

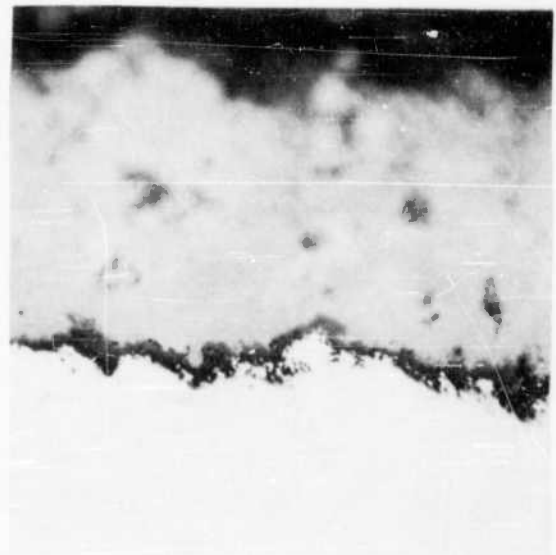


500X

1100°C, 25 min.



100X



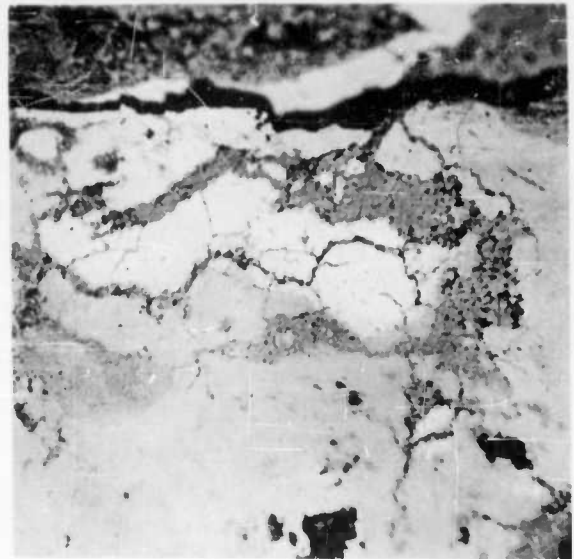
500X

1200°C, 35 min.

Fig. 17 -- Photomicrographs of metal-oxide interfaces, pure tungsten

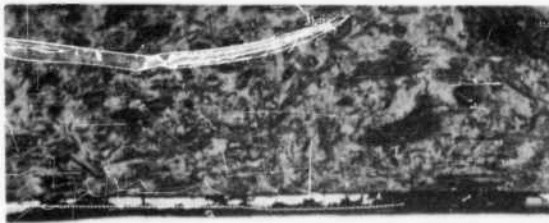


100X



500X

90W-10Ta, 1100°C, 85 min.



100X



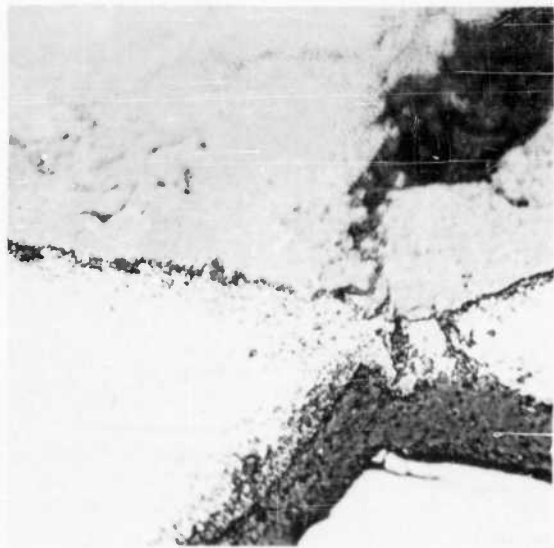
500 X

75W-25Ta, 1100°C, 100 min.

Fig. 18 -- Photomicrographs of metal-oxide interfaces, 90W-10Ta and 75W-25Ta



100X



1200⁰C, 180 min.

500X

Fig. 19 --Photomicrographs of metal-oxide interfaces, 50W-50Ta

data. The type of oxidation is determined by the value of n . Parabolic oxidation rates give a value for n of 2 and for linear rates $n = 1$.

To determine values for n , logarithmic plots of weight gain vs time were made, and the slopes of the lines were determined. Figures 20, 21 and 22 show the plots for the 50W-50Ta, and 90W-10Ta alloys, respectively. The results are summarized in Table 12. The values for n indicate the oxidation of the alloys is not readily characterized by either the parabolic or linear rate laws. However, the 90W-10Ta and 75W-25Ta samples appear to oxidize at a rate which is almost linear while the 50W-50Ta specimens oxidize at a rate which is nearly parabolic. The latter data has not been corrected for WO_3 weight loss.

Figure 23 shows the effect of temperature on the linear rate constants of the three W-Ta alloys. The lines were determined by a least squares fit.

TABLE 12

Summary of Kinetic Data for Oxidation of W Alloys, 7.6 cm of Hg of Oxygen

Temp. °C	Linear Rate Constant, mg/cm ² /sec			Exponential Constant - n		
	90W-10Ta	75W-25Ta	50W-50Ta	90W-10Ta	75W-25Ta	50W-50Ta
800	---	---	0.167	---	---	1.70
900	3.98	1.33	0.889	1.03	1.40	1.45
1000	6.67	3.34	0.945	1.14	1.33	1.93
1050	6.89	7.61	---	1.13	1.16	---
1100	12.9	13.32	1.14	1.18	1.04	2.06
1200	23.22	22.78	1.50	1.34	1.21	1.91

EXPERIMENTAL - PRESSURE MEASURING SYSTEM

The experimental results of this study and our earlier study have shown that weight change methods give an incomplete picture of the oxidation reaction when both oxidation and volatilization of the oxide occur. To overcome this difficulty an oxygen consumption method was devised. The apparatus was designed to measure oxygen consumption by measuring the rate at which the pressure in a reservoir at 1 atmosphere decreased as oxygen was bled through a leak valve into the reaction system. The pressure in the reaction system could be maintained at a constant value between 5 and 75 mm of Hg pressure. Figures 24 and 25 show the apparatus. Essentially the microbalance assembly was replaced by a calibrated vessel and three Wallace and Tiernan pressure gauges.

In Figure 26 gauge 0-5080 measures the pressure in the calibrated reservoir at the beginning of the experiment and in the entire calibrated volume during the course of the experiment. The smaller gauges 0-50 and 0-400 measure the pressure at which the tungsten is reacting. The oxygen enters the reaction system through the variable leak metering valve designated 3.

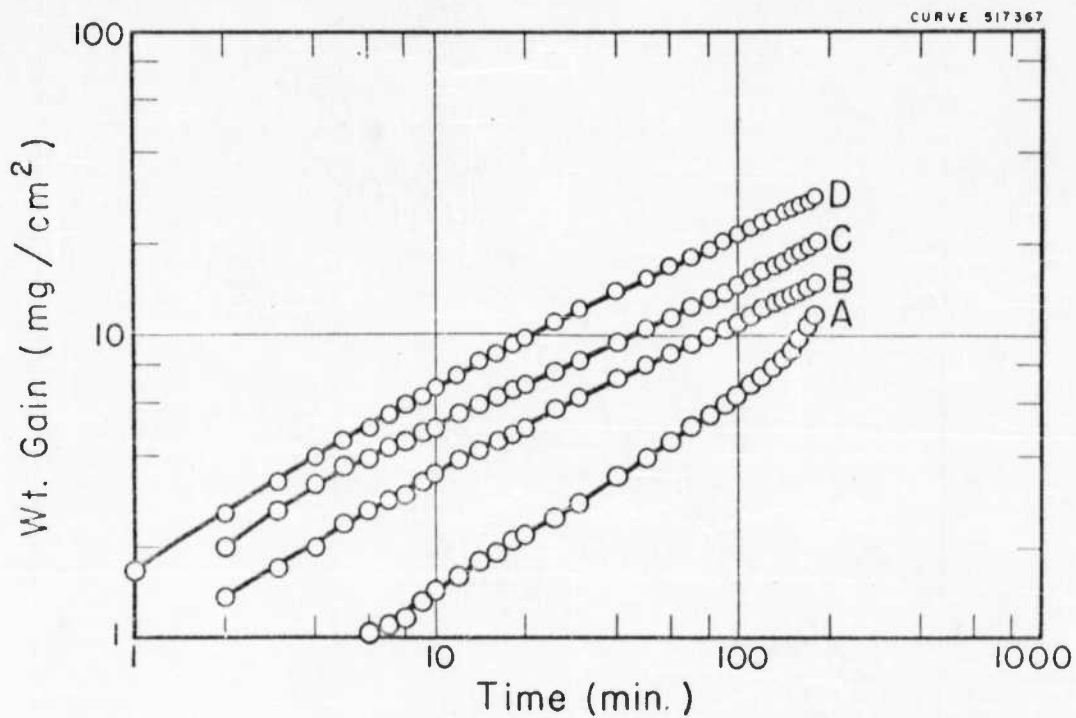


Fig.20-Effect of temperature on oxidation of 50W-50Ta alloy, 900°C-1200°C, 7.6 cm of Hg of O₂.

A-900°C, B-1000°C, C-1100°C, D-1200°C.

(above curves not corrected for vaporization of WO₃)

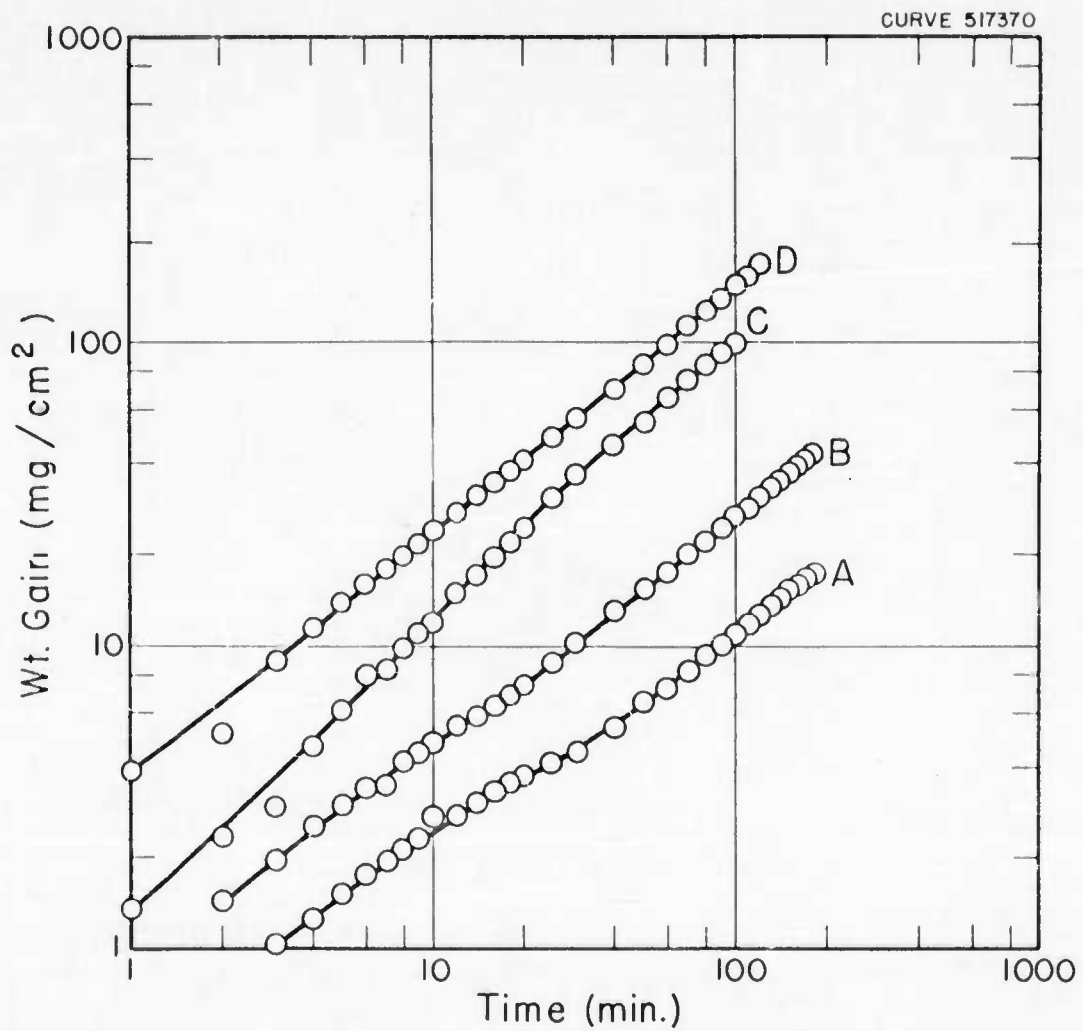


Fig.21 - Effect of temperature on oxidation of 75 W-25 Ta alloy, 900°C-1200°C 7.6 cm of Hg of O₂.
 A-900°C, B-1000°C, C-1100°C, D-1200°C.
 (curves A and B not corrected for vaporization of WO₃)

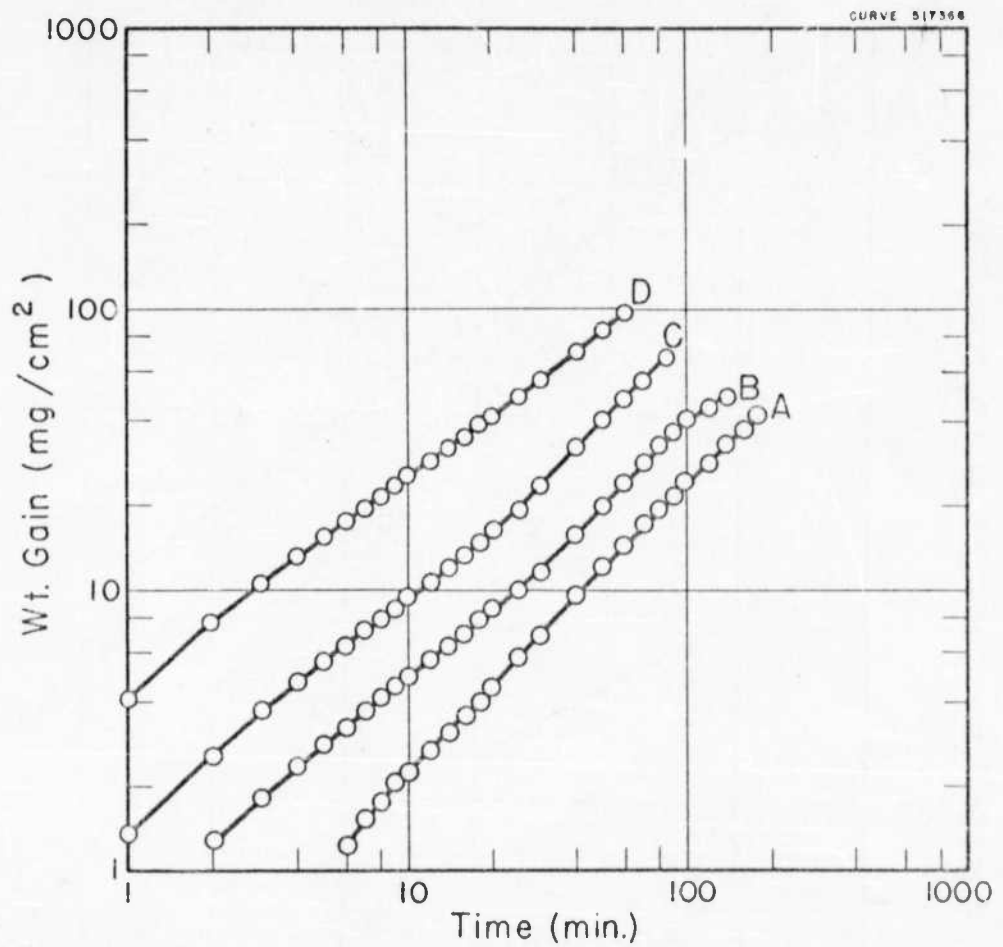


Fig.22- Effect of temperature on oxidation of 90W-10Ta alloy,
 900°C-1200°C, 7.6 cm of Hg of O₂.
 A-900°C, B-1000°C, C-1100°C, D-1200°C
 (curves A and B not corrected for vaporization of WO₃)

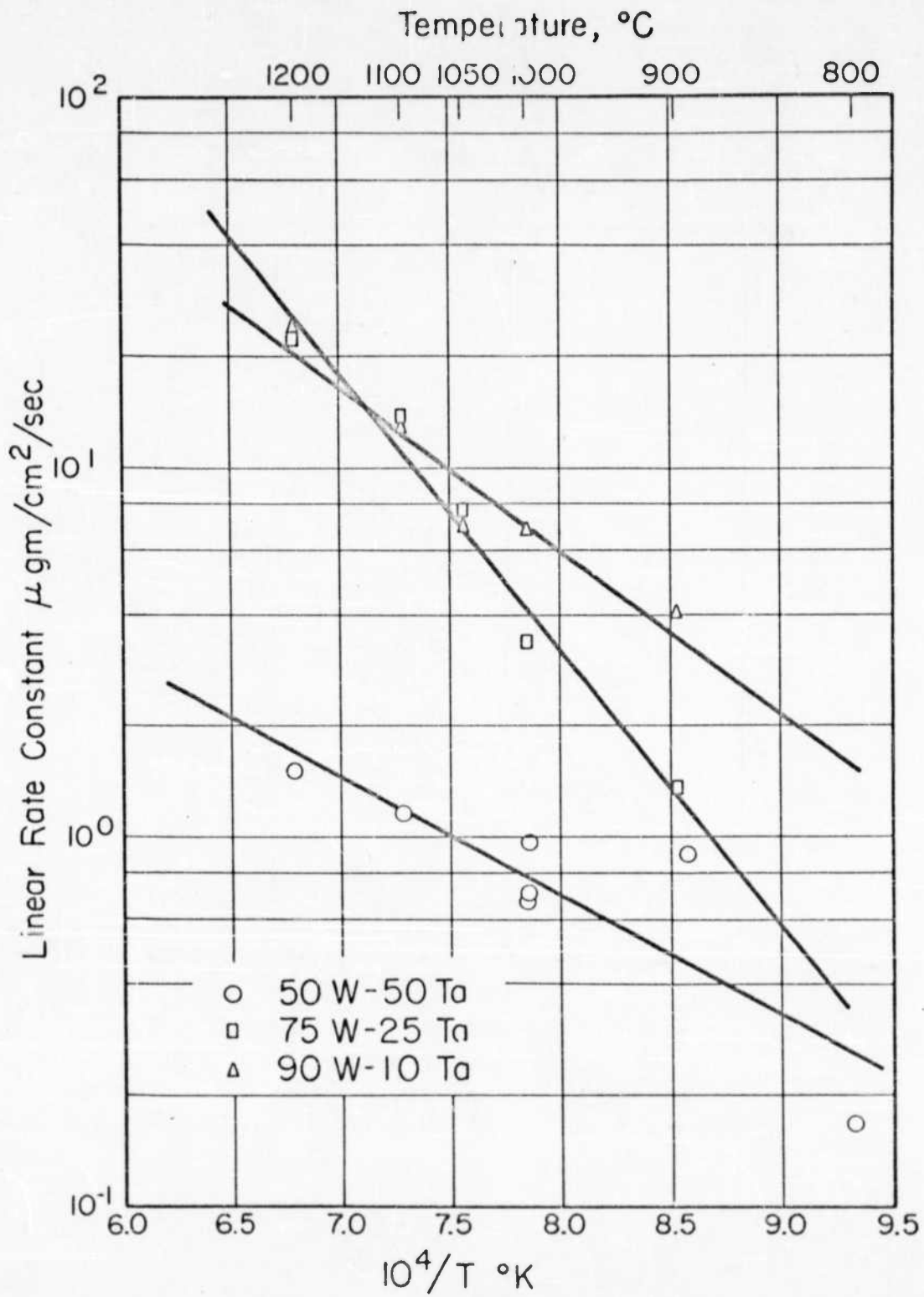


Fig.23-Effect of temperature on linear rate constants for oxidation of W-Ta alloys.

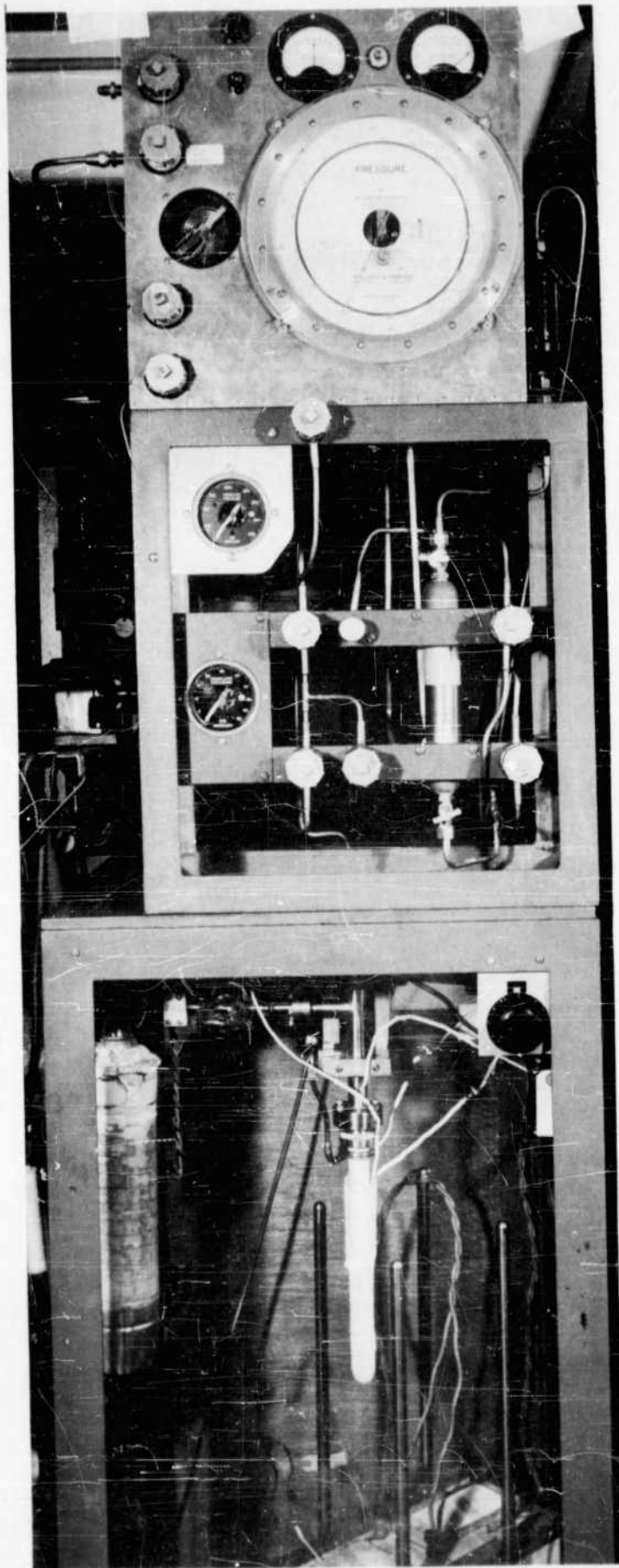


Fig. 24 --Pressure measuring device

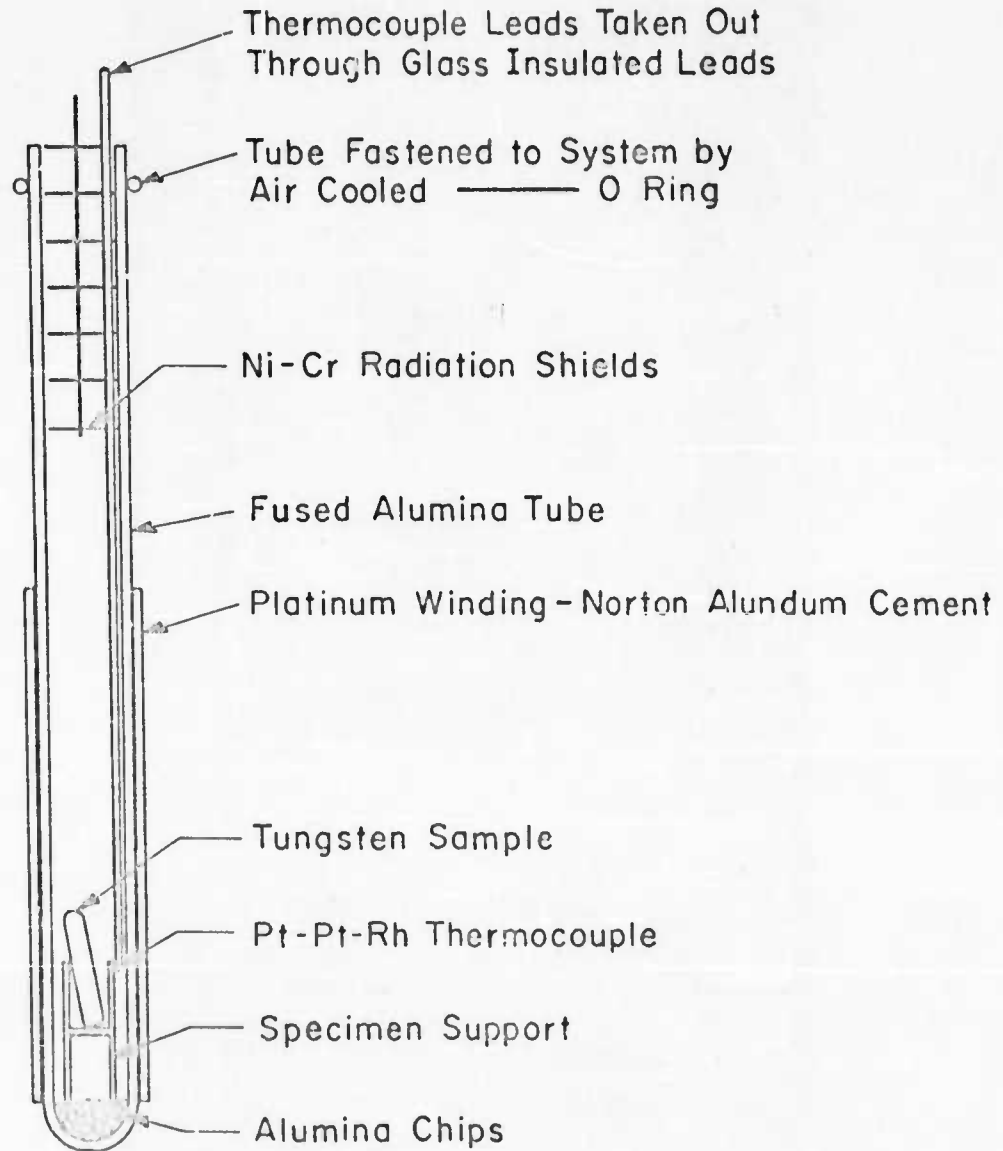


Fig.25-Details of furnace tube and sample support.

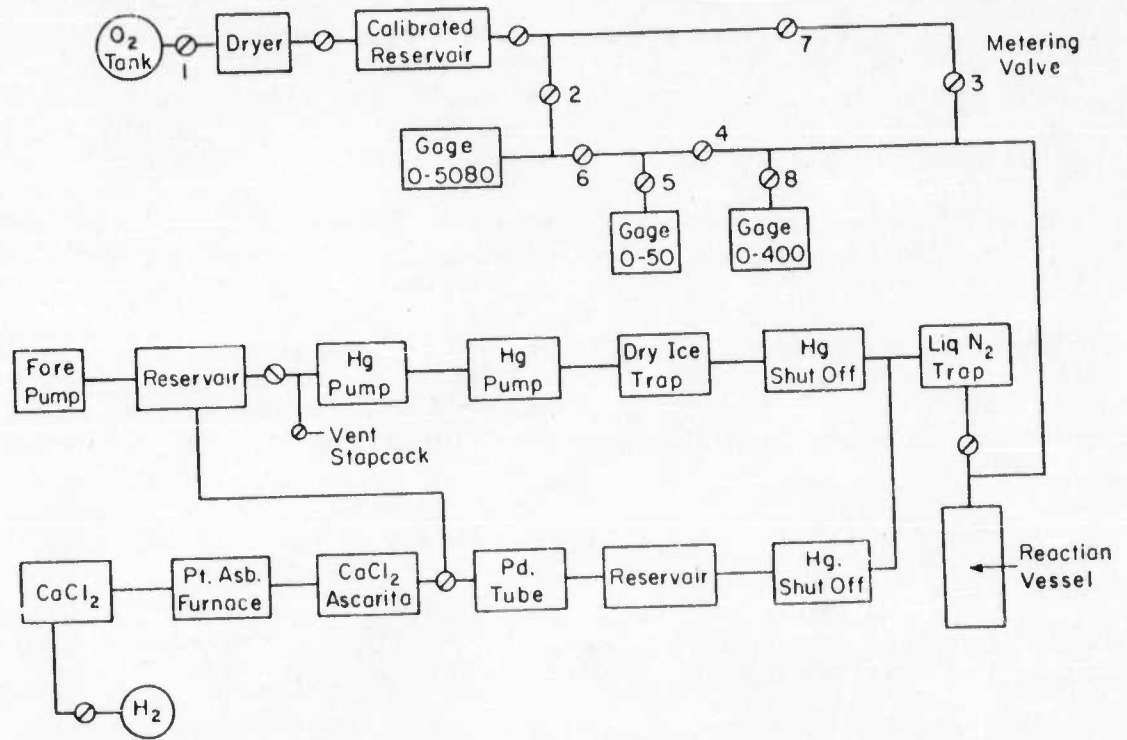


Fig. 26-Schematic diagram reaction system.

The sample and tube details are shown in Figure 25. The alumina tube which contains the sample is attached to the vacuum system by means of flanges and rubber O-rings. An alumina support is used to hold the samples. The furnace temperature is maintained to $\pm 1.5^{\circ}\text{C}$ by the use of a calibrated high sensitivity controller and a calibrated Pt-Pt + 10 per cent Rh thermocouple.

The samples were machined from high purity rod. They were then polished through 4/0 emery paper and washed with petroleum ether and absolute alcohol. The ends were rounded to reduce edge effects noted in the past. The specimens weighed about 9.0 gms and had surface areas of approximately 3.9 cm^2 .

During a typical experiment a known pressure of oxygen was placed in the reservoir. The specimen was heated to temperature by means of a box resistance furnace raised around the tube and the platinum furnace wrapped on the tube. At a predetermined temperature the desired pressure of oxygen was admitted to the reaction vessel. This pressure was read periodically on gauges 0-50 or 0-400 shown in Figure 26.

The flow of oxygen from the storage reservoir to the reaction vessel to maintain a constant reaction pressure was controlled manually by means of the variable leak valve 3 in Figure 26.

In a typical analysis of an experiment, let P_i be the pressure in the storage system having in this case a total volume of 258.1 cc. Let P_r be the pressure in the reaction system having a volume of 372.2 cc. P_i must first be corrected for the dilution effect caused by expansion into the reaction vessel. This is done by means of the formula

$$P_i V_o = P_d V_o + P_r V_r \quad (18)$$

where P_d is the dilution pressure in the reservoir, P_i is the initial pressure in the reservoir, P_r is the reaction pressure, V_o is the original volume; and V_r is the reaction volume. Rearranging the above equation gives

$$P_d = P_i - P_r \frac{V_r}{V_o} \quad (19)$$

For a reaction pressure of 13.6 mm a correction of 22 mm is calculated. In order to determine gas/cm^2 of oxygen reacting ΔP is read from gauge 0-5080 in Figure 30 and corrected. For a sample with a surface area of 3.89 cm^2 a pressure change in the reservoir of 1 mm is equivalent to a weight gain of $1.119 \times 10^{-4}\text{ gm/cm}^2$ of oxygen consumed. Therefore, $1.119 \times 10^{-4} \Delta P = \text{gas/cm}^2$ of oxygen reacting.

RESULTS

1. Kinetic Study

A. Effect of Temperature

Figure 27 shows preliminary oxidation curves for the oxidation of tungsten at

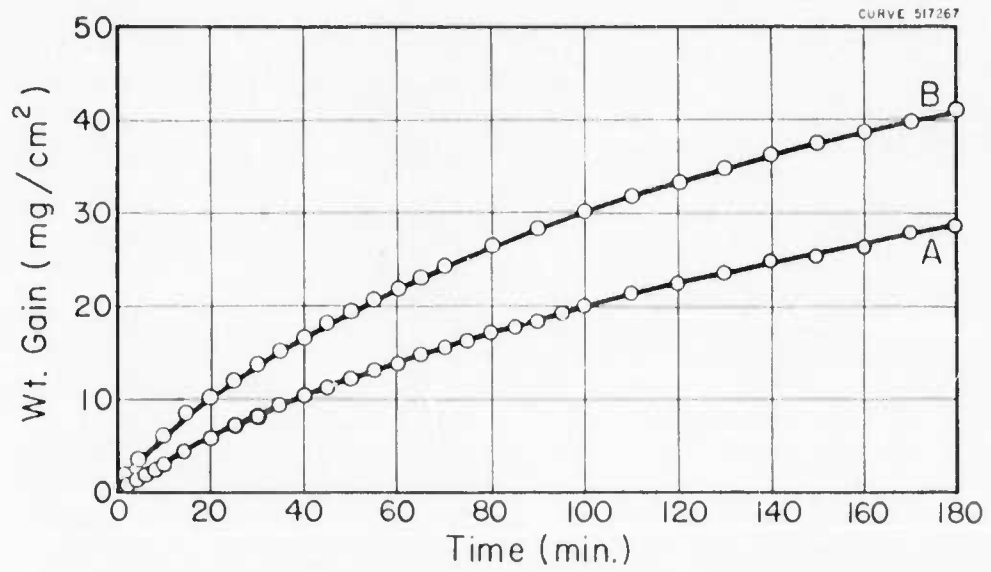


Fig.27-Effect of temperature on oxidation of tungsten 1200°-1250°C,
 0.5 cm of Hg of O₂.
 A-1200°C, B-1250°C.

1200 and 1250°C at 0.5 cm of Hg of oxygen. The oxidation curves indicate the rate of oxidation is decreasing with time. Figure 28 from our earlier study shows the oxidation of wire samples from 1200 to 1300°C at a pressure of 1 mm of Hg of oxygen as determined by the microbalance method. The microbalance method indicates the difference between oxygen consumption and loss of WO_3 from the oxidized sample. The pressure method indicates only oxygen consumption. Figures 27 and 28 should not be used for precise calculations since the oxygen pressure was not the same. With the wire specimens shown in Figure 28 most of the tungsten was oxidized, while in the rod specimens shown in Figure 27, only a small fraction of the sample was reacted.

DISCUSSION - PRESSURE CHANGE METHOD

Although a number of experiments were made with this apparatus, experimental difficulties were encountered. The variable leak valves available were found to be inadequate for controlling the pressure in the reaction system. This made it difficult to obtain good experimental data.

It was also found that tungsten should not be in contact with alumina or other ceramic materials at temperatures above 1100°C. Tungsten trioxide solid and alumina appear to form a eutectic mixture with a melting point below 1200°C. This difficulty was overcome by using a platinum liner in the alumina furnace tube.

Tungsten trioxide vapor was found to react with the alumina furnace tube as shown by a discoloration of the tube. After an appreciable exposure of the tube to tungsten trioxide vapor the furnace tube was found to crack and to leak.

The pressure change method is probably satisfactory for the study of fast oxidation reactions especially when used in conjunction with the microbalance method. This will be tried in the future when better variable leak valves become available.

It also appears that if the temperature is to be extended upwards some way must be found to limit the reaction of tungsten trioxide with the ceramic furnace tube.

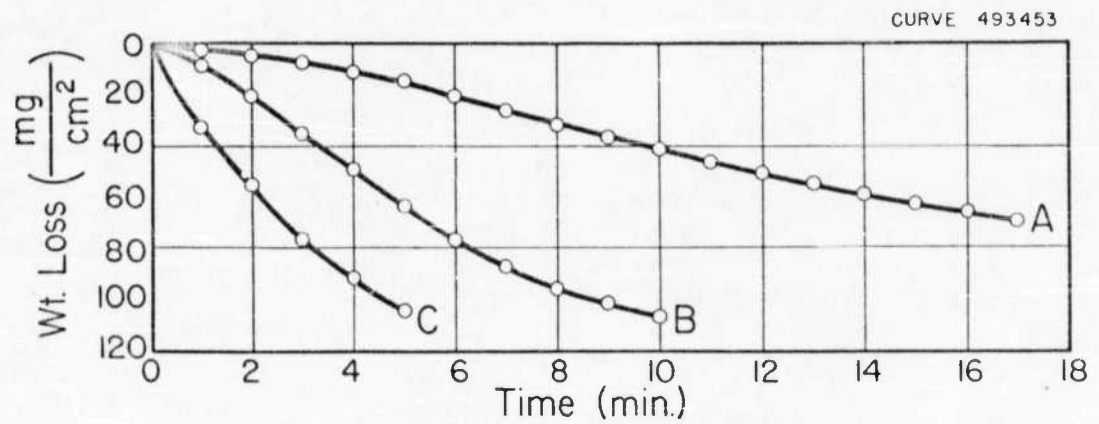


Fig.28-Oxidation of tungsten, wire sample, 1200°—
1300° C, 0.0013 atm. O₂, abraded, A — 1200° C,
B — 1250° C, C — 1300° C.

SECTION III. OXIDATION OF TUNGSTEN AT HIGH TEMPERATURES

APPARATUS

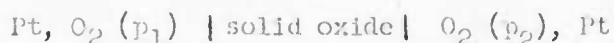
Since we have had difficulty measuring oxidation rates at temperatures above 1200° in the two systems described above, a third system was designed for these studies. This apparatus is shown in Figures 29 and 30. It consists of a water cooled Pyrex furnace tube in which the sample is held on the tip of an alumina thermocouple protection tube. The leads to the thermocouple are brought out through a press seal in the bottom of a ground glass cap which is fitted to the bottom of the furnace tube. Since the sample is heated inductively, the thermocouple leads are shielded to filter out induced r.f. current. The success of the filtering is demonstrated by the lack of change in the e.m.f. of the thermocouple when the induction furnace is turned on and off.

The sample, in the form of a pellet 0.5 inches in diameter and 0.75 inches long, is oxidized in a stream of argon and oxygen. The amount of gas flowing through the system is measured with a flow meter, and the concentration of oxygen in the gas exhaust is measured with the oxygen gauge described below. A glass wool plug keeps oxide powder from being swept through the oxygen gauge. A window protected by a shutter permits temperature measurement with an optical pyrometer.

The oxygen gauge is shown schematically in Figure 31. It consists of a gas tight stabilized zirconia tube through which the gas mixture is flowed. Platinum electrodes are sealed inside and outside the tube to measure the e.m.f. of the oxygen concentration cell. A thermocouple measures the temperature at the electrodes. Compressed air, flowed outside the tube, is used as the oxygen standard. The cell leads attached to the electrodes are shielded with 3 mil platinum sheet. The gauge is heated with a controlled furnace to between 800 and 1000°C to decrease the resistance of the zirconia tube, permitting a small current to be drawn from the cell.

The current from the oxygen cell is passed through a decade resistance box and into a Leeds and Northrup current amplifier. The output from the current amplifier is fed to a 10 MV recorder. This arrangement permits continuous recording of a wide range of voltages from the oxygen cell.

The oxygen cell was developed at this Laboratory by Weissbart and Ruka²¹. It embodies the principles of a concentration cell of the type



where the solid electrolyte is $(\text{ZrO}_2)_{.85}(\text{CaO})_{.15}$, the oxygen pressure p_1 is that flowing through the tube, and p_2 is the reference pressure, in this case, oxygen in air. The e.m.f. of the cell for the reaction



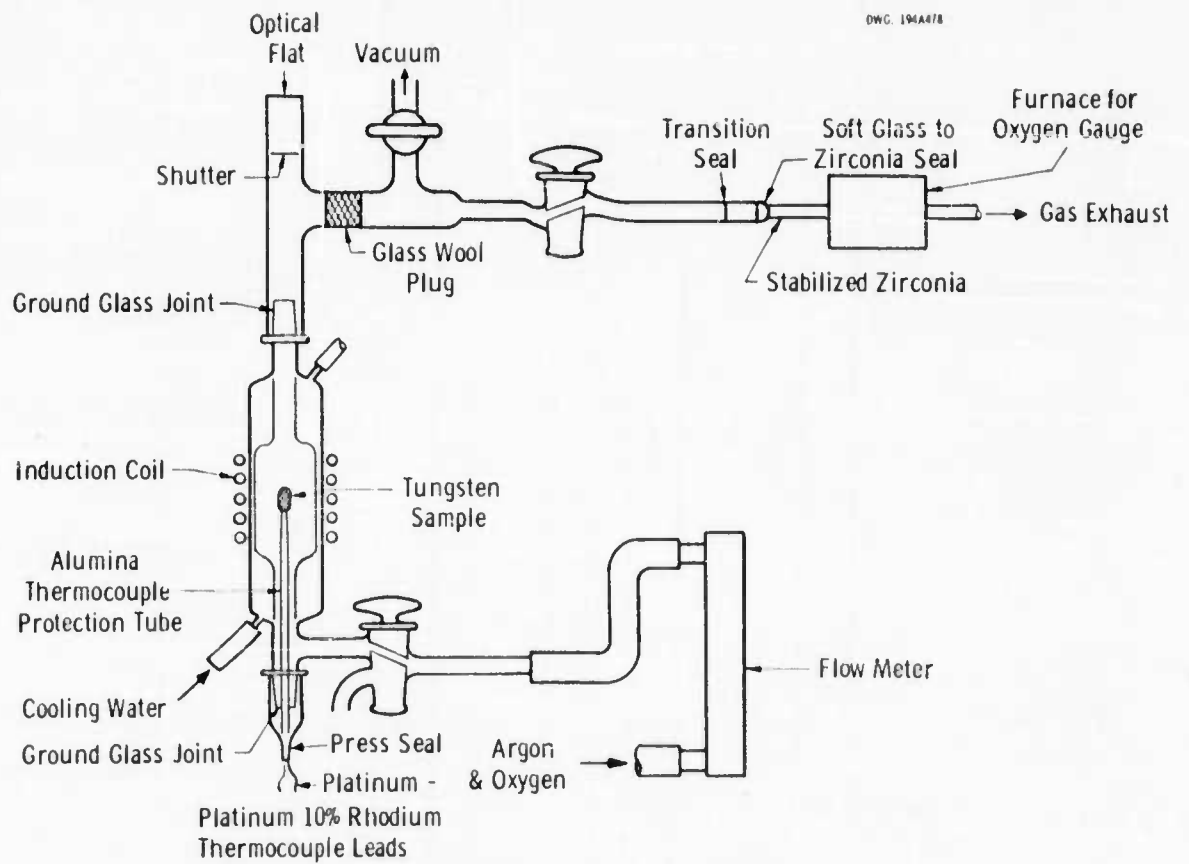


Fig. 29--System for high temperature oxidation measurements

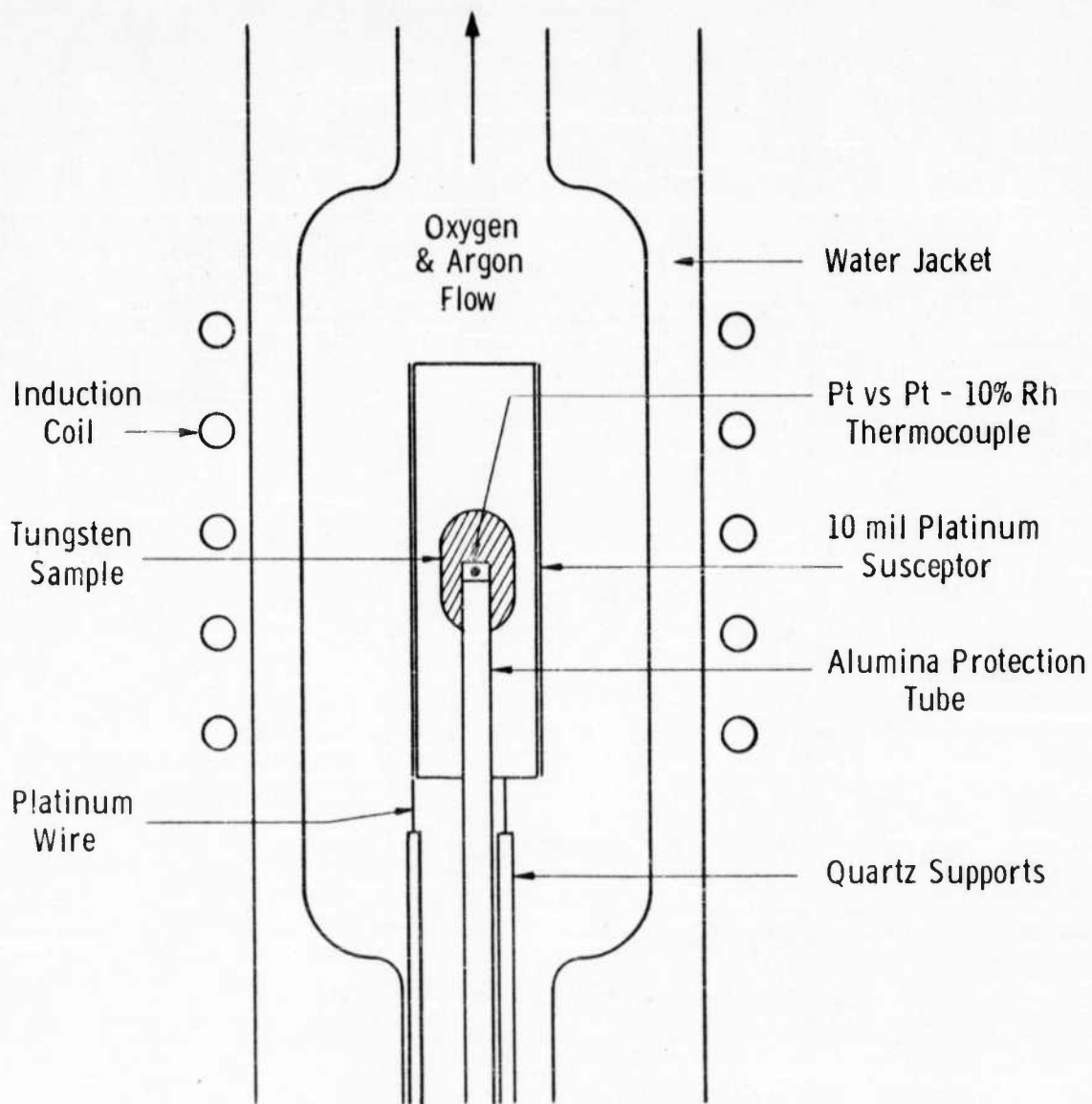


Fig. 30 --Furnace detail with platinum susceptor in place

DWG 2948928

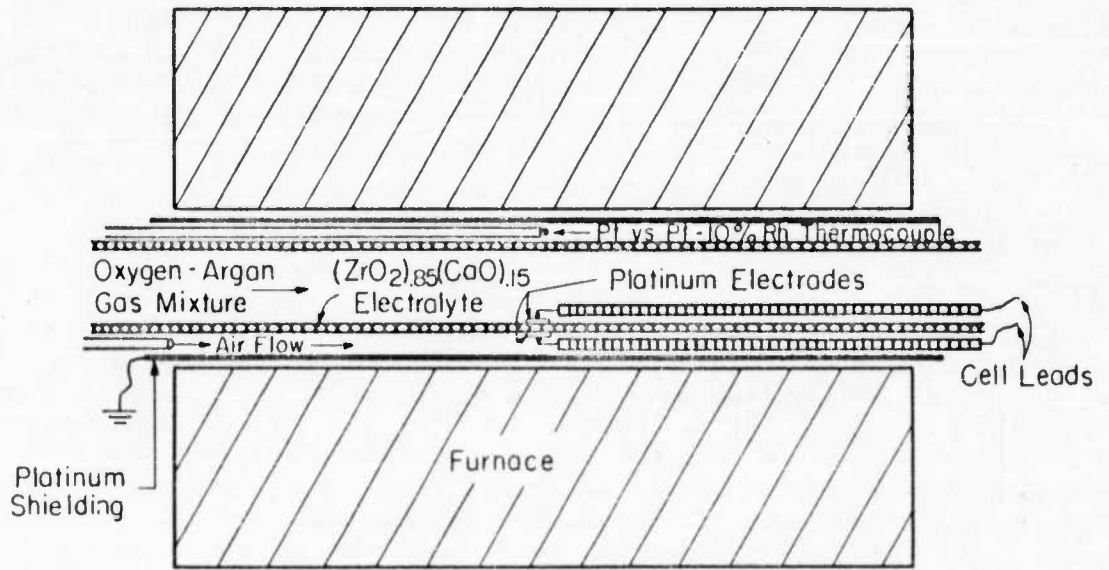


Fig.31—Oxygen gauge schematic diagram.

is

$$E = \frac{RT}{nF} \ln \frac{p_2}{p_1} = 4.96 \times 10^{-5} T \log \frac{p_2}{p_1} \quad (20)$$

In measurements made by Weissbart and Ruka the gauge showed a very small error ($< 1\%$) at 100 mm, the pressure measured here.

SAMPLES

The sample material was obtained in the form of ground 1/2 inch tungsten rods which had been formed by swaging sintered powder rods. The material was quite dense and free of pores. The principal impurities as determined from spectroscopic analysis are in ppm: Ca, 10; Cu, 40; Fe, 15; Si, 10; Mo, < 40 ; Nb, < 100 ; and Zr, < 40 . The rods were cut into 3/4 inch lengths, both ends were rounded by grinding, and holes were drilled approximately 2/3 of the way through for mounting them on the thermocouple tubes.

PROCEDURE

The samples were cleaned in NaOH, rinsed, dried, weighed, and placed inside the furnace. The furnace was evacuated and filled with argon. The sample was brought up to temperature and the argon-oxygen mixture was flowed over the sample. In some measurements the argon-oxygen mixture was flowed over the sample from the beginning. There was a lag between the time the sample started to oxidize and the time the oxygen-argon mixture reached the oxygen gauge. This lag was greater when argon was displaced by the mixed gases and, of course, it also depended on the flow rate. Flow rates less than 300 cc/min were found to require more than 8 minutes to displace the argon. High flow rates lowered the temperature of the gauge below the temperature measured with the thermocouple. At lower gauge temperatures this became more pronounced and was compensated for by measuring the e.m.f. of a known oxygen concentration and calculating the true temperature of the gauge for this flow rate.

During a measurement, the e.m.f. was recorded continuously, while the temperature and flow rate were controlled manually. The temperature was usually held to within $\pm 20^\circ$ while the flow rate was within $\pm 10\%$. These quantities were recorded and a mean temperature and flow rate were used to characterize each experiment.

At the conclusion of a measurement the sample was cooled in the flowing gas mixture.

RESULTS

Measurements were made using two procedures: 1) the sample was heated inductively in a stream of cold gas, 2) a platinum susceptor, as shown in Figure 30, was heated inductively and this in turn heated the sample and gas by radiation and convection.

The results of the experiments on the samples heated inductively between 800 and 1700°C are shown in Figures 32 and 33 and tabulated in Table 13. All but three of these measurements indicate a linear oxidation rate. The three deviates occurred at 1470, 1478 and 1698°C.

TABLE 13

Oxidation of Tungsten Samples in One Atmosphere of 21% O₂-79% Ar
Samples Heated Inductively

Temperature °C	Time Minutes	Rate g-cm ⁻² -sec ⁻¹ x 10 ⁶
807	35	5.83
808	92	3.80
1026	31	31.7
1218	38	63.3
1226	30	61.7
1470	27	233
1478	30	243
1698	25	347

Oxidation may be expressed by the equation

$$W^n = kt \quad (21)$$

where W is the weight gain of oxygen/cm², k and n are constants, and t is time. For a linear rate, the exponent n is 1, and for a parabolic oxidation rate, n is 2. The values of n for these three runs are: 1.25, 1.15, and 1.07. Since these numbers are closer to unity than they are to 2, the values may be considered to represent a linear rate.

Samples from these measurements are shown in Figure 34. The fact that the oxide grows either from the metal or from a very thin oxide layer next to the metal is suggested by the oxide structure on the sample oxidized at 1218°C. Here the oxide grows normal to the surface, leaving a ridge at the line where the ends are rounded. At higher temperatures the oxide forms a loose shell around the sample, as in the case of the 1666°C measurement. The oxide in this case apparently vaporizes from the metal condensing on the inside of the oxide shell. The ridge observed at lower temperatures is evidently filled by the condensing oxide gas.

Figures 35 and 36 present the results of measurements made with the samples heated by radiation from the inductively heated platinum susceptor. All but the measurement at 1396°C indicate linearity. The value of n for the deviating case is 1.14, or again the oxidation rate is quite close to being linear. The rate constants are tabulated in Table 14. Figure 37 shows oxidized samples after removal from the furnace. In some of the measurements heated by induction there was a reaction between

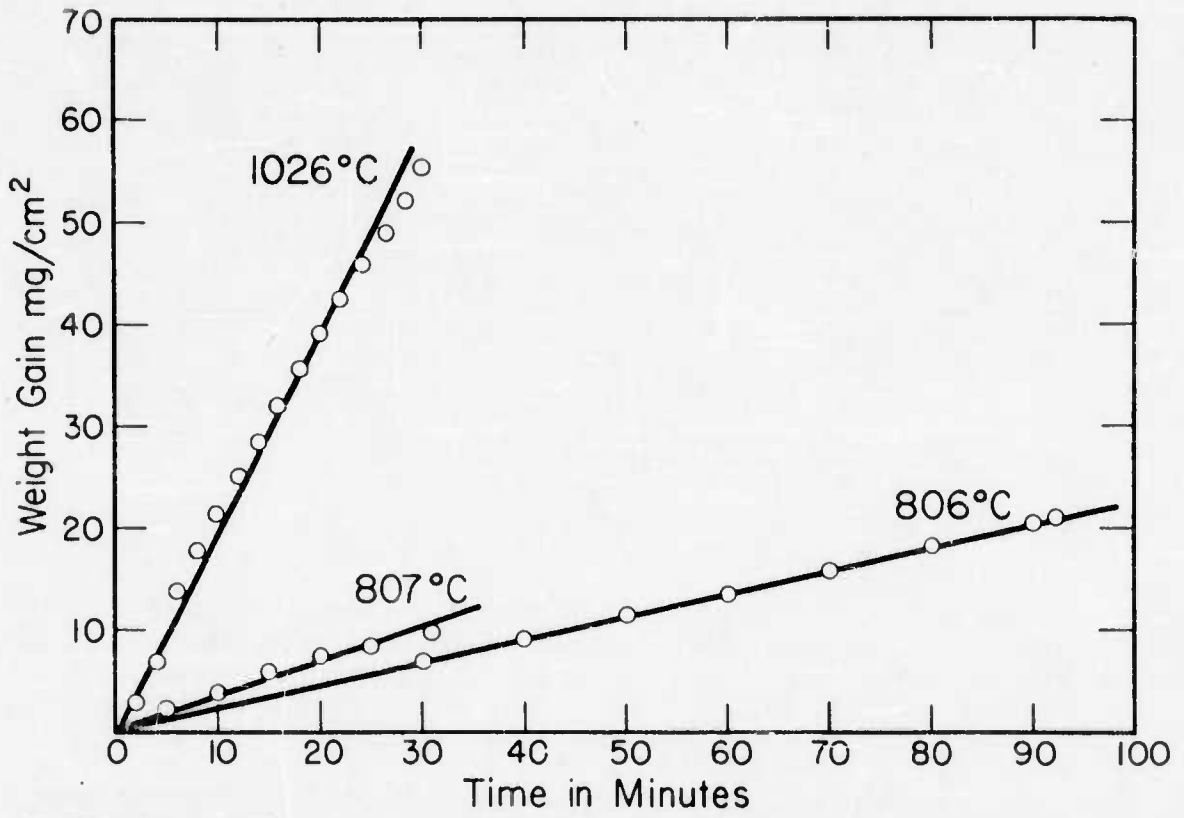


Fig.32 - Oxidation of tungsten in 21% O₂ - 79% Argon. Sample heated by induction.

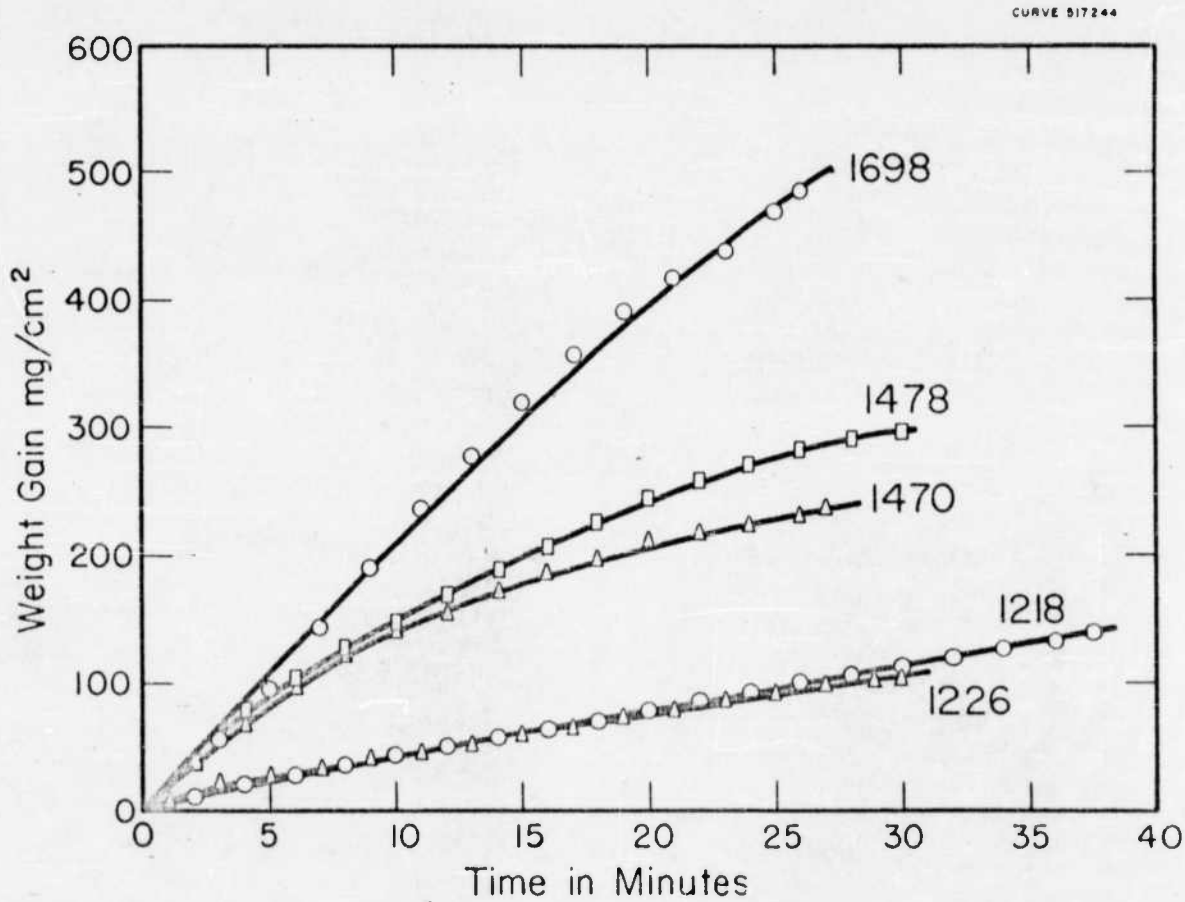
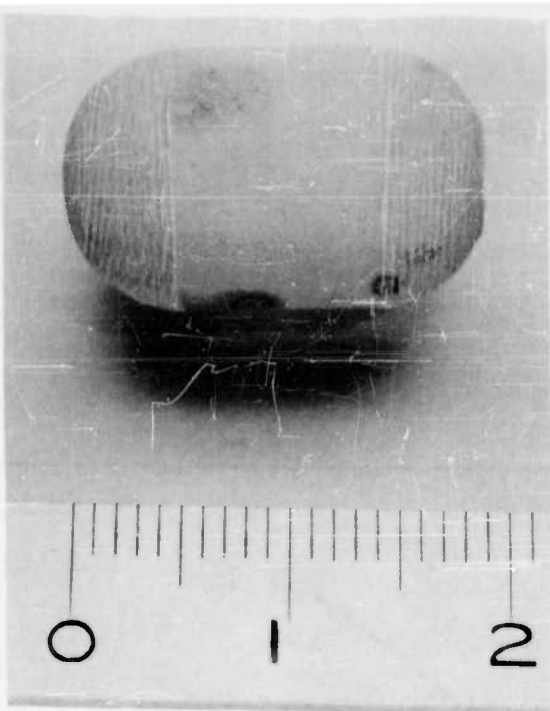
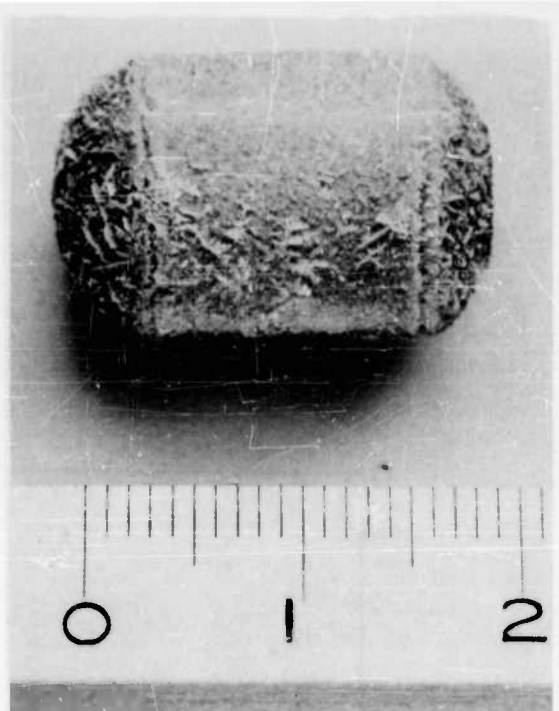


Fig.33- Oxidation of tungsten in 21% O₂ - 79% Argon. Sample heated by induction.



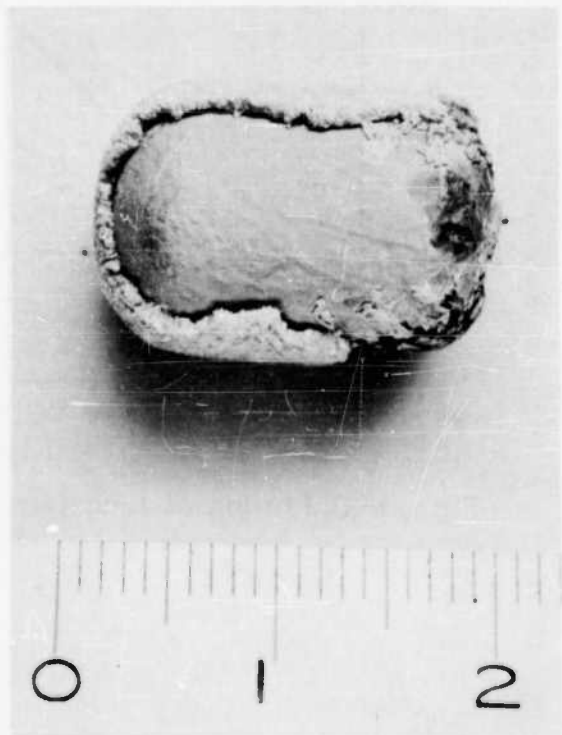
807⁰C - 92 min.



1218⁰C - 38 min.



1470⁰C - 27 min.



1666⁰C - 16 min.

Fig. 34-Tungsten oxidized in 21% O₂ - 79% Ar. Samples heated by induction

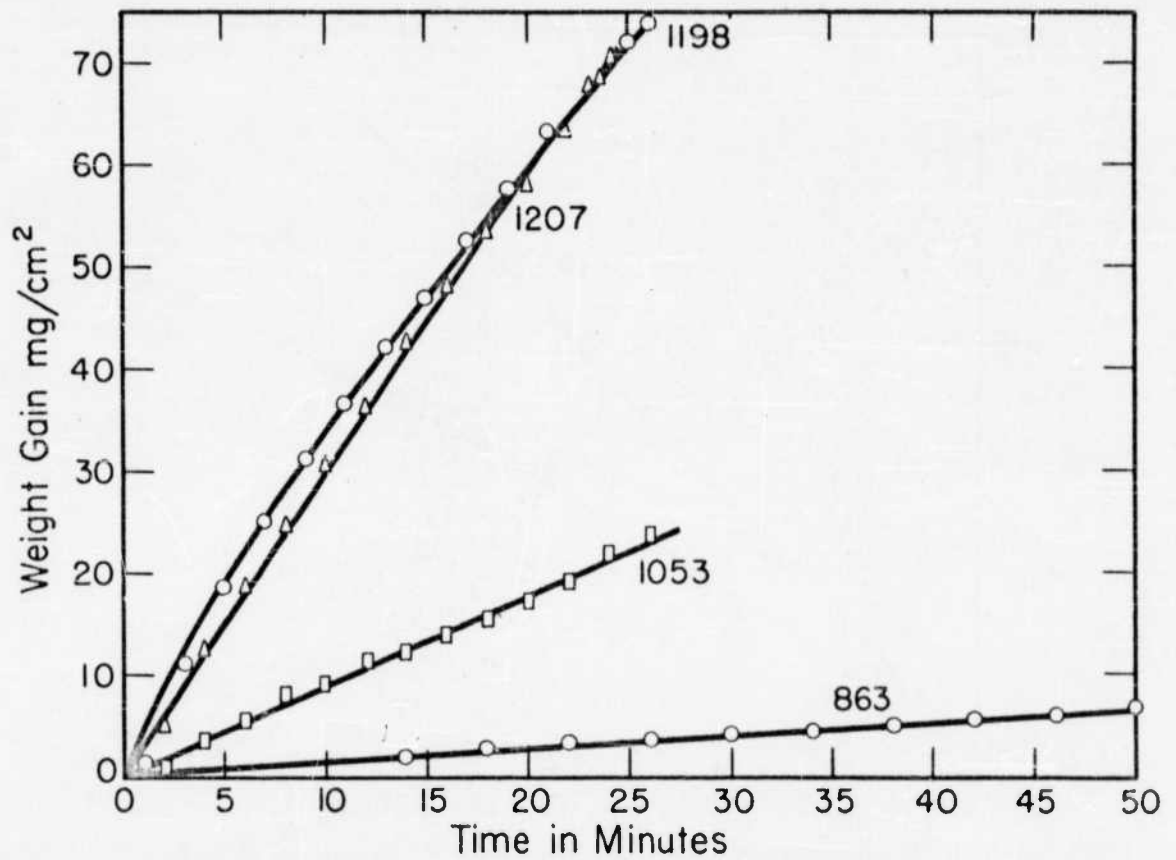


Fig. 35-Oxidation of tungsten in 21% oxygen - 79% Argon. Sample heated by radiation.

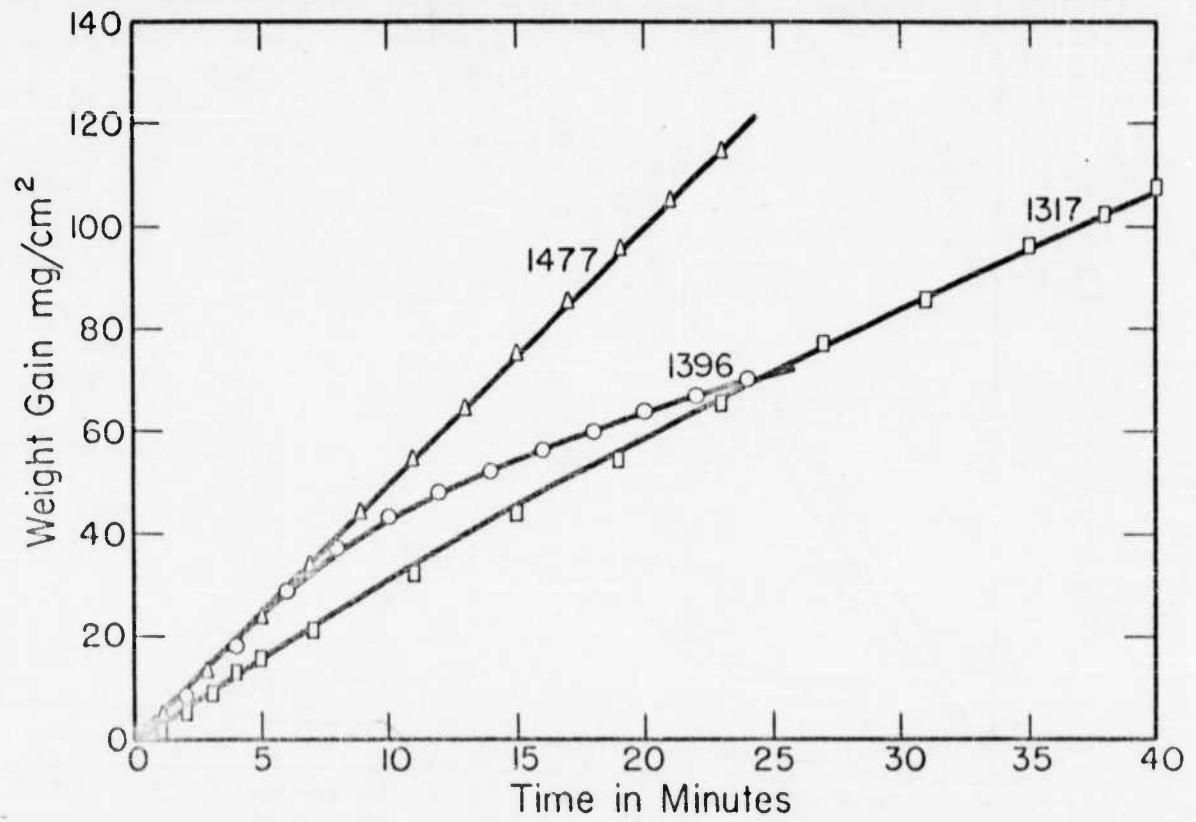


Fig.36-Oxidation of tungsten in 21% oxygen-79% Argon. Sample heated by radiation.



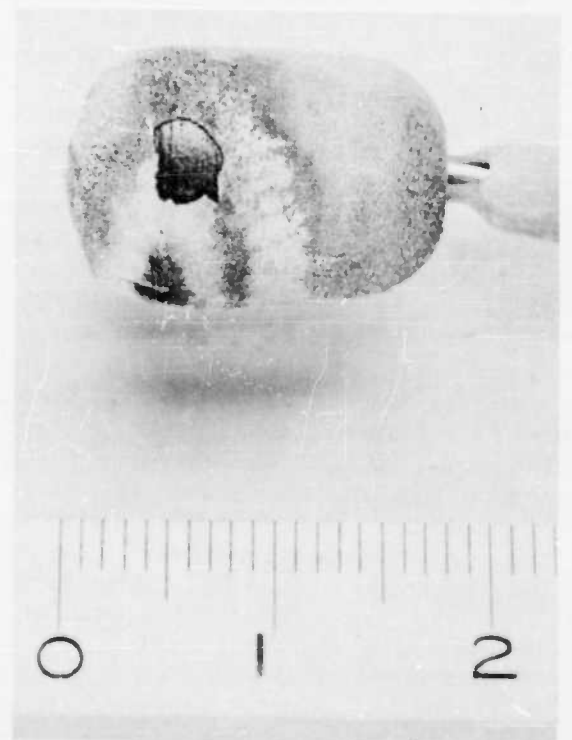
1198⁰C - 27 min.



1317⁰C - 40 min.



1396⁰C - 24 min.



1477⁰C - 24 min.

Fig. 37 -- Tungsten oxidized in 21% O₂ - 79% Ar. Samples heated by radiation

TABLE 14

Oxidation of Tungsten Samples in One Atmosphere of 21% O₂-79% Ar
Samples Heated by Radiation

Temperature °C	Time Minutes	Weight Loss %
863	54.5	2.23
1053	26	11.7
1198	27	55.5
1207	23.5	49.2
1317	40.5	50.0
1396	24	71.7
1477	23.5	81.7

the alumina tube and WO₃. This was much more pronounced when the gas and sample were heated by radiation. The sample oxidized at 1477°C, exhibited in Figure 37, still has part of the thermocouple attached to it. The reaction between WO₃ and alumina is evident at the point where the tube enters the sample. These two oxides appear to form a low melting eutectic. The samples in these measurements lost more oxide by vaporization than those heated in cold gas. The oxide remaining on the sample also appeared to be somewhat more coherent, although in neither case was there evidence that the oxide offered a barrier to oxygen gas.

To determine the amount of vaporization occurring during the oxidation process, samples were weighed after removal from the furnace. From the initial weight, final weight and extent of oxidation, a calculation could be made to determine the amount of WO₃ lost. Some oxidation measurements were checked by removing the oxide mechanically and weighing the tungsten which was left. The weight of tungsten consumed could then be compared to the oxygen consumed. Differences were less than 15%. The case with which the yellow WO₃ oxide was removed again indicates that this oxide could not form a protective layer. However, the thin layer of blue oxide was much more difficult to remove. The blue oxide is believed to be W₁₈O₄₉.

Figure 38 shows the rate of formation of WO₃ and its rate of evaporation during oxidation, as calculated above. At temperatures above 1350°C the oxide appears to evaporate as fast as it is formed under the conditions of these experiments. What is more important is that the curve representing the rate of formation does not change slope above the intersection of the evaporation curve. This indicates that: 1) the rate of oxidation of tungsten is independent of its evaporation rate, and 2) the WO₃ does not form a protective layer. The latter conclusion may be drawn from the fact that the thickness of the WO₃ layer decreases toward zero above 1350. This data shows that the rate of oxidation without any significant amount of WO₃ present is controlled by the same activated process as it is with thick layers of WO₃ present.

Figure 39 compares evaporation rates of WO₃ under three different conditions: 1) in a vacuum, 2) in 1 atmosphere of dry air using Spelsier's¹⁷ data, 3) evaporation in 1 atmosphere of argon and oxygen. In the latter two cases, for the same evaporation rate there is approximately 90° difference in the temperature. Part of this difference could be due to error in temperature measurement.

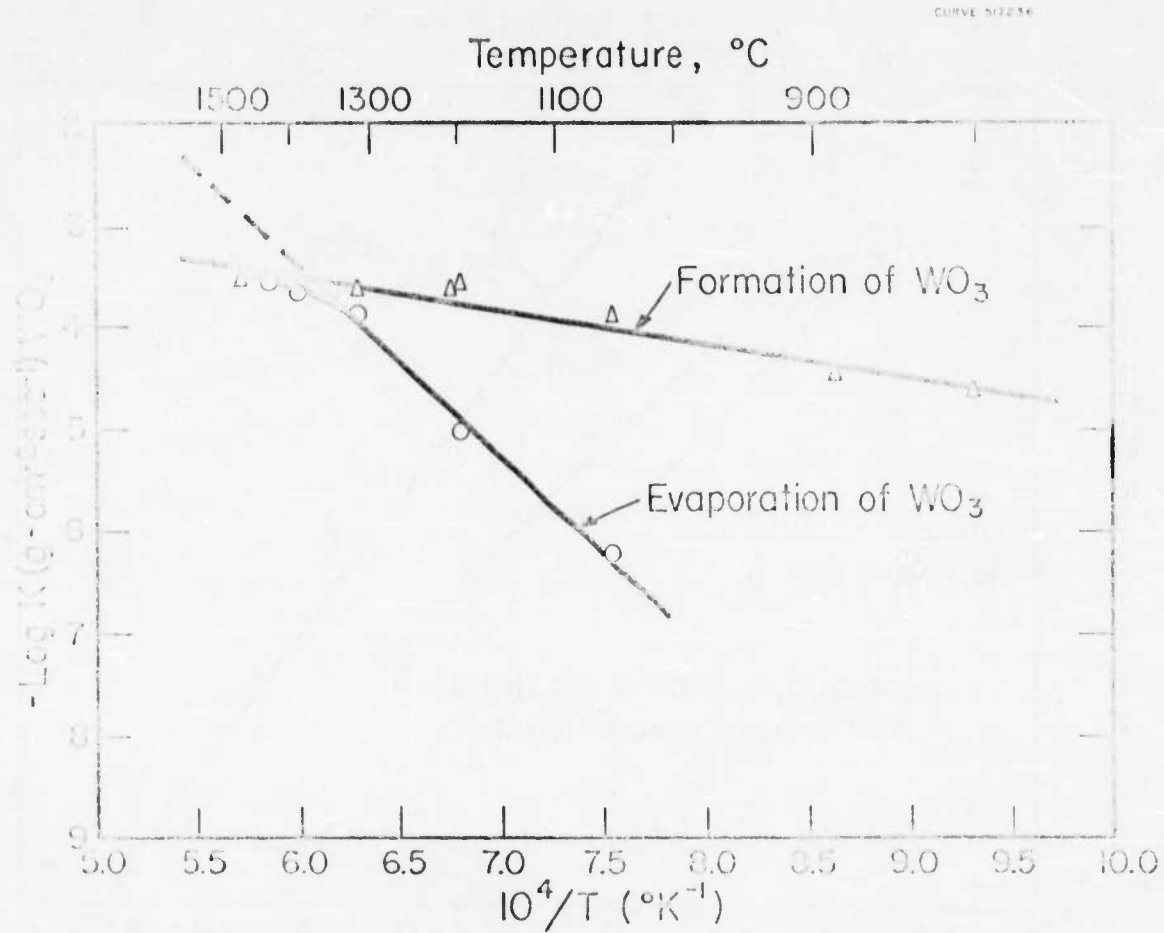


Fig.33-Logarithm of the rate constants for formation and vaporization of WO₃ versus 1/T.

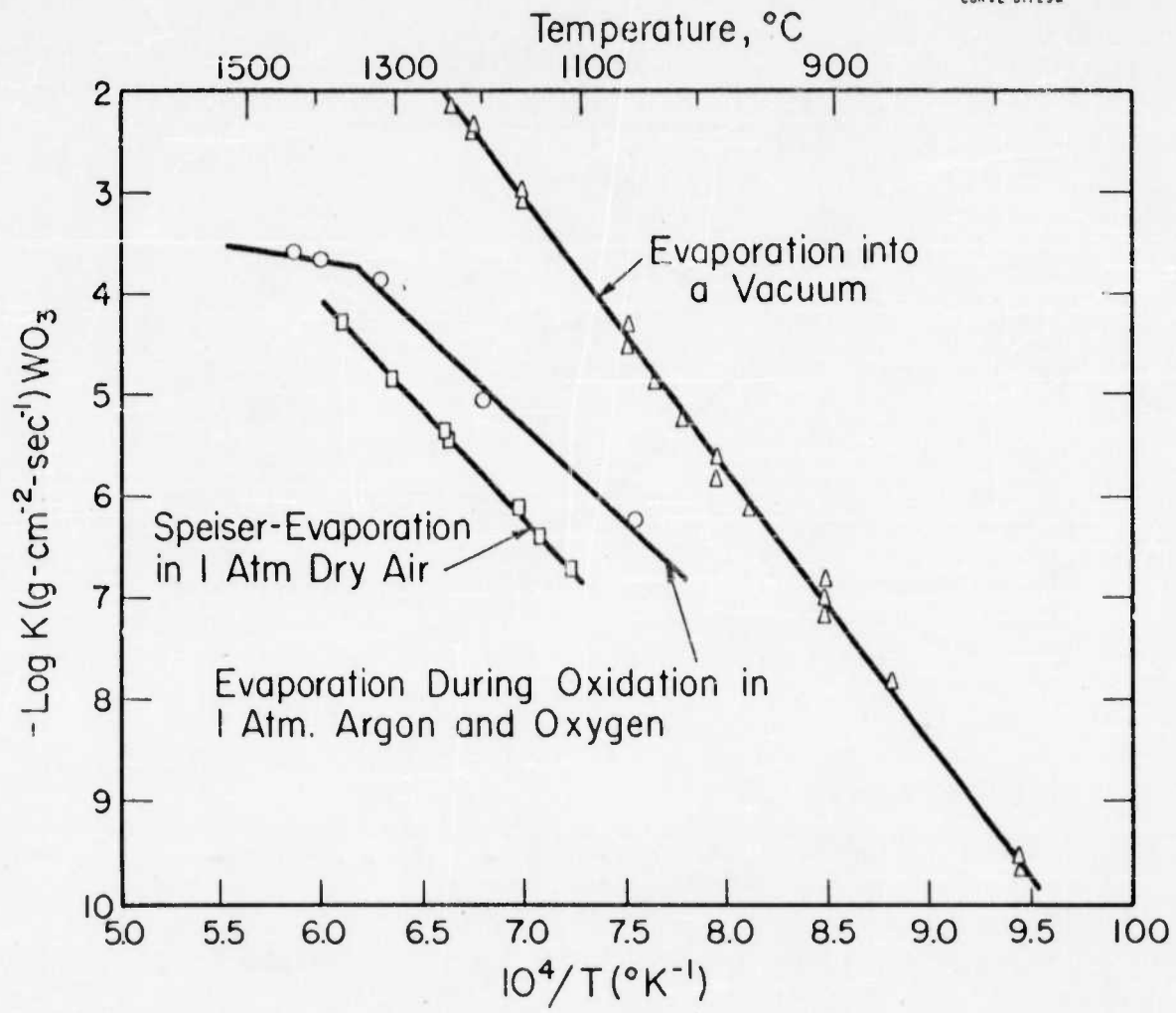


Fig.39-Logarithm of evaporation rate of WO₃ versus reciprocal of absolute temperature.

In these experiments the thermocouple used to measure temperature was checked against an optical pyrometer sighted on a black body hole drilled in the top of a tungsten specimen. When the platinum susceptor was used the difference in the two temperature measurements was no greater than the reproducibility of the pyrometer reading. In the case of samples heated inductively, i.e., without a susceptor, the pyrometer readings were about 28° higher than those read with a thermocouple. These calibrations were carried out in an argon atmosphere and the correction made to the appropriate measurements. It appears that thermocouple error without a susceptor was due to heat losses through the protection tube.

There is no reason to question Speiser's¹⁷ evaporation measurements in 1 atmosphere of air since evaporation rates in lower pressures of oxygen reported earlier (See Figure 7) are in excellent agreement with his data. However, the possibility exists that the surface temperatures of the two samples are different. In the case of evaporation of WO_3 there is a heat loss of about 120 kcal/mole of W_3O_9 , whereas in the case of oxidation of tungsten and evaporation of WO_3 there is a net heat gain of around 470 kcal/mole of W_3O_9 produced. This would require, in our experiments, that a thermal gradient of about 70° (dividing the 90° difference in amounts proportional to the heats of combustion and evaporation) exist between the thermocouple junction and the surface of the metal.

This possible error, around 70° , would apply to oxidation rates also. Since measurements of surface temperatures in these experiments is not feasible, causes of such a discrepancy cannot be definitely established.

Figure 40 presents a comparison between the linear rates of oxidation achieved by each of the two methods, i.e., heating inductively and radiantly. Both measurements were made at the same pressures. From the slopes of these curves, heats of activation of 21.0 ± 1.0 and 23.4 ± 2.9 kcal are calculated for the inductively and radiantly heated samples, respectively.

The measurements made with the platinum susceptor are about $1/2$ as fast as those in which the hot sample reacted with a cold gas. Figure 13 shows the variation in the rate of reaction of tungsten with oxygen as a function of the oxygen pressure at $1200^{\circ}C$. However, as Langmuir¹⁸ established at lower pressures, it is not the oxygen pressure which determines the rate of reaction, but the rate at which molecules strike the surface. Since, at a given pressure, the rate of striking is inversely proportional to the square root of the temperature, a hot gas should react more slowly than a cold gas at the same pressure. If the pressure dependence discussed earlier (Equation 17) is converted to collision frequency dependence and applied to this case, the difference between the two curves may be calculated. When this is done, the mean ratio of the rate of reaction of the radiantly heated sample to the inductively heated one is 0.71 as compared to the observed value of 0.48. On the other hand, if the rate of oxidation is directly proportional to the collision frequency, as found by Langmuir at lower pressures, then the mean ratio of the two rates would be 0.46. Thus, there is a significant difference in the results obtained by the two heating methods and this difference is apparently due to the collision frequency of the gas with the sample. This treatment does not consider the possibility that a blanket of gas near the inductively heated sample may be at a higher temperature than that at the walls of the water cooled container. This effect would decrease the difference between the two curves below the observed differential.

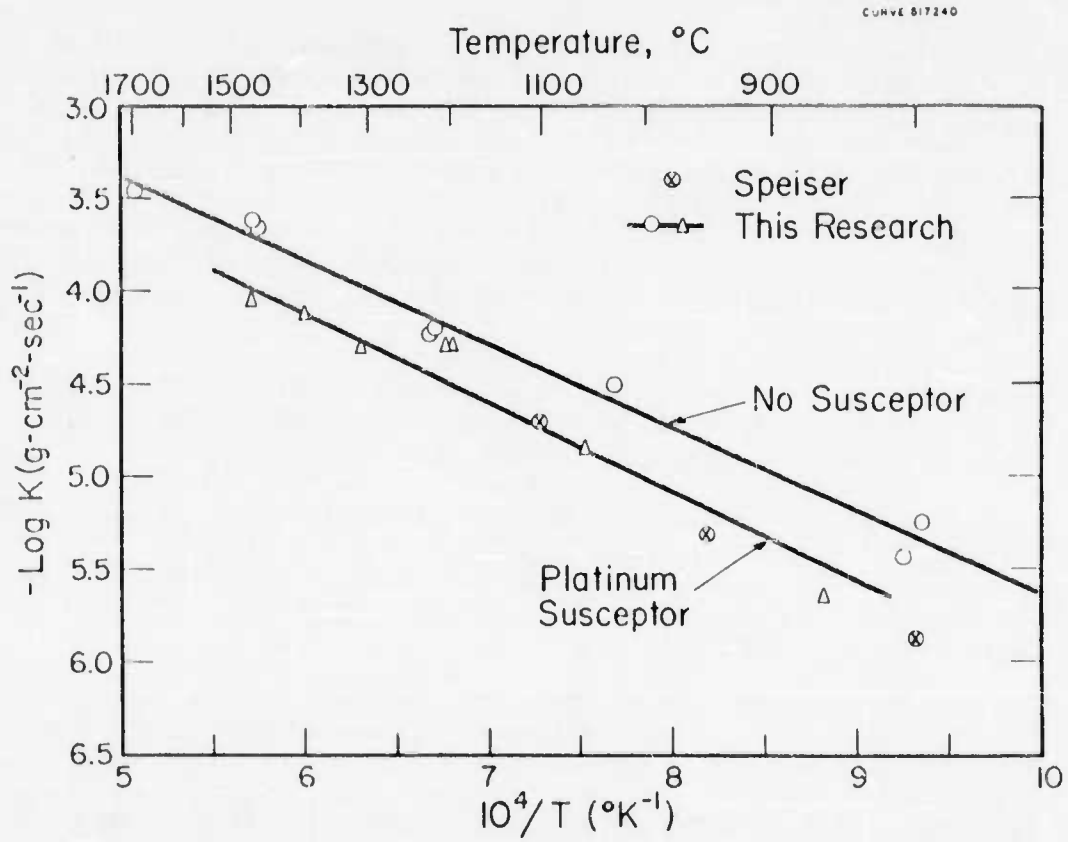


Fig.40-Logarithm of tungsten oxidation rate versus $1/T$ in 21% O_2 -79% A.

Some data obtained by Speiser²² are also plotted in Figure 40. These fall within our scatter for the radiantly heated samples. His data were obtained under conditions similar to ours, that is, his samples were heated by radiation and oxidized in a gas mixture with a total pressure of 1 atmosphere.

Figure 41 compares samples heated inductively in 0.2 atmosphere oxygen and 0.8 atmosphere argon with values calculated from Langmuir¹⁸ at 5×10^{-2} mm of O_2 for a tungsten filament in a cold gas. Langmuir found that the oxidation rate of tungsten between 800 and 2500°C was proportional to a temperature dependent constant multiplied by the collision frequency of oxygen molecules with the metal surface. The pressure, 5×10^{-2} mm, is the upper limit at which this relation was observed. Inasmuch as the two curves are parallel, it seems reasonable to assume that the same mechanism is operating for both pressures. A heat of activation of 22.4 ± 0.8 kcal for Langmuir's curve agrees well with our value of 21.0 ± 1.0 kcal at higher pressures. At the lower pressures used by Langmuir there were probably no more than a few monolayers of oxide on the tungsten surface, especially at the higher temperatures. This is further confirmation that a thicker layer of oxide is not protective since the activation energy for a "clean" surface is practically the same as that found with a considerable amount of oxide on the surface. Furthermore, the low pressure measurements strongly suggest that measurements at higher temperatures in 0.2 atmosphere O_2 and 0.8 atmosphere Ar will follow the extrapolated curve presented in Figure 41.

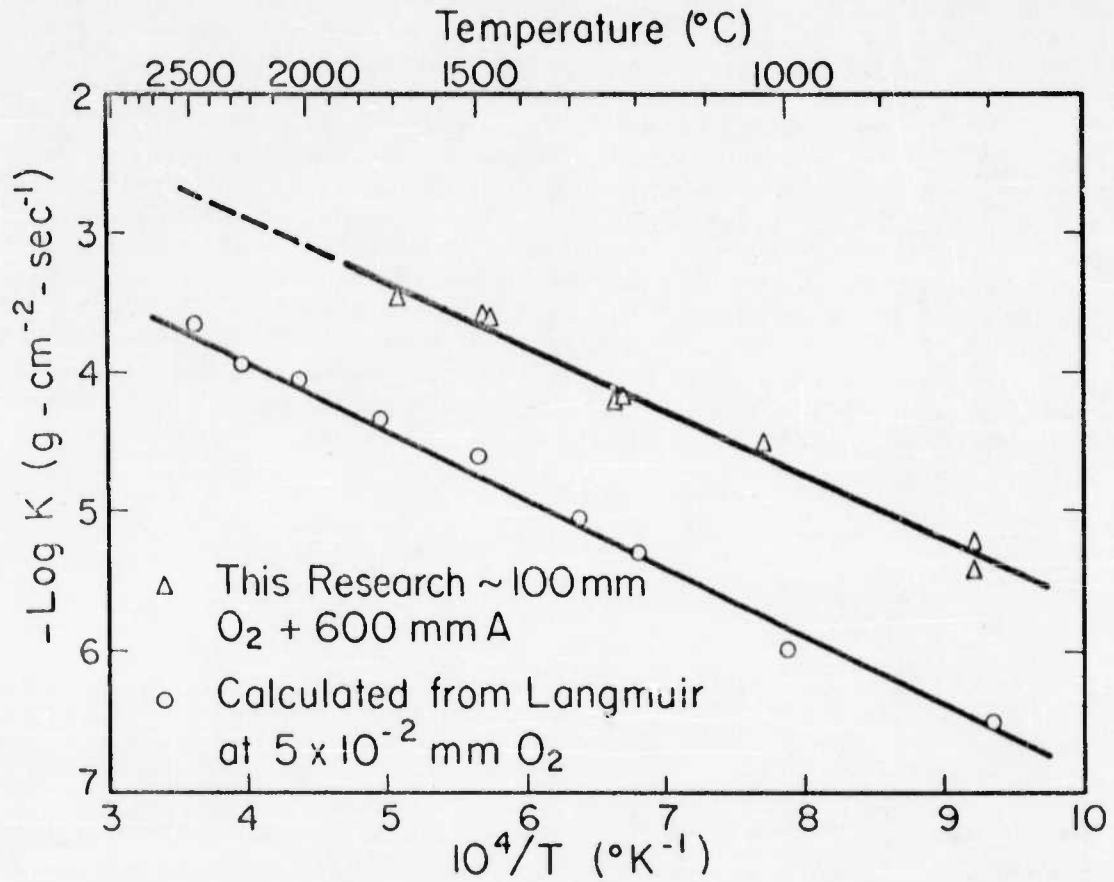


Fig. 41 — Logarithm of oxidation rate of tungsten at 100 mm and 5×10^{-2} mm vs. $1/T$.

SECTION IV. SUMMARY AND CONCLUSIONS

In this report we have presented the results of investigations into the following areas: 1) the vapor pressure over WO_2 , 2) rate limiting factors in vaporization processes, 3) thermodynamics of the tungsten oxides, 4) oxidation rates of tungsten-tantalum alloys between 800 and 1200°C, 5) oxidation rates of tungsten from 800 to 1700°C, and 6) effects of oxygen pressure and oxide evaporation rates on the kinetics of tungsten oxidation. In the course of these inquiries several pieces of equipment have been designed, including: 1) a device for measurement of oxidation rates by determining gas consumption, 2) a high temperature vacuum induction furnace, 3) an Invar vacuum balance, and 4) a new apparatus for making high temperature oxidation rate studies.

The pressure of W_3O_9 measured over WO_2 and W is virtually the same in either tungsten or platinum Knudsen cells and is consistent with the thermal properties of WO_2 and WO_3 . Failure to approach equilibrium in the solid phases at a rate greater than the evaporation rate at temperatures below the 1200 to 1250°C range is believed to be caused by an activated process of high activation energy (> 146 kcal). It is suggested that this procedure may be nucleation and/or growth of the other phases.

Free energy and heat of formation are calculated for the two tungsten oxide phases, $W_{18}O_{49}$ and $W_{20}O_{58}$, from vapor pressures obtained in this study and from literature data. These values are believed to be more reliable than previously reported estimates based on less complete data.

A contrivance has been produced to measure oxidation rates by determining the rate of pressure decline in a reservoir which feeds a constant pressure reaction vessel. The device has not always performed satisfactorily, for the micrometer valve used to bleed the reservoir was faulty, and the alumina furnace tube in which tungsten samples were oxidized has reacted with the tungsten oxide. This situation can be remedied by using an automatic constant pressure manostat and by lining the alumina furnace with platinum.

A new vacuum balance has been constructed of Invar (a material with a very low thermal expansion coefficient) to study oxidation rates of tungsten and tungsten-tantalum alloys. The tungsten measurements were made to determine the kinetic effects of oxygen pressure. Although there is considerable uncertainty about the measurements, it appears that rate may be controlled by dissociation of O_2 to atoms. At lower pressures Langmuir found that the rate of reaction is proportional to the frequency of collision of oxygen molecules with the surface. More accurate data are needed to establish the pressure dependence of the oxidation rate.

Measurements on the tungsten-tantalum alloys indicate that addition of tantalum improves the oxidation resistance of tungsten. At 1200°C 90W-10Ta and 75W-25Ta each oxidize at 40% of the tungsten rate, while the oxidation rate of 50W-50Ta appears to be about 10% of tungsten alone. Some question of the accuracy of this latter measurement exists, since the quantity of WO_3 lost by evaporation is not known. Further study of the 50-50 alloy is planned.

Apparatus for the measurement of oxidation rates up to 1700°C has been constructed. In this equipment the oxidation rate is determined by measuring the oxygen concentration in a known mixture of argon and oxygen after it has flowed over the sample. The oxidation of tungsten between 800 and 1700°C has been found to be independent of the oxide evaporation rate, to be linear, to result in either no protection or the formation of a very thin barrier layer and to form an oxide which grows from the metal or a very thin oxide film. If a protective oxide layer is formed, it is probably $W_{18}O_{49}$. However, the identification by x-ray diffraction of oxides other than WO_3 is uncertain due to the apparent failure of the solid phases to come to equilibrium with adjacent oxide layers. The principal evidence for the presence of a protective film is the strong adherence of a purple scale to the underlying metal. On the other hand, neither the shape of the kinetic curves nor the evident resemblance in mechanism between this work and Langmuir's low pressure measurements supports the hypothesis that a protective layer is present at high temperatures.

LIST OF REFERENCES

1. E. A. Gulbransen, K. F. Andrew, P. E. Blackburn, T. P. Copan, and A. Merlin, "Oxidation of Tungsten and Tungsten Based Alloys," WADC TR 59-575, Part I (March, 1960).
2. K. Ueno, J. Chem. Soc. Japan, 62, 990 (1941).
3. J. Berkowitz, W. A. Chupka, and M. G. Inghram, "Polymeric Gaseous Species in the Sublimation of Tungsten Trioxide," J. Phys. Chem. 27, 85 (1957).
4. P. E. Blackburn, M. Hoch, and H. L. Johnston, "The Vaporization of Molybdenum and Tungsten Oxides," J. Phys. Chem. 62, 769 (1958).
5. J. P. Coughlin, "Contributions to the Data on Theoretical Metallurgy," Bureau of Mines Bulletin 542, U.S. Govt. Printing Office, Washington (1954).
6. G. Huff, E. Squitieri and P. E. Snyder, "The Heat of Formation of Tungstic Oxide, WO_3 ," J. Am. Chem. Soc. 70, 3380 (1948).
7. L. Wöhler and P. Günther, "Das Wasserdampfgleichgewicht über Eisen, Wolfram, und deren Oxyden," Ztschr. Elektrochem., 29, 276 (1923).
8. Z. Shibata, "The Heterogeneous Equilibrium of Tungsten and Its Oxides with Carbon Monoxide and Carbon Dioxide," Tech. Repts. Tôhoku Imp. Univ., 8, 255 (1929).
9. W. B. Pearson, "A Handbook of Lattice Spacings and Structures of Metals and Alloys," Pergamon Press, New York, 1958.
10. E. G. King, W. W. Weller, and A. U. Christensen, "Thermodynamics of Some Oxides of Molybdenum and Tungsten," Bureau of Mines Report of Investigations 5664, U.S. Govt. Printing Office, Washington (1960).
11. I. A. Vasil'eva, Ya. I. Gerasimov, and Yu. P. Simanov, "The Equilibrium of Tungsten Oxides with Hydrogen," Zhur. Fiz. Khim., 31, 682 (1957).
12. R. C. Griffis, "Equilibrium Reduction of Tungsten Oxides by Hydrogen," J. Electrochem. Soc., 106, 418 (1959).
13. A. D. Mah, "The Heats of Formation of Tungsten Trioxide and Tungsten Dioxide," J. Phys. Chem., 81, 1582 (1959).
14. A. P. Beard, "The Enthalpy, Heat Capacity, and Entropy of Tungsten Trioxide Between 0° and 1000° Centigrade," Doctoral Dissertation, Department of Chemistry, Carnegie Institute of Technology, 1951.
15. K. K. Kelley, "The Entropies of Inorganic Substances; Revision of Data," Bureau of Mines Bulletin 477, U.S. Govt. Printing Office, Washington, (1950) and H. Seltz, F. J. Dunkerley, and B. J. DeWitt, "Heat Capacities and Entropies of Molybdenum and Tungsten Trioxides," J. Am. Chem. Soc., 65, 600 (1943).

16. R. J. Ackermann, R. J. Thorn, C. Alexander, and M. Tetenbaum, "Free Energies of Formation of Gaseous Uranium, Molybdenum, and Tungsten Trioxides," *J. Phys. Chem.*, 64, 350 (1960).
17. R. Speiser, "Research on the Oxidation Behavior of Tungsten," AF 33(616)-5721, Report 831-1, 1958.
18. I. Langmuir, "Chemical Reactions at Very Low Pressures, I. The Clean-up of Oxygen in a Tungsten Lamp," *J. Am. Chem. Soc.*, 35, 105 (1913) and "Chemical Reactions at Low Pressures," *ibid.*, 37, 1139 (1915).
19. A. Magneli, "X-Ray Studies on the System Molybdenum Trioxide-Tungsten Trioxide," *Acta. Chem. Scand.*, 3, 88 (1949).
20. A. Magneli, "Crystal Studies on γ -Tungsten Oxide," *Arkiv. Kemi.*, 1, 233 (1949).
21. J. Weissbart and R. Ruka, "Oxygen Gauge," to be published in *Rev. Sci. Instr.*
22. R. Speiser, "Research on the Oxidation Behavior of Tungsten," AF 33(616)-5721, Report 831-4, 1959.

UNCLASSIFIED

WESTINGHOUSE ELECTRIC CORPORATION, RESEARCH LABORATORIES, Pittsburgh, Pa. OXIDATION OF TUNGSTEN AND TUNGSTEN BASED ALLOYS, by P. E. Blackburn, K. F. Andrew, E. A. Galbraisen and F. A. Brassart - June 1961 - 74p. incl. figs. and tables. (Project 7351) (WADC TR 59-575, Pt II) (Contract AF 33(616)-5770) Unclassified Report

This paper describes the results of studies related to the oxidation of tungsten and its alloys.

The pressure of WO_3 polymers over WO_2 was measured in a tungsten Knudsen cell and found to agree with measurements in a platinum cell. Literature data for WO_2 and WO_3 were combined with vapor pressures determined

(over)

in this project to give thermodynamic values for $W_{18}O_{49}$ and $W_{20}O_{48}$.

Tungsten oxidation rates have been measured from 800 to 1700°C and in pressures of oxygen between 2×10^{-1} and 10^{-2} atmospheres. The effects of oxygen pressure indicate that the rate may be governed by oxygen dissociating to atoms at the reacting surface. The oxidation rate is demonstrated to be independent of the oxide evaporation rate. All of the evidence indicates that if an oxide barrier layer is present at temperatures above 800°C it must be very thin.

Studies on the oxidation of tantalum-tungsten alloys between 800 and 1200°C indicate that the 90-50 alloy has the greatest oxidation resistance, oxidizing at a rate as much as 10 times slower than tungsten alone.

UNCLASSIFIED

UNCLASSIFIED

WESTINGHOUSE ELECTRIC CORPORATION, RESEARCH LABORATORIES, Pittsburgh, Pa. OXIDATION OF TUNGSTEN AND TUNGSTEN BASED ALLOYS, by P. E. Blackburn, K. F. Andrew, E. A. Galbraisen and F. A. Brassart - June 1961 - 74p. incl. figs. and tables. (Project 7351) (WADC TR 59-575, Pt II) (Contract AF 33(616)-5770) Unclassified Report

This paper describes the results of studies related to the oxidation of tungsten and its alloys.

The pressure of WO_3 polymers over WO_2 was measured in a tungsten Knudsen cell and found to agree with measurements in a platinum cell. Literature data for WO_2 and WO_3 were combined with vapor pressures determined

(over)

in this project to give thermodynamic values for $W_{18}O_{49}$ and $W_{20}O_{48}$.

Tungsten oxidation rates have been measured from 800 to 1700°C and in pressures of oxygen between 2×10^{-1} and 10^{-2} atmospheres. The effects of oxygen pressure indicate that the rate may be governed by oxygen dissociating to atoms at the reacting surface. The oxidation rate is demonstrated to be independent of the oxide evaporation rate. All of the evidence indicates that if an oxide barrier layer is present at temperatures above 800°C it must be very thin.

Studies on the oxidation of tantalum-tungsten alloys between 800 and 1200°C indicate that the 90-50 alloy has the greatest oxidation resistance, oxidizing at a rate as much as 10 times slower than tungsten alone.

UNCLASSIFIED

UNCLASSIFIED

WESTINGHOUSE ELECTRIC CORPORATION, RESEARCH LABORATORIES, PITTSBURGH, PA. OXIDATION OF TUNGSTEN AND TUNGSTEN BASED ALLOYS, by P. E. Blackburn, K. F. Andrew, E. A. Galbraisen and F. A. Brassart - June 1961 - 74p. Incl. figs. and tables. (Project 7351) (WADC TR 59-575, Pt II) (Contract AF 33(616)-5770) Unclassified Report

This paper describes the results of studies related to the oxidation of tungsten and its alloys.

The pressure of W_2O_3 polymers over WO_2 was measured in a tungsten Knudsen cell and found to agree with measurements in a platinum cell. Literature data for WO_2 and WO_3 were combined with vapor pressures determined

(over)

In this project to give thermodynamic values for W_2O_5 and W_2O_6 .

Tungsten oxidation rates have been measured from 800 to 1700°C and in pressures of oxygen between 2×10^{-1} and 10^{-2} atmospheres. The effects of oxygen pressure indicate that the rate may be governed by oxygen dissociating to atoms at the reacting surface. The oxidation rate is demonstrated to be independent of the oxide evaporation rate. All of the evidence indicates that if an oxide barrier layer is present at temperatures above 800°C it must be very thin.

Studies on the oxidation of tantalum-tungsten alloys between 800 and 1200°C indicate that the 50-50 alloy has the greatest oxidation resistance, oxidizing at a rate as much as 10 times slower than tungsten alone.

UNCLASSIFIED

UNCLASSIFIED

WESTINGHOUSE ELECTRIC CORPORATION, RESEARCH LABORATORIES, PITTSBURGH, PA. OXIDATION OF TUNGSTEN AND TUNGSTEN BASED ALLOYS, by P. E. Blackburn, K. F. Andrew, E. A. Galbraisen and F. A. Brassart - June 1961 - 74p. Incl. figs. and tables. (Project 7351) (WADC TR 59-575, Pt II) (Contract AF 33(616)-5770) Unclassified Report

This paper describes the results of studies related to the oxidation of tungsten and its alloys.

The pressure of W_2O_3 polymers over WO_2 was measured in a tungsten Knudsen cell and found to agree with measurements in a platinum cell. Literature data for WO_2 and WO_3 were combined with vapor pressures determined

(over)

In this project to give thermodynamic values for W_2O_5 and W_2O_6 .

Tungsten oxidation rates have been measured from 800 to 1700°C and in pressures of oxygen between 2×10^{-1} and 10^{-2} atmospheres. The effects of oxygen pressure indicate that the rate may be governed by oxygen dissociating to atoms at the reacting surface. The oxidation rate is demonstrated to be independent of the oxide evaporation rate. All of the evidence indicates that if an oxide barrier layer is present at temperatures above 800°C it must be very thin.

Studies on the oxidation of tantalum-tungsten alloys between 800 and 1200°C indicate that the 50-50 alloy has the greatest oxidation resistance, oxidizing at a rate as much as 10 times slower than tungsten alone.

UNCLASSIFIED

UNCLASSIFIED

WESTINGHOUSE ELECTRIC CORPORATION, RESEARCH LABORATORIES, PITTSBURGH, Pa. OXIDATION OF TUNGSTEN AND TUNGSTEN BASED ALLOYS, by P. E. Blackburn, K. F. Andrew, E. A. Galbransen and F. A. Brassart - June 1961 - 74p. incl. figs. and tables. (Project 7351) (WADC TR 59-575, Pt II) (Contract AF 33(616)-5770) Unclassified Report

This paper describes the results of studies related to the oxidation of tungsten and its alloys.

The pressure of WO_3 polymers over WO_2 was measured in a tungsten Knudsen cell and found to agree with measurements in a platinum cell. Literature data for WO_2 and WO_3 were combined with vapor pressures determined

(over)

In this project to give thermodynamic values for $W_{19}O_{49}$ and $W_{20}O_{48}$.

Tungsten oxidation rates have been measured from 800 to 1700°C and in pressures of oxygen between 2×10^{-1} and 10^{-2} atmospheres. The effects of oxygen pressure indicate that the rate may be governed by oxygen dissociating to atoms at the reacting surface. The oxidation rate is demonstrated to be independent of the oxide evaporation rate. All of the evidence indicates that if an oxide barrier layer is present at temperatures above 800°C it must be very thin.

Studies on the oxidation of tantalum-tungsten alloys between 800 and 1200°C indicate that the 50-50 alloy has the greatest oxidation resistance, oxidizing at a rate as much as 10 times slower than tungsten alone.

UNCLASSIFIED

UNCLASSIFIED

WESTINGHOUSE ELECTRIC CORPORATION, RESEARCH LABORATORIES, PITTSBURGH, Pa. OXIDATION OF TUNGSTEN AND TUNGSTEN BASED ALLOYS, by P. E. Blackburn, K. F. Andrew, E. A. Galbransen and F. A. Brassart - June 1961 - 74p. incl. figs. and tables. (Project 7351) (WADC TR 59-575, Pt II) (Contract AF 33(616)-5770) Unclassified Report

This paper describes the results of studies related to the oxidation of tungsten and its alloys.

The pressure of WO_3 polymers over WO_2 was measured in a tungsten Knudsen cell and found to agree with measurements in a platinum cell. Literature data for WO_2 and WO_3 were combined with vapor pressures determined

(over)

In this project to give thermodynamic values for $W_{19}O_{49}$ and $W_{20}O_{48}$.

Tungsten oxidation rates have been measured from 800 to 1700°C and in pressures of oxygen between 2×10^{-1} and 10^{-2} atmospheres. The effects of oxygen pressure indicate that the rate may be governed by oxygen dissociating to atoms at the reacting surface. The oxidation rate is demonstrated to be independent of the oxide evaporation rate. All of the evidence indicates that if an oxide barrier layer is present at temperatures above 800°C it must be very thin.

Studies on the oxidation of tantalum-tungsten alloys between 800 and 1200°C indicate that the 50-50 alloy has the greatest oxidation resistance, oxidizing at a rate as much as 10 times slower than tungsten alone.

UNCLASSIFIED

UNCLASSIFIED

WESTINGHOUSE ELECTRIC CORPORATION, RESEARCH LABORATORIES, PITTSBURGH, Pa. OXIDATION OF TUNGSTEN AND TUNGSTEN BASED ALLOYS, by F. E. Blackburn, K. F. Andrew, E. A. Gulbraansen and F. A. Brassart - June 1961 - 74p. incl. figs. and tables. (Project 7321) (WADC TR 59-575, Pt II) (Contract AF 33(616)-5770) Unclassified Report

This paper describes the results of studies related to the oxidation of tungsten and its alloys.

The pressure of W_3 polymers over WO_3 was measured in a tungsten Knudsen cell and found to agree with measurements in a platinum cell. Literature data for WO_2 and WO_3 were obtained with vapor pressures determined

(over)

In this project to give thermodynamic values for WO_3 and WO_2 .

Tungsten oxidation rates have been measured from 500 to 1700°C and in pressures of oxygen between 2×10^{-4} and 10^{-2} atmospheres. The effects of oxygen pressure indicate that the rate may be governed by oxygen dissociation at the reacting surface. The oxidation rate is demonstrated to be independent of the oxide evaporation rate. All of the evidence indicates that if an oxide barrier layer is present at temperatures above 500°C it must be very thin.

Studies on the oxidation of tantalum-tungsten alloys between 500 and 1200°C indicate that the W-50 alloy has the greatest oxidation resistance, oxidizing at a rate as much as 10 times slower than tungsten alone.

UNCLASSIFIED

UNCLASSIFIED

WESTINGHOUSE ELECTRIC CORPORATION, RESEARCH LABORATORIES, PITTSBURGH, Pa. OXIDATION OF TUNGSTEN AND TUNGSTEN BASED ALLOYS, by F. E. Blackburn, K. F. Andrew, E. A. Gulbraansen and F. A. Brassart - June 1961 - 74p. incl. figs. and tables. (Project 7321) (WADC TR 59-575, Pt II) (Contract AF 33(616)-5770) Unclassified Report

This paper describes the results of studies related to the oxidation of tungsten and its alloys.

The pressure of WO_3 polymers over WO_2 was measured in a tungsten Knudsen cell and found to agree with measurements in a platinum cell. Literature data for WO_2 and WO_3 were combined with vapor pressures determined

(over)

In this project to give thermodynamic values for WO_3 and WO_2 .

Tungsten oxidation rates have been measured from 500 to 1700°C and in pressures of oxygen between 2×10^{-4} and 10^{-2} atmospheres. The effects of oxygen pressure indicate that the rate may be governed by oxygen dissociation at the reacting surface. The oxidation rate is demonstrated to be independent of the oxide evaporation rate. All of the evidence indicates that if an oxide barrier layer is present at temperatures above 500°C it must be very thin.

Studies on the oxidation of tantalum-tungsten alloys between 500 and 1200°C indicate that the W-50 alloy has the greatest oxidation resistance, oxidizing at a rate as much as 10 times slower than tungsten alone.

UNCLASSIFIED